Experimental and Numerical Investigation of the Dynamic Seat Comfort in Aircrafts

by

Hakan Ciloglu

Bachelor of Science in Engineering, NTUU KPI, 2010

A Thesis Submitted in Partial Fulfillment of the Requirements for the Degree of

Masters of Applied Science in Engineering

In the Graduate Academic Unit of Mechanical Engineering

Supervisor(s): Atef Mohany, PhD, P. Eng, Mechanical Engineering

Hossam Kishawy, PhD, P. Eng, Mechanical Engineering

Faculty of Engineering and Applied Science

University of Ontario Institute of Technology

Oshawa, Ontario, Canada, 2013

Abstract

This research focuses on the dynamic seat comfort in aircrafts specifically during takeoff, landing and cruise through turbulence flight conditions. The experiments are performed using a multi axis shaker table in the Automotive Centre of Excellence (ACE) at the University of Ontario Institute of Technology subjected to sample takeoff, landing and cruise vibration recordings obtained onboard of an actual flight. The input vibrations introduced to the aircraft seats during actual flight conditions and during the experiments in the ACE are compared and it is concluded that the given flight conditions were successfully replicated for the interest of this thesis.

The experiments are conducted with two different aircraft seats, economy class and business class. Furthermore, to investigate the importance of seat cushion characteristics in addition to economy and business class seat cushions, three laboratory made cushions were included in the investigation as well. Moreover, the effect of passenger weight is also discussed by conducting the experiments with 1 and 2 identical dummies.

It is concluded that static seat properties play a significant role in the comfort perception level as well as flight conditions. Among the three flight condition, landing appeared to be the most uncomfortable case comparing to takeoff and cruise.

In addition to experimental work, a numerical study to simulate the flight conditions is undertaken with the initial work of CAD modelling. The simulated responses of the seat is partially matching with experimental results due to unknown parameters of the cushion and the connections of the aircraft seat that cannot be created in the CAD model due to unknown manufacturing processes.

Acknowledgements

It is a pleasure to thank a great number of people who made this thesis possible. First of all, I would like to express my sincere thanks to my supervisors Dr. Atef Mohany and Dr. Hossam Kishawy for their guidance, support and patience throughout my study.

I would also like to thank Dr. Ibrahim Dincer for supporting me from the beginning and his clear-sighted suggestions during my studies at UOIT. Cordial thanks to Dr. David Arthurs for his help during my experimental studies. In addition to the kind help I got from UOIT, more specifically ACE staff and faculty, I am very grateful to the members of Dr. Mohany's research team, Nadim Arafa, Mohammed Alziadeh and Ahmad Omar. I wish to express my warm thanks to them who have given continuous encouragement, support and assistance during my research. It was a privilege for me to work with such a team during the course of my study.

Very special thanks to Canan Acar, Dr. Kemal Ozdemir, Hasan Ozcan, Ahmet Ozbilen and all my friends for their friendship and support which has motivated me throughout my study.

Finally, I wish to thank my family for all their endless support, patience and encouragement throughout my life. Besides these, I would also like to express my great debt of gratitude to my family believing in me. This thesis is dedicated to my mother, father and brother. If there is any honor in this degree, it belongs to them.

Table of Contents

Abstract ii

Acknowledgements iii

Table of Contents iv

List of Tables vii

List of Figures viii

Nomenclature xii

Chapter 1 1

1.1 Global Airline Industry 2

1.2 Flight Physiology: Vibration in Aviation 5

1.2.1 Sources of Vibration in Aviation 7

1.2.2 Response of Human Body to Vibration 7

1.2.3 Human Physiological and Subjective Responses to Vibration 9

1.2.4 Whole-Body Vibration Exposure Standards 10

1.2.5 Vibration Mitigation 12

1.3 Aircraft Seat Design 12

1.4 Scope of This Study 14

Chapter 2 16

2.1 Dynamic Seat Comfort in Heavy Vehicles: Measurements and Developments 17

2.1.1 Improvements towards Seat Design 18
2.1.2 Developments towards Cabin Suspension 21
2.1.3 Effect of Tire Pressure and Type on Vibration Transmissibility 24
2.1.4 Reported Improvements 26
2.2 Factors Effecting Seat Transmissibility 27
2.2.1 Seat Characteristics 28
2.2.2 Sitting Posture 30
2.2.3 Input Vibration 33
2.2.4 Apparent Mass 33
2.2.5 Age 37
2.3 Seat Comfort Measurement Methods 37
Chapter 3 43
3.1 Experimental Setup 44
3.1.1 Vibration Exciters 44
3.1.2 Performance Specification and Measurement 45
3.1.3 Data Acquisition and Processing 46
3.1.4. Complete Experimental Setup 47
3.2 Experimental Procedure 50
3.2.1 Signal Processing 50
Chapter 4 54
4.1 Input Comparison for Takeoff 55
4.2 Input Comparison for Landing 57
4.3 Input Comparison for Cruise 58
Chapter 5 62
5.1 Transmissibility 62

5.2 Seat Effective Amplitude Transmissibility 70
Chapter 6 76
6.1 Effect of Weight on the Transmissibility and S.E.A.T 76
6.2 Effect of Cushion on the Transmissibility and S.E.A.T. 78
Chapter 7 82
7.1 Mesh Development and Mesh Sensitivity 83
7.1.1 Modal Analysis 83
7.2 FEA Response for the Given Flight Conditions 86
Chapter 8 92
8.1 Conclusions 92
8.2 Recommendations 94
References 95

List of Tables

Table 2.1: Outcome measurement units employed for different studies. 26
Table 2.2: Summary of the broad-band vibration magnitudes employed (Mandapuram et al., 2012). 35
Table 3.1: Typical operation – capability ranges for various shaker types. 44
Table 5.1: Calculated S.E.A.T. values using ISO–2631. 73
Table 5.2: Calculated S.E.A.T. values using BS–6841. 73
Table 6.1: Calculated S.E.A.T. values using BS–6841 human weighting functions. 78
Table 6.2: Calculated S.E.A.T. values for different cushions. 80
Table 7.1: Identified model frequencies by using FE. 84

List of Figures

Figure 1.1: Annual RPK growth rates, 1987–2007 (ATA, 2008; ICAO, 1971–2005). 3
Figure 1.2: Airline passenger traffic growth by world regions (reproduced from ICAO, 1971–2005; IATA, 2007). 4
Figure 1.3: Orthogonal axes for assessment of human exposure to vibration (BS-6472, 1992) 6
Figure 1.4: Axes for measuring vibration exposures of seated aircraft passengers (Griffin and Helmut, 2011). 8
Figure 1.5: The short–time, one–minute and three–minute human whole–body tolerance limits reported during vertical sinusoidal vibration (Magid et al. 1960). 9
Figure 1.6: Symptoms experienced for frequencies between 1 and 20 Hz at tolerance levels (Magid et al. 1960). 10
Figure 2.1: Segments of suspension control employed by various studies. 17
Figure 2.2: Power spectrum comparisons of input and outputs from two different suspensions (Hostens and Ramon, 2003). 19
Figure 2.3: Calculated S.E.A.T. values for different forward speeds and low (white) and high (black) tire pressure (Hostens et al., 2004). 20
Figure 2.4: Comparison of analytical and experimental acceleration transmissibility of seat suspension (reproduced from Tewari and Prasad (1999)). 20
Figure 2.5: Comparison of weighted rms cabin vertical acceleration of passively, actively and semi–actively suspended cabin (reproduced from Elmadany and Abduljabbar (1990)). 22
Figure 2.6: Reduction in the vertical acceleration using the developed semi-active suspension system (Nell and Steyn, 2003). 22
Figure 2.7: Experimental performance on uneven road (Ieluzzi et al., 2006). 23

Figure 2.8: Displacement of the interior cabin with optimized and un-optimized suspension system (Zehsaz et al., 2011). 24
Figure 2.9: Collected data for different tire inflations (Sherwin et al., 2004). 25
Figure 2.10: Comparison of ride comfort level improvements (by percentage) of selected studies. 27
Figure 2.11: Vertical vibration transmissibility for 10 different cushions for railway passenger seat (Corbridge et al., 1989). 28
Figure 2.12: Effect of posture on the transmission of vibration through a train seat. Mean of 30 subjects (15 male, 15 female) with 0.6 ms–2 r.m.s. random vibration: ——— normal (with backrest, hands in lap); — • — • — • arms on armrests (with backrest); and - - - - back-off (hands in lap) (Corbridge et al., 1989). 29
Figure 2.13: Factors affecting comfort score (Ebe and Griffin, 2001). 30
Figure 2.14: New weighting frequency curves at different backrest angles and current ISO 2631–1 curve (Wk. for z–direction) (Paddan et al., 2012). 32
Figure 2.15: Effect of magnitude on seat transmissibility (Fairley, 1986). 33
Figure 2.16: Effect of the seat backrest on mean apparent mass and inter-subject variability: 1.0 ms–2 rms excitation; mean (------) and ± 1 s.d. (·····) (Toward and Griffin, 2011). 34
Figure 2.17: The lateral apparent mass of all 12 test subjects normalised by sitting mass showing the median and interquartile ranges for lateral oscillation (lower lines) and roll oscillation (upper lines) in response to each magnitude of seat surface lateral acceleration (Gunston, 2003). 36
Figure 2.18: Effect of age on resonance frequency and seat transmissibility (Toward and Griffin, 2011). 37
Figure 2.19: A model of overall seat discomfort on linear scales (Ebe and Griffin, 2000). 38
Figure 2.20: Effect of initial values on features of graphs: (a) linear scales, (b) log-log scale (from Ebe and Griffin, 2000). 40
Figure 2.21: The new proposed design as implemented in testing vehicle (Makhsous et al., 2005). 40
Figure 3.1: Schematic description of the conducted work. 43
Figure 3.2: Designed fixations to the MAST using steel plates. 45
Figure 3.3: Seat pad accelerometer. 46
Figure 3.**5**: Complete attachments of aircraft seat with the accelerometer under the dummy. 47

Figure 3.6: Laboratory–made cushions used in the experiments. 48
Figure 3.7: DMA Q 800 dynamic mechanical analyzer. 49
Figure 3.8: Stress–strain curve for cushion A. 49
Figure 3.9: Stress–strain curve for cushion C 50
Figure 4.1: Experimental setup during actual flight conditions. 54
Figure 4.2: Input comparison for take–off in z–direction. 55
Figure 4.3: Input comparison for take–off in y–direction. 56
Figure 4.4: Input comparison for landing in z–direction. 57
Figure 4.5: Input comparison for landing in y–direction. 58
Figure 4.6: Input comparison for cruise in z–direction. 59
Figure 4.7: Input comparison for cruise in y–direction. 60
Figure 5.1: Comparison of input and output vibration on the seat surface (z-direction) for takeoff. 63
Figure 5.2: Comparison of input and output vibration on the seat surface (z-direction) for landing. 64
Figure 5.3: Comparison of input and output vibration on the seat surface (z-direction) for cruise. 65
Figure 5.4: Transmissibility in z–direction for economy class seats. 66
Figure 5.5: Transmissibility in z–direction for business class seats. 67
Figure 5.6: Transmissibility in x–direction for economy class seats. 68
Figure 5.7: Transmissibility in the x–direction for business class seats. 68
Figure 5.8 Change in the peak transmissibility depending on the weight for takeoff. 69
Figure 5.9 Change in the peak transmissibility depending on the weight for landing. 69
Figure 5.10 Change in the peak transmissibility depending on the weight for cruise 70
Figure 5.11: ISO–2631 human response functions W_z =z–direction, W_y = x–direction. 72
Figure 5.12: BS–6841 human weighting functions W_d = z–direction, W_c = x–direction. 73
Figure 6.1: Effect of number of passengers in transmissibility during take–off. 77
Figure 6.2 Effect of number of passengers in transmissibility during landing. 77
Figure 6.3: Effect of number of passengers in transmissibility during cruise. 78
Figure 6.4: Transmissibility comparison of different cushions during take–off. 79
Figure 6.5: Transmissibility comparison of different cushions during landing. 79

Figure 6.6: Transmissibility comparison of different cushions during cruise. 80
Figure 7.1: CAD model of economy class seats. 82
Figure 7.2: Change in the model frequencies with the increase of tetrahedral element number. . 84
Figure 7.3: First and second mode shapes. 85
Figure 7.4: Third and fourth mode shapes. 86
Figure 7.5: Output acceleration comparison for takeoff without cushion. 87
Figure 7.6: Output acceleration comparison for landing without cushion. 87
Figure 7.7: Output acceleration comparison for cruise without cushion. 88
Figure 7.8: Output acceleration comparison for takeoff including cushion. 89
Figure 7.9: Output acceleration comparison for landing including cushion. 89
Figure 7.10: Output acceleration comparison for cruise including cushion. 90

Nomenclature

a	Acceleration [m/s^2]
G	Power spectral density [$(m/s^2)^2/Hz$]
k	Constant
x (n)	Data sequence
f	Frequency [Hz]
X (k)	Fourier coefficient
W_N	Phase factor
j	Imaginary unit

Greek Symbols

β	Stimulus constant
φ	Stimulus magnitude
Ψ	Sensation magnitude (e.g. discomfort)

Subscripts

f	Input acceleration
rms	Root-mean-square
s	Output acceleration

Acronyms

ACE	Automotive Centre of Excellence
ACGIH	American Conference of Governmental Industrial Hygienists
ANSI	American National Standards Institute
ATA	Air Transport Association of America
ATAG	Air Transport Action Group
BS	British Standards
DFT	Discrete Fourier Transform
DOF	Degree of Freedom
FAA	Federal Aviation Administration
FE	Finite Element
FEA	Finite Element Analysis
FFT	Fast Fourier Transform
GDP	Gross Domestic Product
IATA	International Air Transport Association
ICAO	International Civil Aviation Organization
ISO	International Organization for Standardization
IT	Ischial Tuberosities
JADC	Japan Aircraft Development Corporation
LBP	Low Back Pain
MAST	Multi–Axis–Shaker–Table
NASA	National Aeronautics and Space Administration
PSD	Power Spectral Density
RPK	Revenue Passenger Kilometers

S.E.A.T.	Seat Effective Amplitude Transmissibility
TLV	Threshold Limit Values
UOIT	University of Ontario Institute of Technology
VDV	Vibration Dose Value
VTV	Vibration Total Value
WBV	Whole–Body Vibration

Chapter 1

Introduction

This chapter presents an introduction to the global airline industry, its evolution, and current status. Extraordinary fuel price volatility, increasing costs, global financial crises, fluctuating passenger demands, and tight regulations are some of the major challenges of the aviation industry. The focus of this study is vibration in aviation; therefore, the types and sources of vibration and its effects on aircraft passengers, whole–body vibration exposure standards, vibration mitigation and aviation industry regulations, and aircraft seat design are explained in this chapter.

The vibration that passengers are exposed to during aircraft take–off, cruise, and landing has serious effects on human health which potentially could harm body functions at different levels. To minimize the adverse effects of aviation–related vibration and increase passenger health and comfort, major aviation authorities and industries in the world are putting significant efforts in research and development on monitoring, controlling, and minimization of vibration during aircraft operations. Aircraft seating systems play an important role in reducing the effects of vibration and increasing passenger comfort. However, design and certification of aircraft seating systems is challenging and expensive, therefore, there is a need to accurately simulate and predict the dynamic characteristic and behavior of such systems. For that reason, in this thesis, it

is aimed to develop a methodological approach to simulate and assess dynamic aircraft seat suspension characteristics more economically and accurately. The objectives of this study are explained in detail in the "Scope of This Study" section. And the final section of this chapter provides a brief overview of the general outline of this thesis.

1.1 Global Airline Industry

The global airline industry plays a major role in the creation of global economy by providing service to almost every country in the world. The industry itself is a major economic force. Its operations are strongly connected to other industries, from manufacturing and logistics to tourism. Furthermore, air transportation boosts the economy by offering a wide array of employment opportunities, making it possible to reach a diverse range of markets, people, ideas and information, labor supply, skills, capital, opportunities, and resources. There are few other industries that create the amount of attention generated by the airline industry. Government policy makers, the media, and a vast amount of people directly engaged to aviation industry's operations make the industry very dynamic, yet highly challenging (Ishutkina and Hansman, 2008).

The global airline industry's development was made possible by key technological innovations such as the introduction of commercial jet aircrafts in the 1950s and wide body jumbo jets in the 1970s. During these years, airlines were heavily regulated all over the world which caused the domination of government policies over technological developments, profitability, and competition. By the beginning of 1980s, the airline regulations were loosened in the USA and as a result, the industry became more competitive. The airlines had to keep up with recent innovations and take cost efficiency and operating profitability into account in a competitive environment. This era is also called the liberalization of the airline industry which eventually made the global airline industry a very dynamic and extremely competitive.

Compared to other transportation alternatives, air travel has some clear advantages such as speed, cost, and safety. Among passengers, air travel is seen as the only reasonable long distance transportation alternative. Another great advantage of air travel over other options is that it is the only way of access to some geographically remote destinations. With the help of the liberalization of the industry and economic globalization, the international and domestic air transportation industries grew drastically after 1980s. With more than 2,000 airlines operating more than 23,000 commercial aircrafts, the airline industry today serves to more than 3,700 airports (ATAG, 2008). IATA (2008) records show that there were over 29 million scheduled flights in 2007 which, in total, transported more than 2.2 billion passengers. Since 1980, the world air travel growth was around 5% per year. The change in economic conditions had a significant effect on the yearly growth rate of the aviation industry. There is a strong correlation between the growth in GDP and the industry itself. Based on historical data and economic growth expectations, a minimum of 4–5% annual growth in global air travel is anticipated over the next 10–15 years, which will almost double the industry in the given period of time (JADC, 2002).

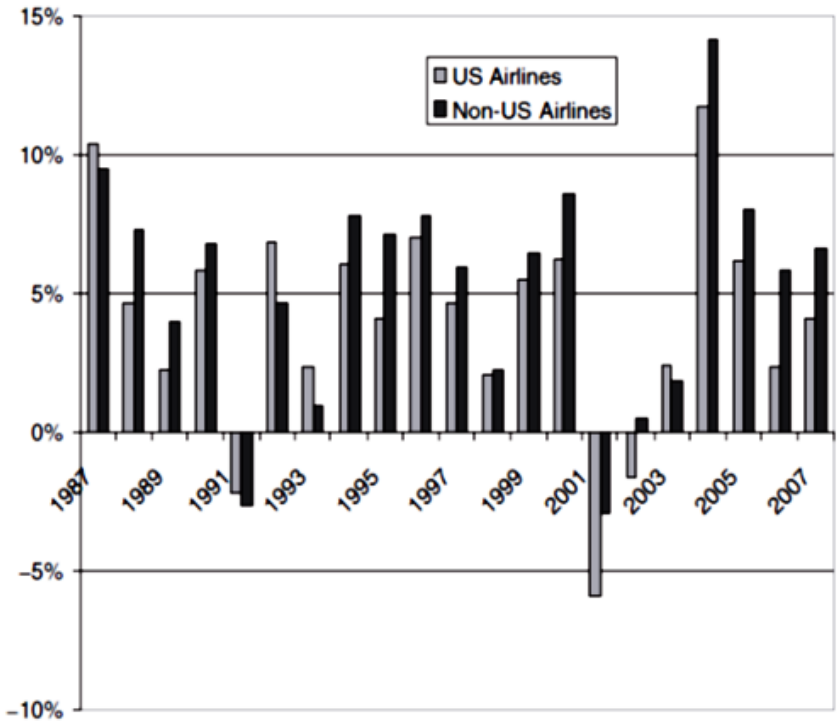

Figure 1.1: Annual RPK growth rates, 1987–2007 (ATA, 2008; ICAO, 1971–2005).

The revenue per passenger kilometers (RPK) is a method of measuring annual air traffic passenger growth rates, which is calculated by multiplying the distance traveled by the number of revenue–paying passengers aboard. The US and non–US RPK growth rates between the years of 1987 and 2007 is presented in Figure 1.1. As mentioned earlier, economic growth is the main factor affecting RPK. Within the time frame of 1987–2007, the RPK and GDP annual growth rates were around 5–6% and 2–3%, respectively. On the other hand, Figure 1.1 shows significant RPK growth rate variation in different years for both US and non–US airlines. Between 1987 and 2007, world RPK growth rate has been negative only twice. The first one, 1991, is a result of the first Gulf War and the following economic recession and fuel crisis. The second one, 2001, is an outcome of the 9/11 terrorist attacks in the US. Furthermore, Figure 1.1 demonstrates that the RPK growth rates of non–US airlines have been outpacing the US airlines with few exceptions. Consequently, the market share of US airlines has fell from 40% in 1987 to less than 32% in 2007.

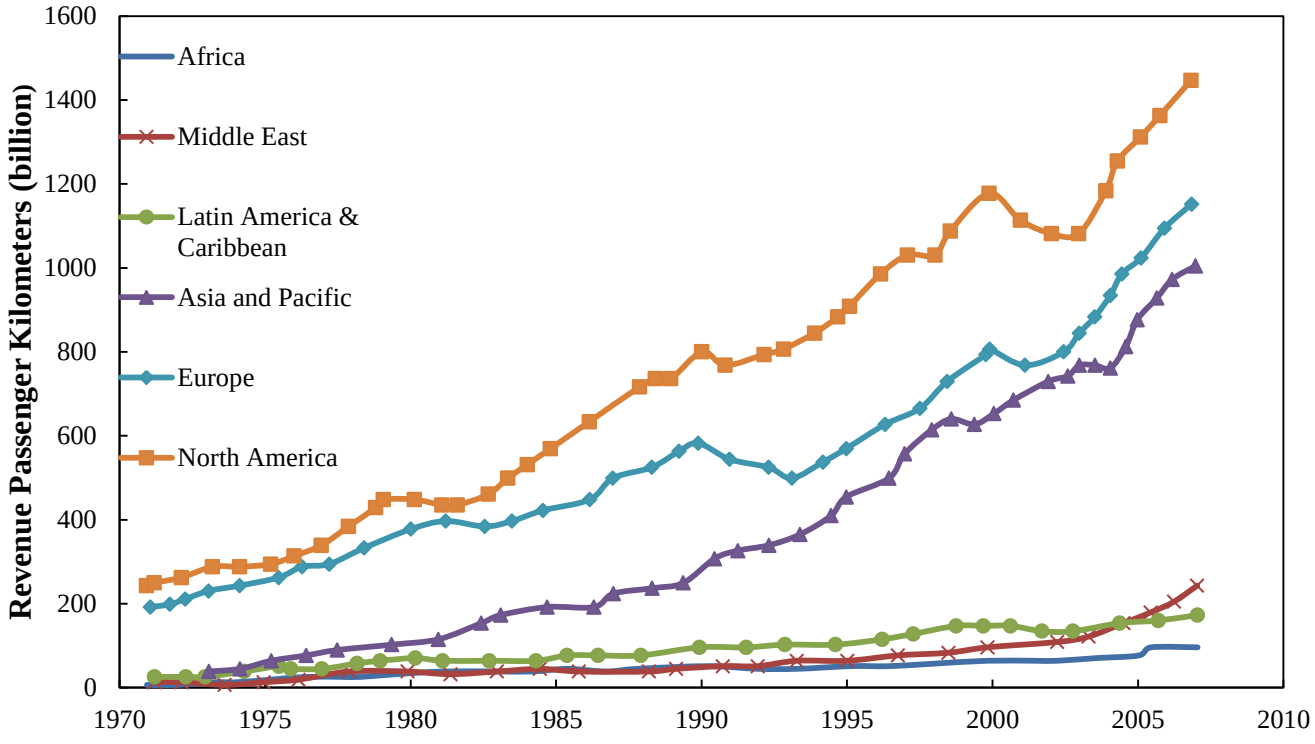

Figure 1.2: Airline passenger traffic growth by world regions (reproduced from ICAO, 1971–2005; IATA, 2007).

The comparison of world regional airline passenger traffic between 1970 and 2008 shown in Figure 1.2 indicates that North America is the leader in terms of air traffic; Europe and Asia–Pacific are the second and third ones, respectively. From Figure 1.2, it can be seen that North American airline traffic was severely affected by the post–effects of 9/11. The negative RPK growth rates of US airlines between 2001 and 2003 presented Figure 1.1 also points out this effect. As a result of its sharp and continuous increase in airline traffic, Asia–Pacific region reached Europe's level in 2007. This increase is expected to continue, therefore, Asia–Pacific region is anticipated to have the world's second largest airline traffic soon.

The sensitive nature of the airline industry makes it potentially vulnerable to possible economic and social crises. Due to its economic and social advantages and significant effect on other industries, the security of the airline industry became a global concern. Therefore, the airline industry generates considerable amount of attention from the government policy makers, the media, and a vast amount of people directly engaged to its operations. Furthermore, the growing airline passenger volume forces the authorities to ensure the safety and reliability of air travel.

1.2 Flight Physiology: Vibration in Aviation

Vibration is the physical movement or oscillation of a mechanical part according to a reference position; it can be periodic, aperiodic, or random. In periodic vibration, oscillatory motion repeats itself in a given time period (e.g. sinusoidal motion, the simplest periodic motion). Shock or transient motions are some examples of aperiodic vibration. The statistical properties are used to define random vibration; in stationary random vibration, these properties are time invariant while in non– stationary vibration, they change with time and are unpredictable.

Frequency, direction, and amplitude are used to distinguish vibration. Frequency, a critical component for a dynamic system, is defined as the number of complete cycles of motion that occurs in a unit of time, its unit Hertz (Hz) also means cycle per second. Multiple frequency components, content and/or spectrum is observed in random vibrations. In aviation, mostly

random and aperiodic vibrations happen. Amplitude is an indicator of the severity of a vibration. Amplitude can be expressed as one of the following engineering units: velocity, acceleration, and/or displacement.

The oscillatory motion generated as a result of vibration is transferred along three axes: fore–and–aft (X), lateral (Y), and vertical (Z).

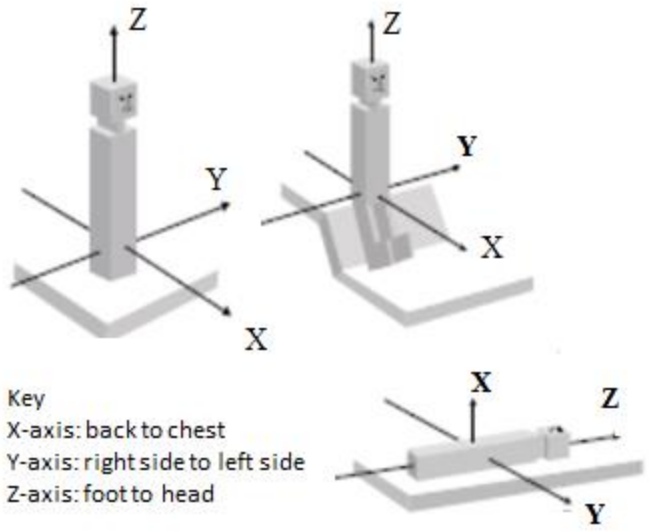

Figure 1.3: Orthogonal axes for assessment of human exposure to vibration (BS-6472, 1992)

The vibration encountered in aviation is transmitted to passengers via body contact (structure–borne) and transmission of sound pressure waves in high noise environments (air–borne). Human body is a dynamic system and it is strongly affected by both of the vibration types. Structure–borne vibration is the main concern of aircraft passengers and the crew, whereas air–borne vibration primarily affects the ground crews who are endangered by aircraft engine noise at high levels.

Aviation industry is negatively affected by vibration because it causes waste of energy, and therefore money, it is a major cause of premature component failure, and last but not least, vibration during operation causes aircraft noise which contributes to crew and passenger discomfort. Therefore, it is very important to address sources of vibration to develop potential solutions for vibration reduction.

1.2.1 Sources of Vibration in Aviation

The sources of vibration during aircraft operation can be classified as internal or external. These sources can be due to mechanical sources, weather and operating conditions, and/or thermal disturbances (Smith and Smith, 2006).

Air turbulence is one of the major vibration sources during the cruise mode of aircraft operation. Air turbulence is caused by local heating or cooling between the air and ground at altitudes below 500 m (or 1,600 ft.). Between 500 m and 10,000 m (or 33,000 ft.), weather and thermal effects contribute to air turbulence. And above 10,000 m, wind shear between moving air masses starts generating turbulence. The various interactions between the ground and air (e.g. thermal, mechanical etc.) have a potential to generate air turbulence (Guignard and King, 1972). Although it has major effects on vibration, the effect of turbulence is outpaced by another major vibration source during take–off and landing, which is road roughness and/or surface irregularities.

1.2.2 Response of Human Body to Vibration

Since human body is adversely affected by vibration, understanding and evaluating the response characteristics of the human body to vibration is extremely important to minimize these negative effects. For this reason, many studies have been conducted to determine the resonance frequency range of the human body. However, these studies have mainly focused on the vibrations in the vertical direction and they used frequency transfer functions to evaluate human resonance, see for instance Basri and Griffin, 2012; Mandapuram et al. 2012; Toward and Griffin, 2011).

One way to identify the regions with high vibration transmission due to the resonance in the body is the use of impedance. It is the ratio of the transferred force on the seat surface and the input velocity to the seat. However, impedance is a complex number and defined by the amplitude of the ratio and the phase angle between the two measurements. Peaks in this ratio of two measurements indicate the body resonance. The main impedance peaks of the human body happen between 4 and 10 Hz and they are produced due to the relative motions of the upper body. Figure 1.4 shows the axes for measuring vibration exposures of seated aircraft passengers.

Another frequency response function is transmissibility, which is defined as the ratio between the input motion measured (usually in the units of acceleration) on the subject and the measured input motion to the supporting structure (passenger seat). Transmissibility plots show peaks around 12 Hz for the head considering the vertical vibration components.

Other body parts, such as the eyes, have been reported by NASA to have a resonance frequency in the vicinity of 20 Hz which significantly affects the visual performance.

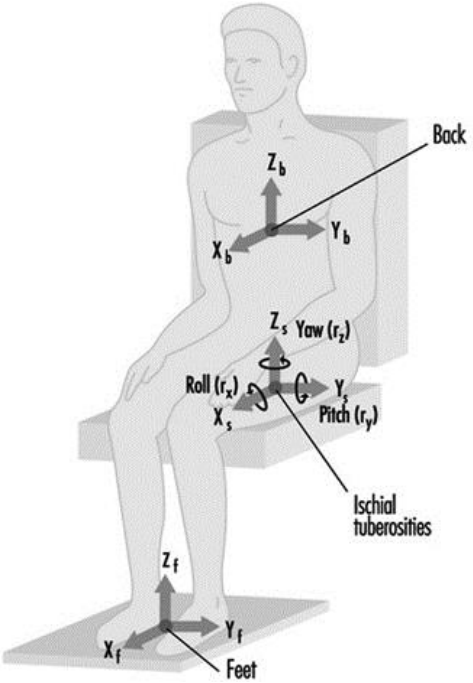

Figure 1.4: Axes for measuring vibration exposures of seated aircraft passengers (Griffin and Helmut, 2011).

Vertical vibration in the z-direction as shown in Figures 1.3 and 1.4 has been the major concern of the aviation industry.

During aircraft flight operations, the whole–body vibration is usually transmitted to passengers through the seating system. The components of the seating system, coupling with the lower and upper body, interface material, and posture have significant effects on vibration transmission.

Passive, active and semi-active suspension systems have been designed by many that are aiming the resonance frequency range (4-12) to reduce the output vibration which reaches to passengers. These systems are mainly employed for rail and ground vehicles but not for aircrafts because of the additional weight. Therefore, there is need in developing new cushion materials to that can reduced the vibration transmission in the aircrafts.

1.2.3 Human Physiological and Subjective Responses to Vibration

There is no reported injury in aviation caused by intense vibration levels. Lucky vibrations levels in aviation remain at lower levels. However, as the whole–body vibration exposure time increases, tolerance levels have been shown to decrease. Figure 1.5 demonstrates the short–time (less than a minute), one–minute and three–minute vibration exposure limits reported by healthy adult males exposed to vertical vibration (Magid, Coermann, and Ziegenrucker, 1960). The figure shows that as the exposure time increases, the tolerance amplitude of the input vibration decreases.

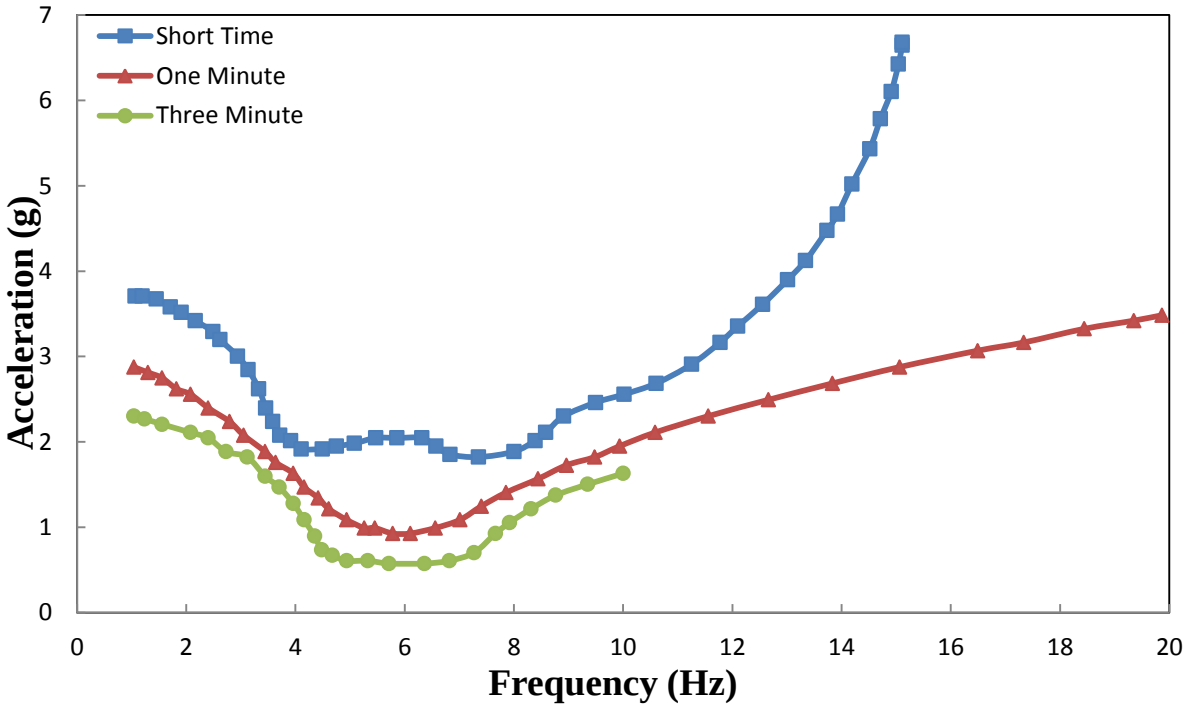

Figure 1.5: The short–time, one–minute and three–minute human whole–body tolerance limits reported during vertical sinusoidal vibration (Magid et al. 1960).

Figure 1.6 shows the most severe symptoms reported associated with 1-20 Hz (cycles per seconds) frequency range.

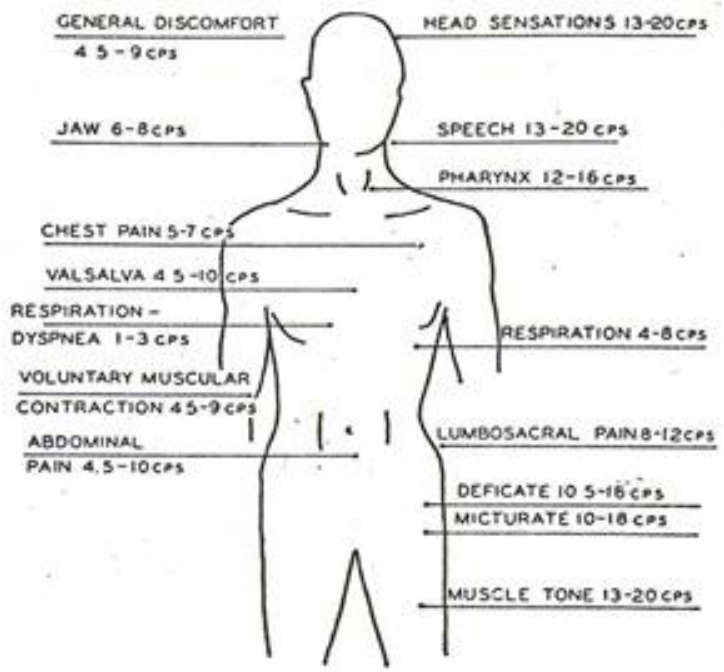

Figure 1.6: Symptoms experienced for frequencies between 1 and 20 Hz at tolerance levels (Magid et al. 1960).

The most commonly health symptoms due to the prolonged vibration exposures have been reported for back pain since the spinal column is the main path that vibration propagates through. However, the sitting posture makes it very difficult to determine which vibration causes to these symptoms (Pope et al. 1983).

1.2.4 Whole-Body Vibration Exposure Standards

Whole–body vibration standards have been developed based on laboratory and field experiments, to provide guidelines for vibration exposure assessments and its effects. The International Organization for Standardization (ISO) offers the ISO 2631–1: 1997 entitled "Mechanical vibration and shock: Evaluation of human exposure to whole–body vibration, Part 1: General

requirements". The document, which is widely used, describes procedures for evaluating whole–body vibration. Additional annexes are provided to inform on possible effects of vibration on comfort perception. The American National Standards Institute (ANSI) acknowledged the ISO 2631–1: 1997 in 2002. The ISO 2631–1: 1997 suggests that accelerations should be measured in the three orthogonal directions (X, Y, and Z) relative to the seated or standing individual (see Figures 1.3 and 1.4).

The standard also suggests that, if the vibration is in multiple directions, first the multiplying factors are applied and then vector sum or the vibration total value (VTV) is obtained based on the rms acceleration values which are in the second order. Moreover, to emphasise the importance of these standards, based on the forth order of weighted functions vibration does values (VDV) are also provided which are more sensitive to the peaks in the exposure.

The American Conference of Governmental Industrial Hygienists (ACGIH, 2002) provides regulations on human vibration exposure due to the interaction with the structures, although its main focus is heavy vehicles. Threshold limit values (TLVs) for the vertical and horizontal axes are defined by calculating weighted rms accelerations through the curves that are time and frequency dependent. The threshold limit value (TLV) describes the limit that most workers may be exposed repetitively with minimum risk of health. However, the ACGIH highlights that the TLVs can only be used for monitoring vibration exposure but not for describing the limits between safe and harmful vibration levels.

Since 2002, The European Union has also established its human vibration standard (Directive 2002/44/EC). Most of these standards are based on ISO guidelines of vibration exposure assessments.

1.2.5 Vibration Mitigation

There are two ways to reduce to vibration transmission or human vibration exposure. It can either be eliminated at the source or be reduced by providing better isolation. However, eliminating the vibration at the source is very difficult and can be highly priced, providing better isolation to reduce the vibration transmissibility seems more practical.

Present methods for providing better isolation and damping to reduce the vibration transmissibility are widely used to reduce high frequency vibration components. However, these methods are not successful in minimizing the low frequency components and since, the low frequency vibrations are more effective for the human body, improving seat comfort still remains a challenge. On the other hand, some seat components, such as seat cushion, that are not adversely affecting vibration transmissibility can change the comfort significantly.

The effect of low frequency vibration components that cause the most discomfort can be reduced by providing rigid coupling between the body and contact surface to prevent repetitive impact, whereas high frequency vibration components can be prevented by removing the contact between seat and body.

1.3 Aircraft Seat Design

Designing aircraft seats is challenging because of the weight and complex geometry of the seats. Generally an aircraft passenger seat consists of the assembly of the three main parts, such as seat base, seat track and seat backrest. In additional to those parts head, leg and arm rests features are attached to provide support to body parts. All these components are designed such that the factors effecting the comfort and safety of the passenger should be minimized. Therefore designing the aircraft seats requires good knowledge of comfort related factors and materials.

In other words, design requirements of the aircraft seats can be summarized in three categories; demands of the customer, expectations of the manufacturer and regulatory legislations. Customer demands contain comfort of the seat and its ergonomics. On the other hand manufacturer expects a seat design that is reliable and cost effective and regulatory legislations cover passengers safety.

The General Aviation Safety Panel (GASP) defined candidate seat dynamic performance standards using the impulse, impact pulse duration, and velocity change data obtained from NASA general aviation full–scale impact tests (Soltis and Nissley, 1990). In 1983, the National Transportation Safety Board (NTSB) conducted a comprehensive study on general aviation dynamic seat characteristics. The NTSB study defined impact survivability limits in the form of vertical and longitudinal velocity change envelope. The GASP candidate seat dynamic performance standards fell within these envelopes further confirmed that they represent survivability impact conditions. The seat dynamic performance standards were defined with the intent to represent general aviation aircraft limits. The proposed performance criteria evaluate the occupant/seat protection system's potential for preventing or minimizing injuries from both primary and secondary impacts and from other occupant skeleton loads (Soltis and Nissley, 1990).

Above mentioned parameters make the design and certification of an aircraft seat very complex and costly. Therefore, to provide a solution for this complexity, computer aided modelling and analysis has become very popular.

Simulating the dynamic characteristics and behaviors of seating systems using computer simulations is a very cost efficient way. Advanced simulation software and tools provide analysis even for complex structures. Consequently, finite element analysis (FEA) method has become well known and reliable design tool to analyze the dynamic behavior of the aircraft seats.

Additionally, the Federal Aviation Administration (FAA) is cooperating with aircraft industries to make FEA a reliable certification tool to even more reduce the seat development cost.

1.4 Scope of This Study

The scope of this study is the development of a methodological approach to assess the dynamic aircraft seat suspension characteristics more economically and with certainty. The main objective of this study is to provide a methodology of computer simulation for aircraft seat certification by comparing experimental results and FEA. The goals of this study can be summarized as:

- To determine whether or not the actual flight conditions can be replicated in laboratory scale
- To develop a finite element model that can perform as close as possible to experiments
- To investigate the effect of weight and static cushion properties in dynamic seat comfort
- To measure the overall seat comfort in dynamic environments during take–off, cruise, and landing

The focus of this research is to develop a simulation methodology for aircraft passenger seats. For this purpose the basic functional, structural, and other design requirements such as comfort for aircraft seats are discussed. This study briefly explains most commonly used finite element analysis applications. Practical challenges in aircraft seat simulation in different areas such as modeling techniques, material properties, manufacturing limitation etc. are discussed.

At the end, three flight conditions are discussed: take–off, landing, and cruise through turbulence. And validation results are presented for these flight conditions.

Chapter 2

Literature Review

As explained in the previous chapter, passengers use airplanes every day and comfort is one of the most important factors in flight satisfaction. Whether it is leg room or cushioning on the seats, passengers ideally would want a comfortable ride for the duration of their flight. Comfort is a relative subject that should be evaluated from a physical point of view. In that sense, seat comfort can be divided into two categories; static comfort and dynamic comfort, Ebe and Griffin (2000), and Shen and Vertiz (1997). Static comfort represents the comfort evaluations depending on the pleasance it produces on subjects, excluding external factors such as vibration, whereas, dynamic comfort deals with the overall seat comfort including external forces and their effect on comfort for subjects. However, a seat that is comfortable in a non-moving vehicle and/or aircraft may have poor dynamic characteristics that make it uncomfortable when the vehicle and/or the aircraft are moving. Moreover, comfort is primarily felt by the human body during a dynamic process rather than a static one (Yousof, 2005).

Unfortunately, dynamic seat comfort in aircrafts has merely been the subject of researchers in the literature therefore there is no significant prove on how it should be evaluated or improved. On the other hand, seat comfort has been extensively investigated especially for heavy vehicle operators since they are exposed to high intensity of vibrations for long periods thus, generating a high risk of health issues. Therefore, evaluation of dynamic seat comfort plays a key role for setting the limits that an operator/passenger can be exposed and for improving the seat comfort.

Here the measurements and developments towards dynamic seat comfort for vehicles are first discussed and then the factors affecting the dynamic seat comfort covered.

2.1 Dynamic Seat Comfort in Heavy Vehicles: Measurements and Developments

Studies that dealt with whole-body vibration, executed laboratory or field studies, and dealt with human studies are included in this review. Figure 2.1 describes the method approached by these studies. The reviewed studies are divided into three sections. Each section reviews the studies depending on their aim. It is set 3 aims that can be undertaken to improve ride comfort for heavy vehicle drivers and prevent any fatigue risk. Some studies are aiming to reduce the vibration reaches to driver by improving the suspension system of the seat whereas others try to prevent this by improving the suspension system of the vehicle itself so that vibration input to the driver's seat would be less. Also, few studies investigated to reduce this effect by changing the tire characteristics.

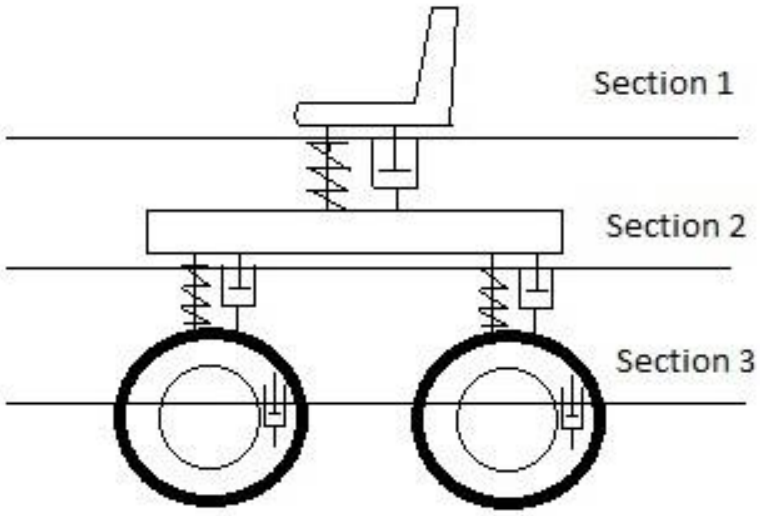

Figure 2.1: Segments of suspension control employed by various studies.

2.1.1 Improvements towards Seat Design

As mentioned previously, one of the three ways to reduce the WBV exposure and risk of any health issues is to develop better seats so that these issues can be prevented. However, improving the seat design to attenuate the vibration is not very easy because they are initially designed as good as possible since the heavy vehicle operators are exposed to high intensity of vibrations during operation. Most of the seats designed with a passive suspension system under the seat where the seat interacts with the vehicle cabin.

One of the early studies in improving the seat design was conducted by Patil and Palanichamy (1988). The mathematical model they introduced for tractor occupant system with a new suspension structure provided good correlation with experimental results. Their introduced seat suspension system is reported to reduce the maximum body amplitude ratio response, acceleration intensity level, transient amplitude, relative amplitude between nearby body parts and pitch response of the chassis, therefore providing highly increased comfort level for tractor drivers.

Boileau and Rakheja (1990) conducted laboratory and field experiments on four existing different types of agricultural vehicle seats. Their comparison based on acceleration transmission revealed the clear advantages of air suspension seat design over mechanical alternatives, especially in terms of vibration attenuation. In the contrary, Wilder et al. (1994) reported that in some situations mechanical seat suspensions provided less transmissibility over pneumatic suspensions. They compared the gas (pneumatic) spring systems to conventional spring systems. Moreover, they also included the effect of sitting posture in vibration transmissibility. While comparing two spring systems, they run each experiment for upright, full back and leaning forward positions. From the experiments they performed, vibration transmissibility in the vertical direction between baseplate and seat pan, gas spring system resulted with less transmissibility for upright and forward positions. However, while sitting with full contact with backrest, standard spring system showed less transmissibility comparing to gas spring system.

Hostens and Ramon (2003) performed a field experiment with a combine at 20km/h to obtain data to be used in the laboratorial studies. For their study, they compared mechanical seat suspension and air suspended seat. For overall comfort judgements, Seat Effective Apmlitude Transmissibility (S.E.A.T.) values are calculated as 77.5% and 63% for mechanical suspension and air suspension seats respectively. Figure 2.2 shows the comparison between input and output signals of mechanical and air suspension systems. It is clear from the figure that output of the air suspension is significantly lower than mechanical suspension.

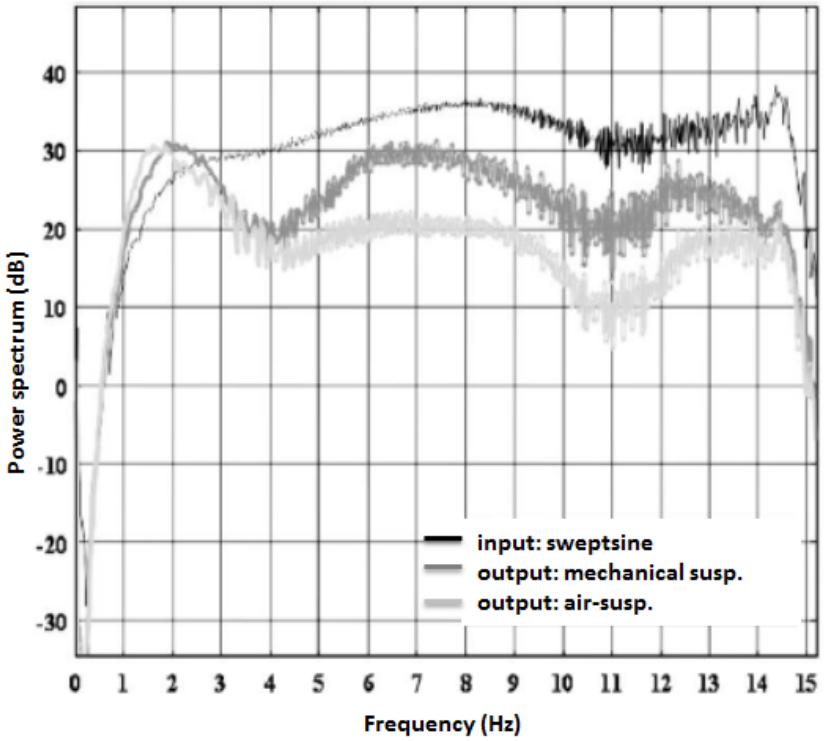

Figure 2.2: Power spectrum comparisons of input and outputs from two different suspensions (Hostens and Ramon, 2003).

A more recent study by Hostens et al. (2004) introduced a new improved passive suspension system. Since agricultural vehicle operators are exposed to high excitation in the range of 1.5-5 Hz and usually the existing seats have natural frequency in this range, their goal was to reduce the resonance frequency. They achieved this with adding extra air volume and variable air damping to a pneumatic seat suspension. Moreover, they provided S.E.A.T. values comparison between high and low tire pressures for different surface and speeds as shown in Figure 2.3.

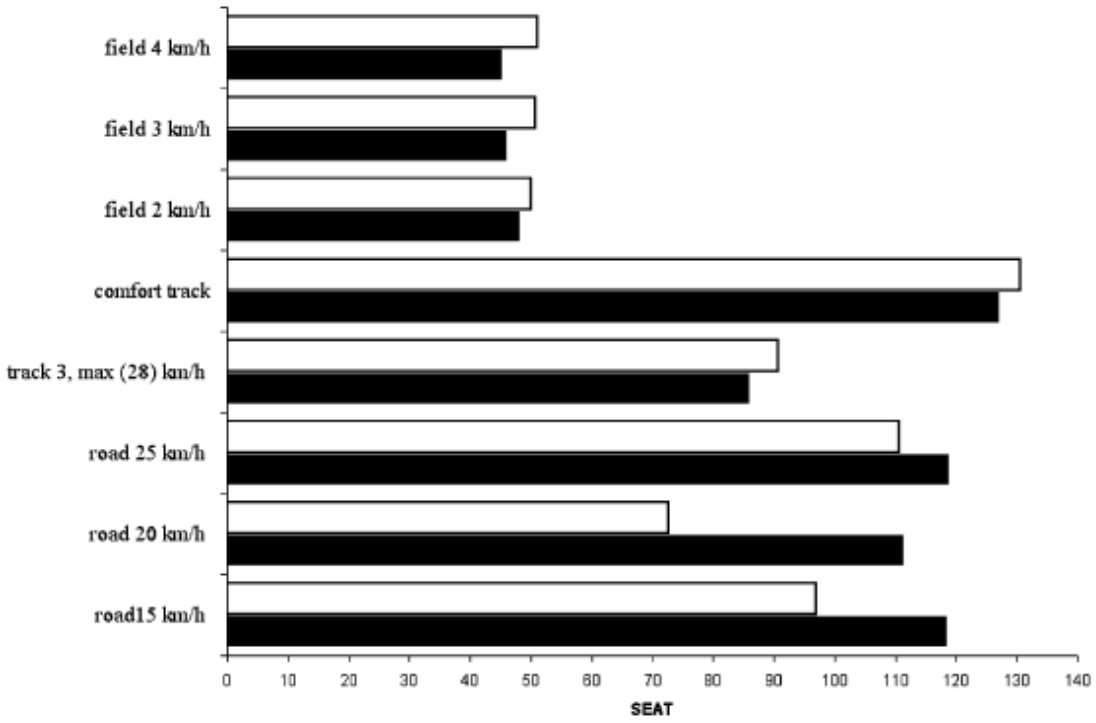

Figure 2.3: Calculated S.E.A.T. values for different forward speeds and low (white) and high (black) tire pressure (Hostens et al., 2004).

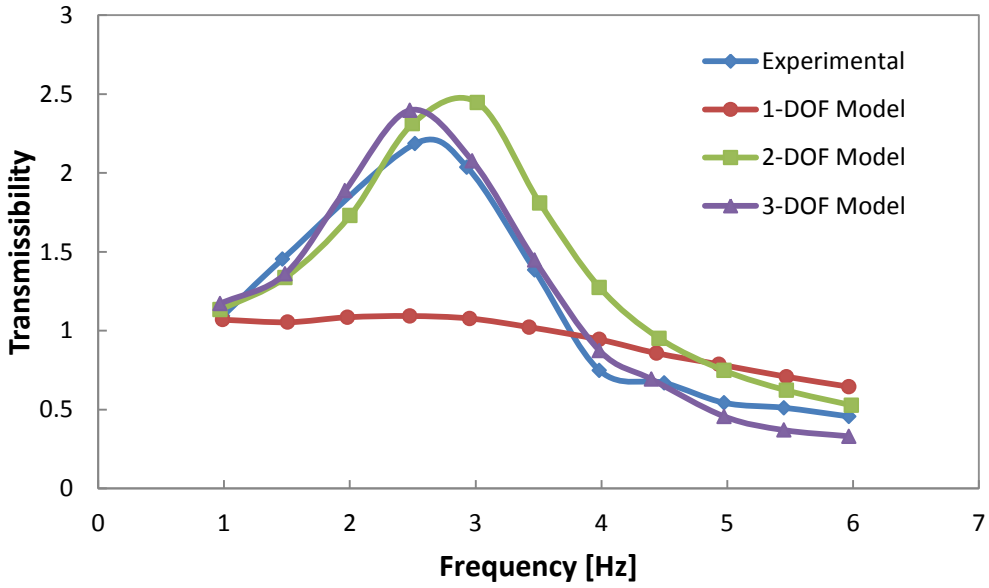

Figure 2.4: Comparison of analytical and experimental acceleration transmissibility of seat suspension (reproduced from Tewari and Prasad (1999)).

Tewari and Prasad (1999) developed a 3–DOF model for computer simulation and compared its accuracy to experimental results in terms of transmissibility. Along with their model they also compared, as shown in Figure 2.4, a 1–DOF and 2–DOF system from published studies by Verma (1970) and Gouw et al. (1990), respectively.

Tewari and Prasad (1999) also investigated the effect of spring constant, damping and operator's mass in transmissibility. They compared three different operator mass along with three different spring and damping constants. Their results indicated that as the spring constant and mass of the operator increases transmissibility is increased as well. However, an opposite trend for damping constant is observed. If the damping constant increases the transmissibility reduces.

2.1.2 Developments towards Cabin Suspension

Agricultural vehicle operators are being exposed to high intensity vibration levels that cause severe health issues such as low back pain (LBP) and intestinal disorders, von Gierke (1979). Therefore, many studies have investigated the reduction of whole-body vibration exposure in agricultural and heavy vehicles by decreasing input vibration to vehicle cabin. WBV and any impact or damage it might cause, can be controlled and minimized by absorbing some of the vibration energy. Vibration damping is one of the most efficient, and therefore heavily used, WBV reduction techniques that decrease some of the vibration effect by changing how fast or slow energy oscillates. The comparative simulation, lab and field experimentation study conducted by Matthews (1966) demonstrated the advantages of hydraulic cylinder damping in the agricultural vehicles suspension system in terms of average acceleration amplitude and order of ride vibration attenuation. Elmadany and Abduljabbar (1990) demonstrated a clear comparison between passive, semi-active and actively suspended cabin of truck. Moreover, they combined the actively damped system with load levelers and included in the comparison as shown in Figure 2.5. It is clear from this figure that the introduced combine system resulted with significant low acceleration outputs.

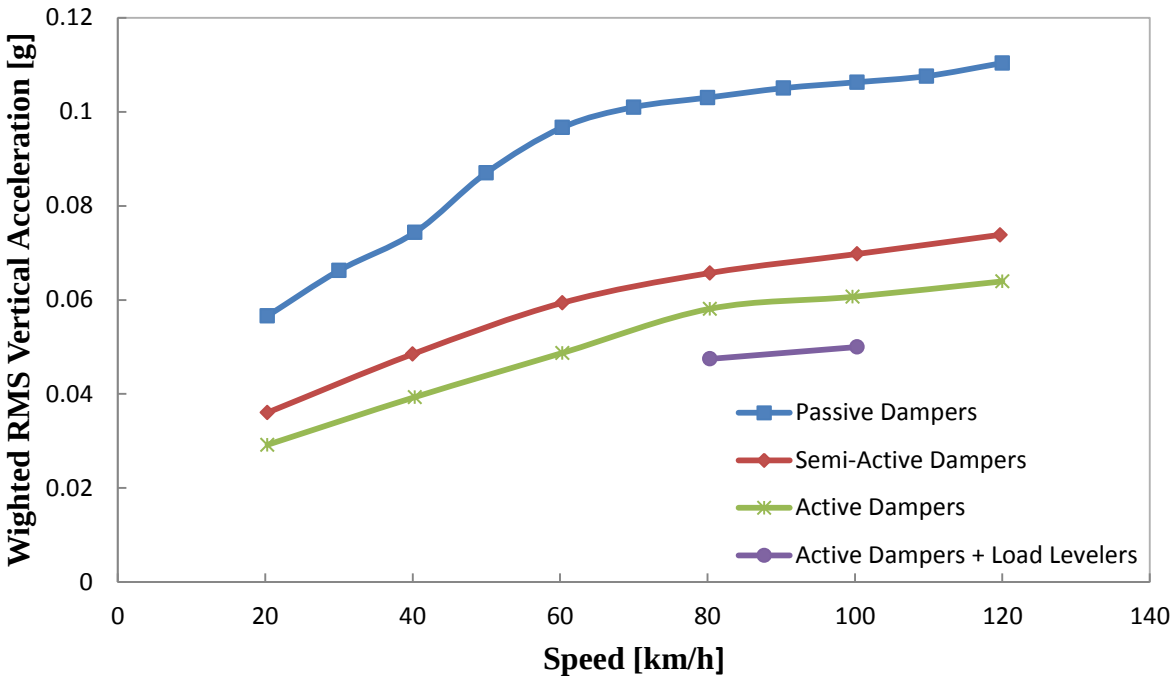

Figure 2.5: Comparison of weighted rms cabin vertical acceleration of passively, actively and semi–actively suspended cabin (reproduced from Elmadany and Abduljabbar (1990)).

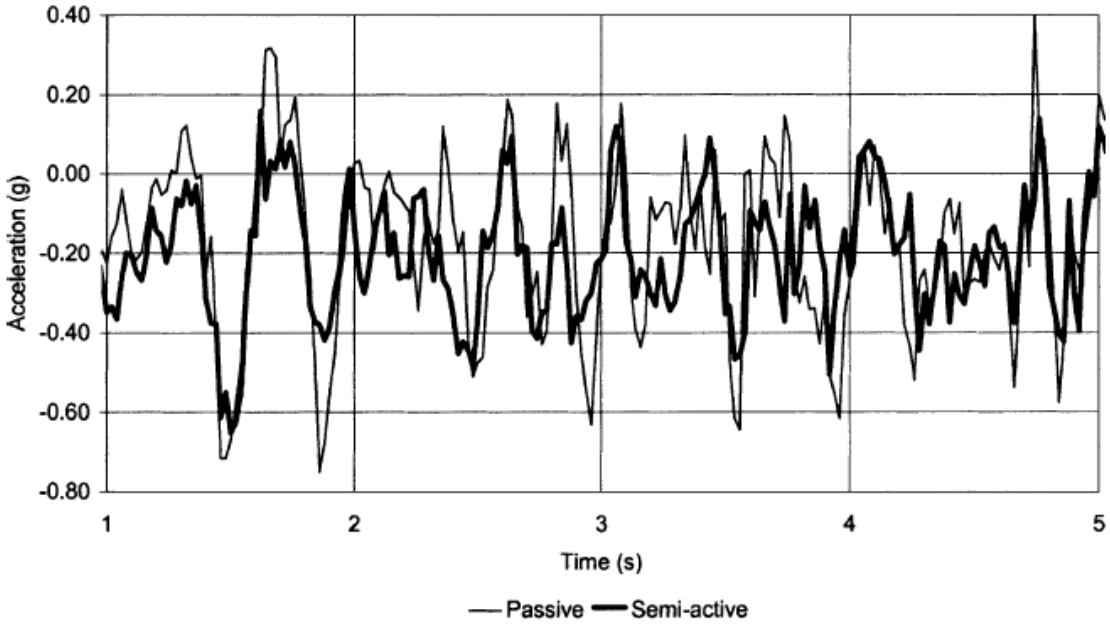

Figure 2.6: Reduction in the vertical acceleration using the developed semi-active suspension system (Nell and Steyn, 2003).

Els et al. (2007) reported that good ride comfort and good handling for agricultural vehicles require completely different characteristics in terms of spring and damping constants of the vehicle suspension. Therefore, the suspension system should be capable of switching between two cases depending on the road roughness. Using a twin accumulator hydro-pneumatic spring combined with an on-off semi-active hydraulic damper can help eliminate this problem based on the idea developed by Eberle and Steele (1975). Nell and Steyn (2003) have developed a semi–active suspension system that keeps the handling characteristics unaffected while providing a more comfortable ride. The reduction in the vertical acceleration is shown in Figure 2.6.

Similarly, Ieluzzi et al. (2006) developed a semi-active suspension control system for a heavy truck. The semi-active suspension system reduced acceleration values by 17% as shown in Figure 2.7 while unchanging the handling characteristics of the truck.

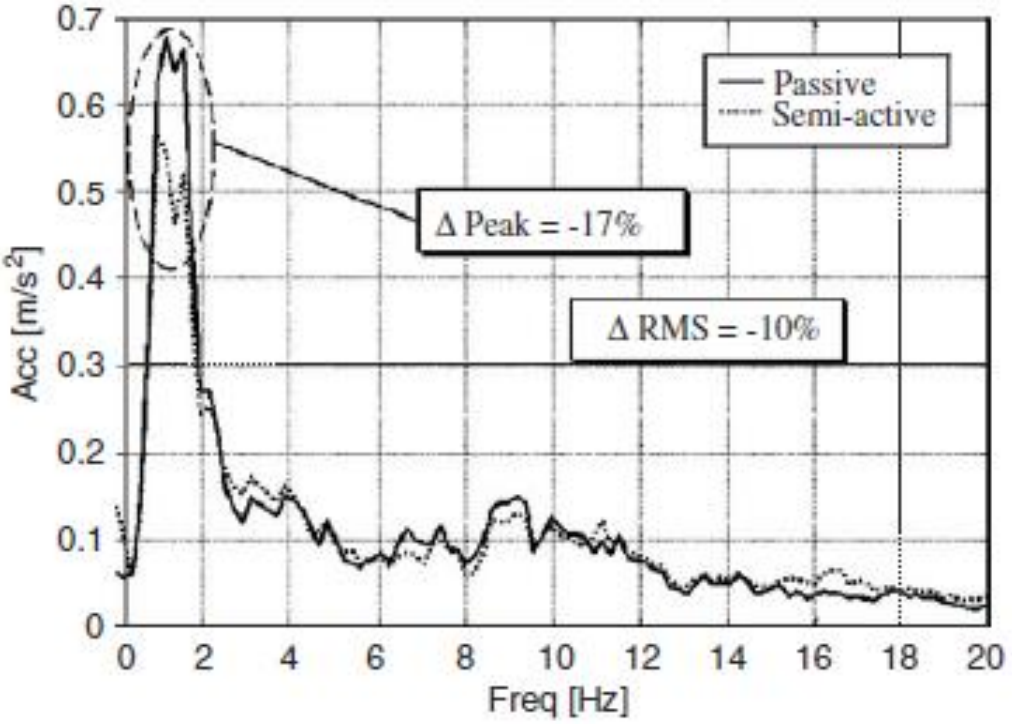

Figure 2.7: Experimental performance on uneven road (Ieluzzi et al., 2006).

Uys et al. (2007) conducted an investigation to determine the spring and damper settings that will result with optimal ride comfort of an off-road vehicle, on different tracks and at different

speeds. These settings were required for the design of a four stage semi-active hydro-pneumatic spring damper suspension system. They reported that optimal ride comfort suspension settings depend on road's roughness and speed of the vehicle.

Zehsaz et al. (2011) focused on the reduction of agricultural vehicle vibration transmission caused by road roughness. From the measurements taken in the tractor cabin, FE model and the dynamic model developed they have optimized the vehicle suspension parameters and they compared them to un-optimized result as shown in Figure 2.8. It is concluded that with the optimized parameters, dynamic comfort was increased and risk of fatigue was reduced.

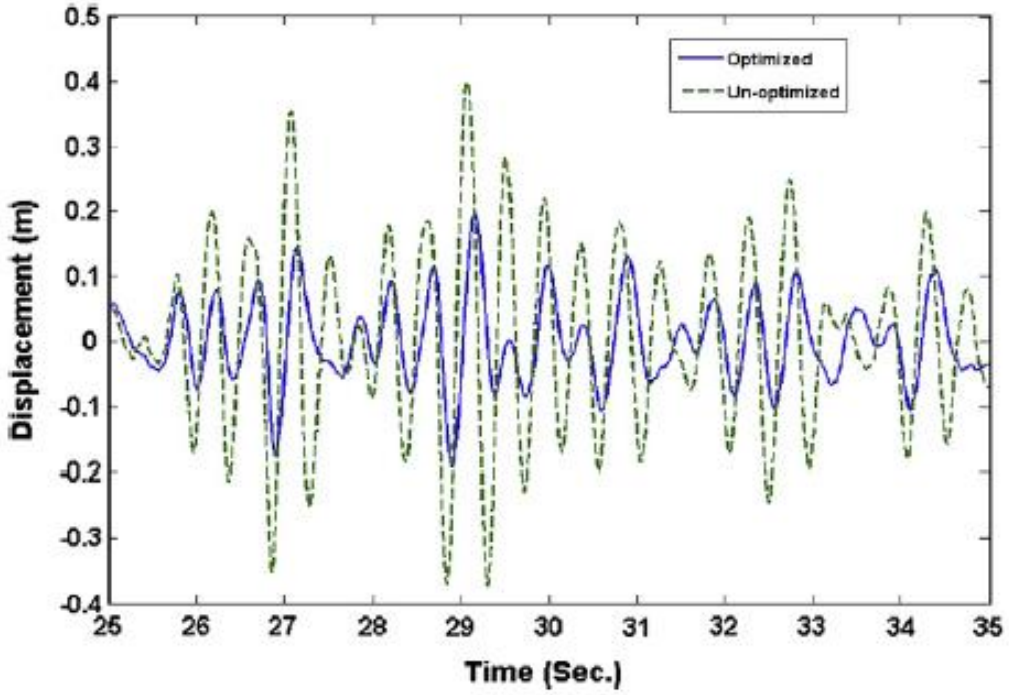

Figure 2.8: Displacement of the interior cabin with optimized and un-optimized suspension system (Zehsaz et al., 2011).

2.1.3 Effect of Tire Pressure and Type on Vibration Transmissibility

As the tires behave like suspensions, effects of tire characteristics have been also investigated to reduce the vibration transmission to vehicle cabin and eventually to occupant. However this

effect might be depended on the speed of the vehicle or road roughness. Sherwin et al. (2004) investigated the effect of tire pressure on transmissibility at different pressure levels (414 kPa, 345 kPa, 138 kPa). They calculated the transmissibility and tires with lower pressure produce less transmissibility as shown in Figure 2.9. However, they did not mention what are the limitations to reduce the tire pressure. Moreover, they calculated the transmissibility using the ratio of the cabin chassis accelerations to seat accelerations. But, the transmissibility curves are calculated by many using the ratio of the output acceleration to input acceleration.

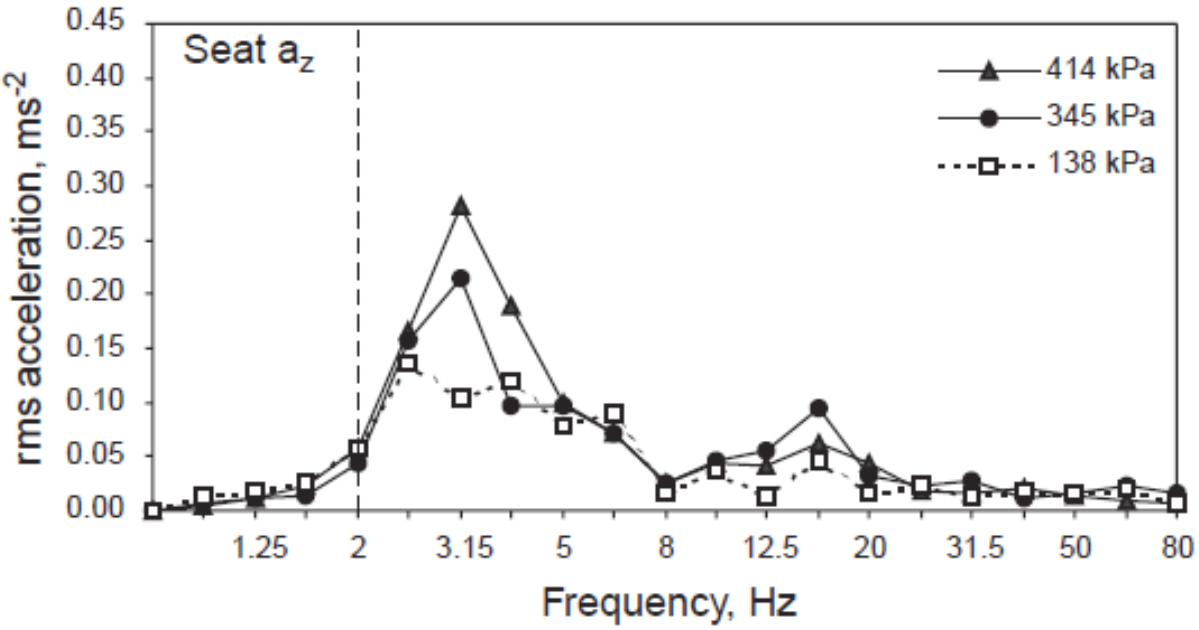

Figure 2.9: Collected data for different tire inflations (Sherwin et al., 2004).

Depending on the work, some environments may have slippery surface or consist of sands. In that case, heavy duty vehicles such as caterpillars may require additional chains on the tire to provide friction. Consequently, the chains around the tires will definitely affect the riding comfort. Blood et al. (2012) discussed the effect that additional chains have on tires. They compared ladder chains and basket chains to tires without chains for different tasks, specifically plowing, scooping and dumping. They concluded that ladder chains cause the most vibration exposure over basket chains. Blood et al. (2012) also reported that ladder chains exceeded WBV limits recommended by ISO–2631–1 for the front-end loader operator's thus, increased risk for LBP issues for operators. In the contrary, Malchaire et al. (1996) reported that the type of tire

does not significantly affect vibration magnitude on the cabin therefore on the seat surface as well. However, they have also found that high tire pressure tends to increase vibration magnitude which agrees with the finding of Sherwin et al. (2004) and Hostens et al. (2004).

2.1.4 Reported Improvements

Some of the improvements that are achieved by various studies are summarized in Figure 2.10. However, since it is not practical for all studies to have same output values, Figure 2.10 only indicates the improvements that were achieved in specific outcome values employed by different studies. Table 2.1 show the outcome measurements employed for each study that are presented in Figure 2.10.

Table 2.1: Outcome measurement units employed for different studies.

References	Outcome Measurements
Elmandy and Abduljabbar (1990)	a_{rms} [m/s^2]
Sherwin et al. (2004)	a_{rms} [m/s^2]
Deprez et al. (2005)	VDV [$m/s^{1.75}$]
Zehsaz et al. (2001)	a_{rms} [m/s^2]
Wilder et al. (1994)	a_{rms} [m/s^2]
Ieluzzi et al. (2006)	a [m/s^2]
Sankar and Alfonso (1993)	PSD [$(m/s^2)^2$/Hz]
Nell and Steyn (2003)	VDV [$m/s^{1.75}$]
Uys et al. (2007)	a_{rms} [m/s^2]

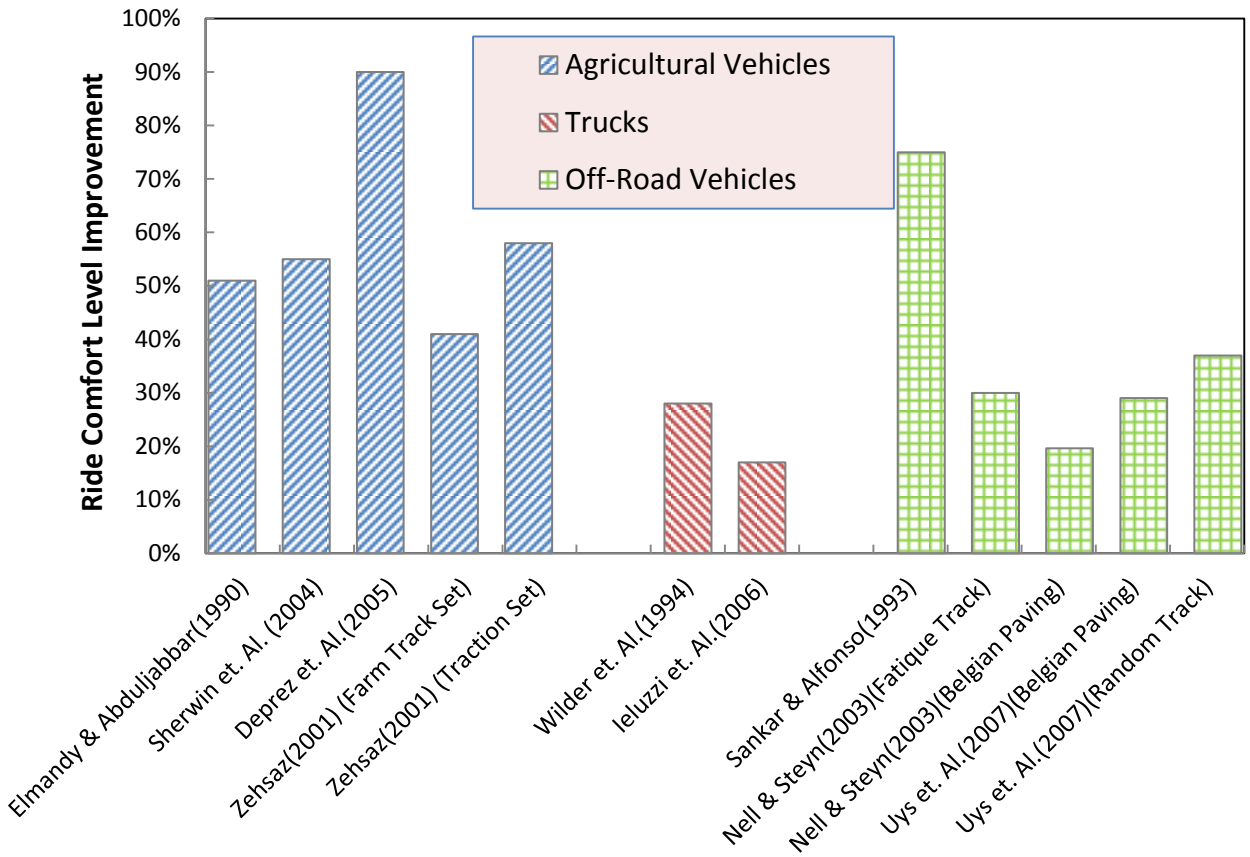

Figure 2.10: Comparison of ride comfort level improvements (by percentage) of selected studies.

Since the focus of the current study is to characterize and improve seat comfort, the following section is a review of the development work in the literature that only dealt with seat even in passenger vehicles.

2.2 Factors Effecting Seat Transmissibility

As vibration transmitted through the seat and its perception are dependent on the input location of vibration, the occupant and the characteristics of the seat (e.g. cushion properties and backrest position) it is very difficult to measure. Although vibration transmitted through the seat is difficult to measure, it is possible to evaluate seats depending on their discomfort created on occupants due to vibration.

2.2.1 Seat Characteristics

It seems that seat characteristics have more significant impact on the transmission of the vertical vibration than the occupant or the input location of vibration (Corbridge, 1989). Corbridge (1989) discussed influencing factors of seat, occupant and vibration on seat transmissibility and the effect of seat transmissibility on vehicle ride for railway vehicles. Moreover, comparison of seat transfer function in the vehicle and laboratory results was performed. Results indicate that the most effective factor of vibration transmissibility is seat characteristics. Performed experiments with ten different seat cushions resulted with significant difference in ride comforts as shown in Figure 2.11.The second influencing factor appears to be occupant's physical characteristics, specifically posture of upper body as they compared three different sitting postures in Figure 2.12. The least influencing factors stated as the factors associated with the vibration input.

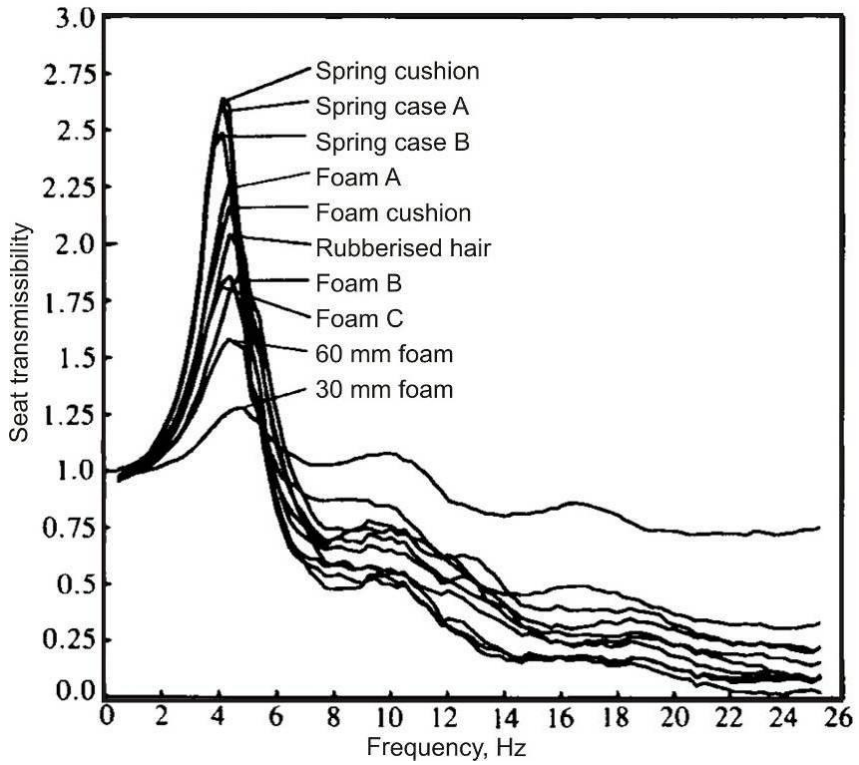

Figure 2.11: Vertical vibration transmissibility for 10 different cushions for railway passenger seat (Corbridge et al., 1989).

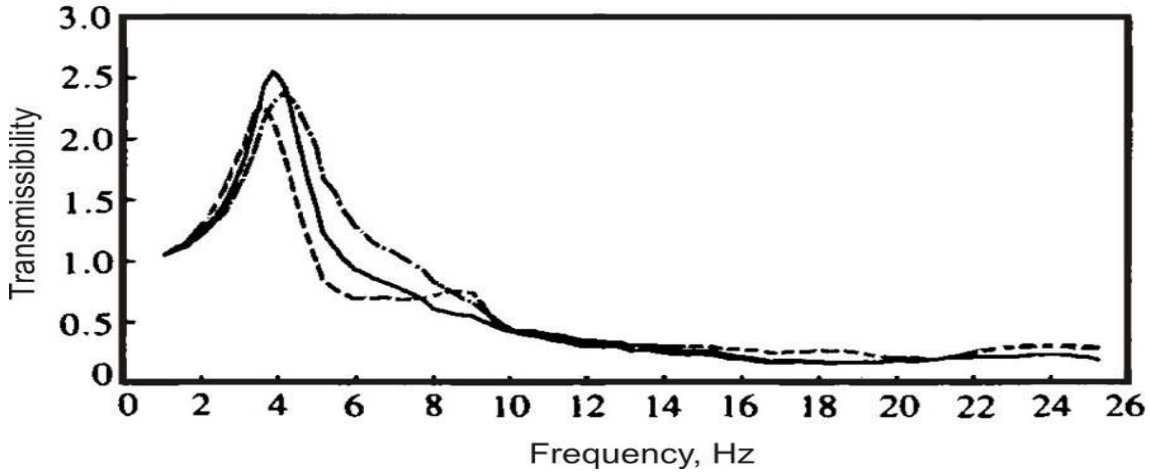

Figure 2.12: Effect of posture on the transmission of vibration through a train seat. Mean of 30 subjects (15 male, 15 female) with 0.6 ms–2 r.m.s. random vibration: ——— normal (with backrest, hands in lap); — • — • — • arms on armrests (with backrest); and - - - - back-off (hands in lap) (Corbridge et al., 1989).

Ebe and Griffin (2001) investigated the effects of static seat properties to provide clear understanding of static seat comfort (without vibration) using Scheffe's method of paired comparison. This method was applied to different cushions with the same foam hardness but different foam compositions and the comfort of each foam was classified by the gradient of force-deflection curve. Therefore, a linear relationship between the sample stiffness (gradient of force-deflection curve) and seat comfort was presented. However, a similar comfort evaluation of different foams of same composition with different stiffness was conducted and results indicate that the relationship between seat comfort and foam stiffness was nonlinear. Additionally, it is reported that comfort feeling due to cushion may be affected by two factors; bottoming and foam hardness. Figure 2.13 shows the effectiveness of two factors (foam hardness and bottoming) with the change of sample stiffness. If sample stiffness increases bottoming feeling becomes the dominant factor in judgment of seat comfort while high sample stiffness causes foam hardness to be decisive.

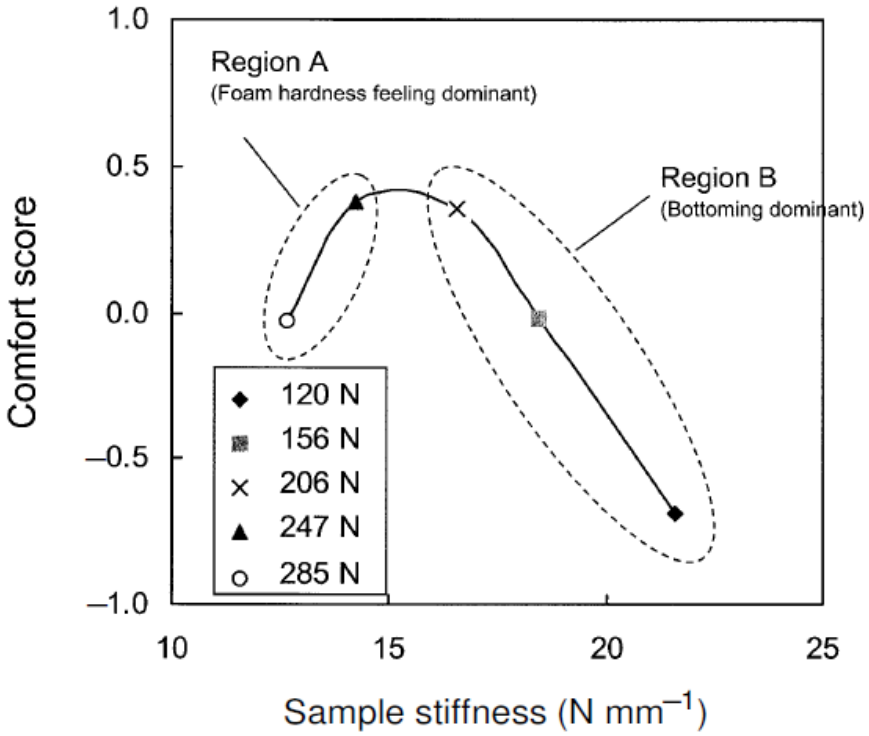

Figure 2.13: Factors affecting comfort score (Ebe and Griffin, 2001).

One may think that seat cover may have an influence on seat comfort however, Corbridge and Griffin (1989) have performed their experiments on a train seat with the seat cover and without it. There was not noteworthy difference in the transmissibility of vibration.

White et al. (2000) discussed the dynamic behavior of 3 inch cube of foam material at different pressure levels. It is proposed that an increase in compression level from 30 to 40 and 50%, results in a decrease in the resonance frequency as the vibration magnitude was increased from 0.1g to 0.25g.

2.2.2 Sitting Posture

Although static seat comfort seems to be affected mostly by the characteristics of the cushion, sitting posture is also very important factor that affects the comfort directly and even plays a role in dynamic conditions. In the literature, sitting posture is taken into account for measuring the

discomfort due to vibration and its transmissibility. Hence, the shape and the slope of the seats should also be considered as an influencing factor because, those properties (shape and slope of the seat) play significant role in sitting posture.

Discomfort is described as the unpleasant feeling in human body due to muscle tension or spinal pressure. For travelling occupants seat backrest angle is the most significant factor that affects the spinal pressure. As the backrest becomes closer to horizontal state the pressure on spinal discs reduces.

Since position of the backrest shapes the human posture while sitting, the importance of the backrest in whole-body vertical vibration has been investigated by Basri and Griffin (2012). They examined the variable discomfort due to backrest position with an inclined backrest at 0°, 30°, 60°, 90° and without backrest. Moreover, where many studies predict the whole-body vibration assuming same vibration frequency, Basri and Griffin (2012) performed experiments at different frequencies (from 1 to 20 Hz at 0.2 to 2.0 m s -2 r.m.s.). The following remarks can be drawn from this study:

- At frequencies greater than 8 Hz, to cause same discomfort with backrest lower vibration magnitude is required comparing to seats without backrest.
- Backrest causes change in apparent mass depending on frequency. If the frequency of vibration is greater than principal resonance frequency apparent mass increases, otherwise decreases.

Standards such as BS 6841 and ISO 2631–1 can lead us to measure the transmissibility of vibration through the seat and whole-body vibration exposure, however, these standards consider the backrest position either upright (90°) or fully horizontal (0°), Paddan et al. (2012). In that sense, effect of the backrest position should also be considered in inclined backrest positions as they are most commonly appear.

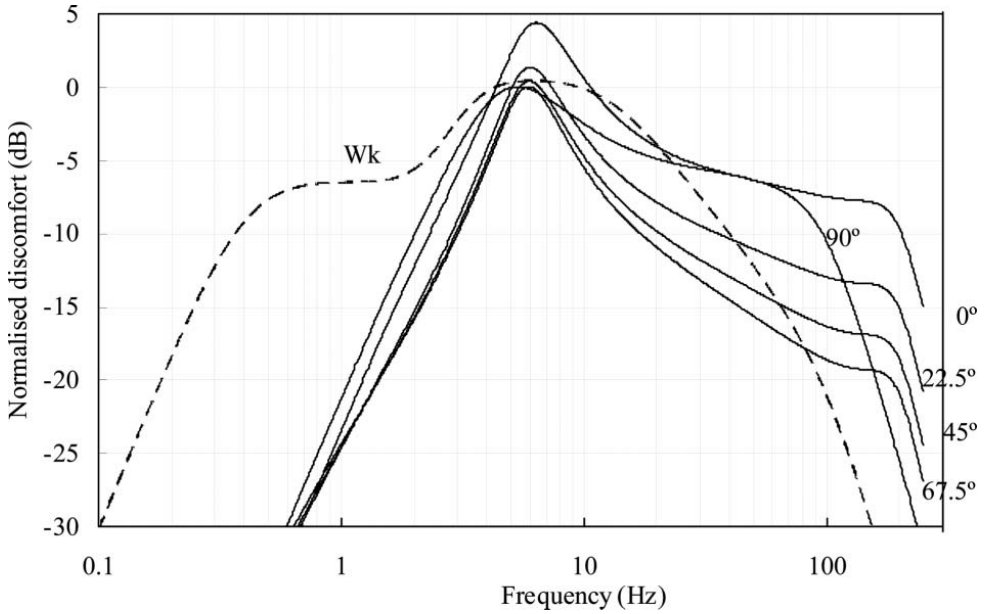

Figure 2.14: New weighting frequency curves at different backrest angles and current ISO 2631–1 curve (Wk. for z–direction) (Paddan et al., 2012).

Paddan et al. (2012) have also investigated the transmissibility of vibration and its human perception for inclined backrest positions (67.5°, 45° and 22.5°) and presented a new set of frequency weighting curves. The study was conducted in two main parts. Aim of the first part is to compare effect of vibration frequency in perceived comfort at different backrest angles. The second part aims to investigate the effect of backrest angle at a certain vibration frequency (8 Hz). Data obtained from the experiments provided new frequency weighting curves (see Figure 2.14). It is concluded that as the angle of backrest becomes closer to recumbent position, perceived discomfort increases because, vibration exposure becomes maximum. On the other hand, upright backrest provides less contact with backrest causing increased spinal pressure consequently increased discomfort. Figure 2.14 shows the weighting frequency curve of ISO 2631–1 in the vertical direction for upright and recumbent position and new weighting frequency curves of Paddan et al (2012).

2.2.3 Input Vibration

Apparent mass is one of the factors that also affect the transmissibility, which also depends on level of input vibration. Hence, the magnitude of vibration is able to change the resonance frequency of seated human body (Toward, 2010).

Fairley (1986) has investigated the transmissibility of a car seat with six subjects at six different vibration magnitudes between 0.2 and 2 r.m.s. It is proven as the magnitude of vibration increases, the mean resonance frequency reduces from 5 to 3 Hz, and therefore, transmissibility at resonance frequency also reduces from 1.9 to 1.5 as shown in Figure 2.15.

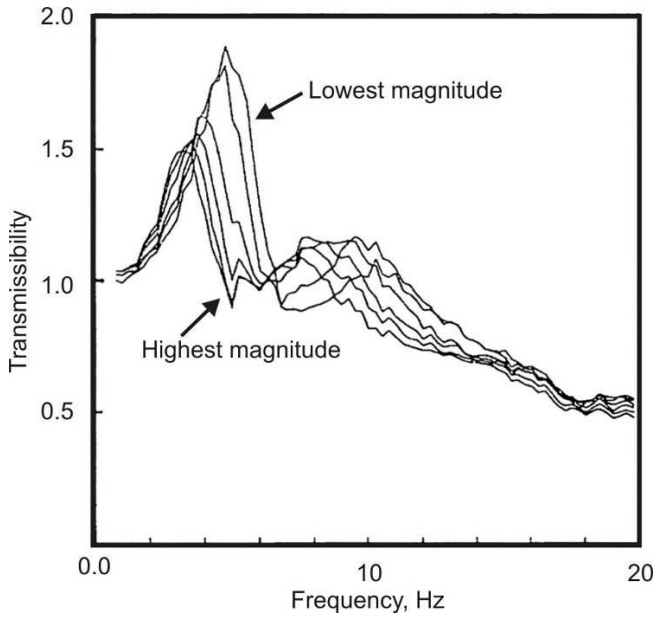

Figure 2.15: Effect of magnitude on seat transmissibility (Fairley, 1986).

2.2.4 Apparent Mass

Previous studies have shown that apparent mass affects the seat transmissibility. Toward and Griffin (2011) discussed change of apparent mass by subjects physical characteristics and effects of vibration magnitude and backrest on inter-subject variability. They conducted experiments with 80 adults to measure vertical apparent mass at frequencies between 0.6 to 20 Hz with four different backrest positions (without backrest, upright backrest without foam, inclined backrest

without foam and inclined backrest with foam) and three different random vibration magnitudes (0.5, 1.0 and 1.5 ms–2 r.m.s.). The results are summarized in Figure 2.16.

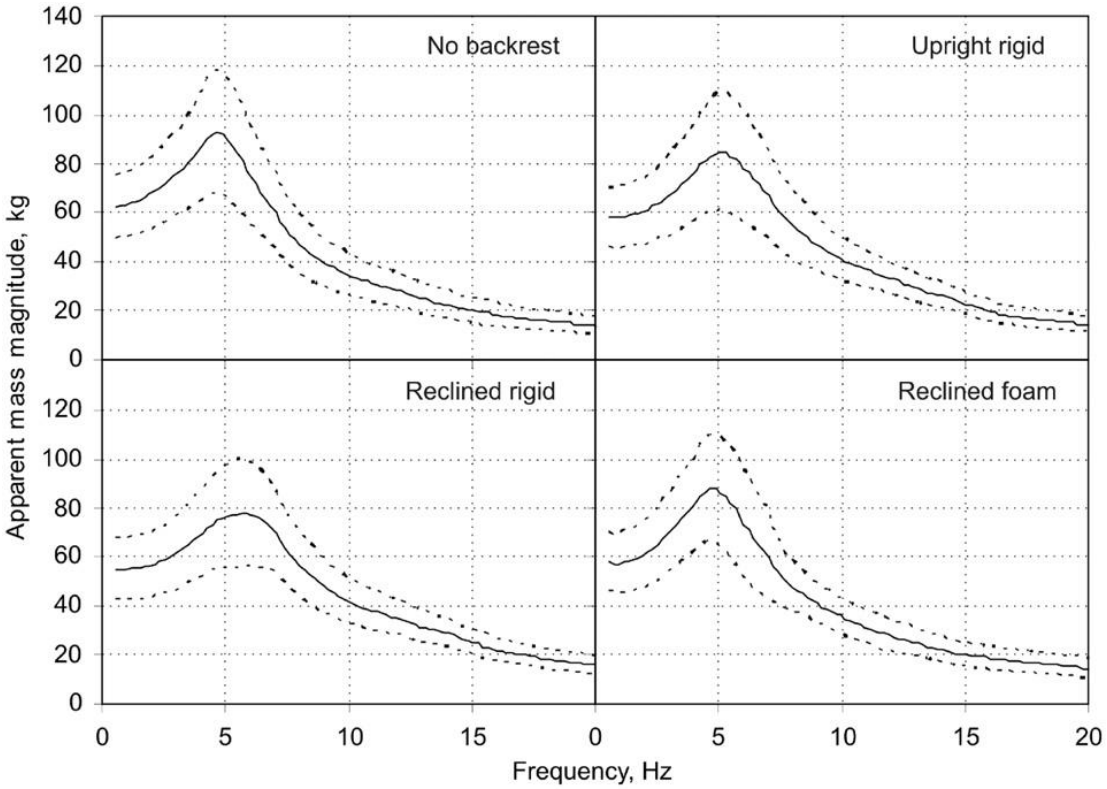

Figure 2.16: Effect of the seat backrest on mean apparent mass and inter-subject variability: 1.0 ms–2 rms excitation; mean (------) and ± 1 s.d. (·····) (Toward and Griffin, 2011).

Toward and Griffin (2011) also found that the most influencing factor on apparent mass appears to be body weight at 0.6 Hz, resonance and 12 Hz. Moreover, it is pointed that when describing apparent mass, factors such as age, body mass index, posture, weight and vibration magnitude should be taken into account.

Mandapuram et al. (2012) investigated apparent mass and seat to head vibration transmissibility response functions of seated subjects under whole-body vibration exposure to fore-aft (x), vertical (z) and lateral (y) which were applied individually and simultaneously with 9 subjects. Table 2.2 summarizes the proposed results.

Table 2.2: Summary of the broad-band vibration magnitudes employed (Mandapuram et al., 2012).

Vibration Magnitudes (rms, m/s^2)			**Overall rms**
x-axis	**y-axis**	**z-axis**	
0.25	-	-	- 0.25 m/s^2 single axis
-	0.25	-	
-	-	0.25	
0.4	-	-	- 0.4 m/s^2 single axis
-	0.4	-	
-	-	0.4	
0.23	0.23	0.23	- 0.4 m/s^2 three axis
0.4	0.4	0.4	- 0.7 m/s^2 three axis

Mandapuram et al. (2012) also derived two new frequency response functions based on cross- and auto spectral density of the response and excitation signals (H_1 and H_v, respectively) to measure apparent mass and head vibration transmission. Response of the seated body to simultaneous three–axis vibration derived using H_v frequency response function. It is suggested that H_v estimator can be used for measuring biodynamic response of subjects exposed to multi-axis vibration (Mandapuram et al., 2012).

Standards such as ISO 2631–1, 1997 and BS 6841, 1987 measure whole body vibration transmitted through seat to occupants consider vibrations only in vertical and horizontal direction. Therefore, a separate guidance is usually provided for assessment of rotational oscillation. However, provided information for rotational oscillation is measured with horizontally oriented accelerometers and expected to be effected by gravitational components (Gunston, 2003).

Gunston (2003) compared lateral apparent mass of seated human body in response to lateral and roll motions. Lateral apparent mass values obtained from rigid seat without a backrest within 0.2

and 2 Hz frequencies with three different magnitudes (0.05, 0.1 and 0.2 ms–2 r.m.s) and results are presented in Figure 2.17. In this study, using Fairley and Griffin (1989) parameters, it is concluded that normalised lateral apparent mass in response to rotational oscillation found to be greater than in response to lateral oscillation.

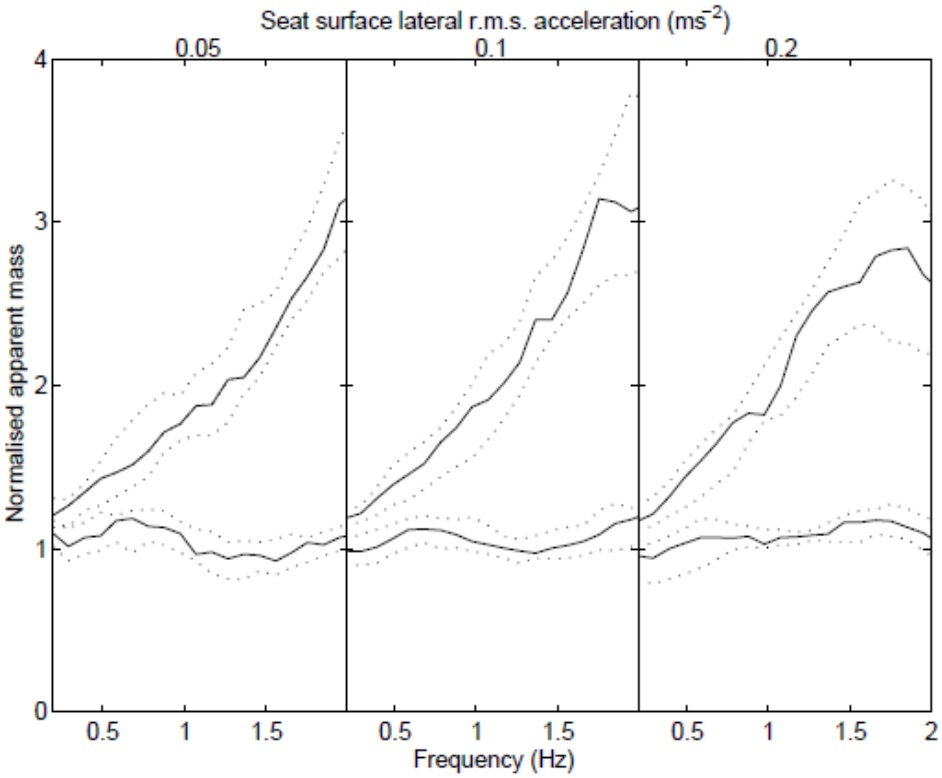

Figure 2.17: The lateral apparent mass of all 12 test subjects normalised by sitting mass showing the median and interquartile ranges for lateral oscillation (lower lines) and roll oscillation (upper lines) in response to each magnitude of seat surface lateral acceleration (Gunston, 2003).

The hypothesis that at low frequencies the lateral apparent mass in response to roll oscillation will be similar to that obtained in response to lateral oscillation must be rejected for the frequency range (between 0.2 and 2 Hz). Changes in lateral apparent mass with magnitude over the frequency range investigated were small compared with the inter-subject variability.

2.2.5 Age

Toward and Griffin (2011) also investigated the effect of age in seat vibration transmissibility since elderly people might be more sensitive to a certain exposure comparing to younger people. They conducted the study with 80 subjects' ages from 18 to 65 years old. When they compared the results, not only an increase in the seat transmissibility was observed, but also an increase in the resonance frequency as shown in Figure 2.18. A conclusion can be drawn from their study that testing for seat transmissibility requires a good selection of subjects in order to quantify the seat transmissibility objectively.

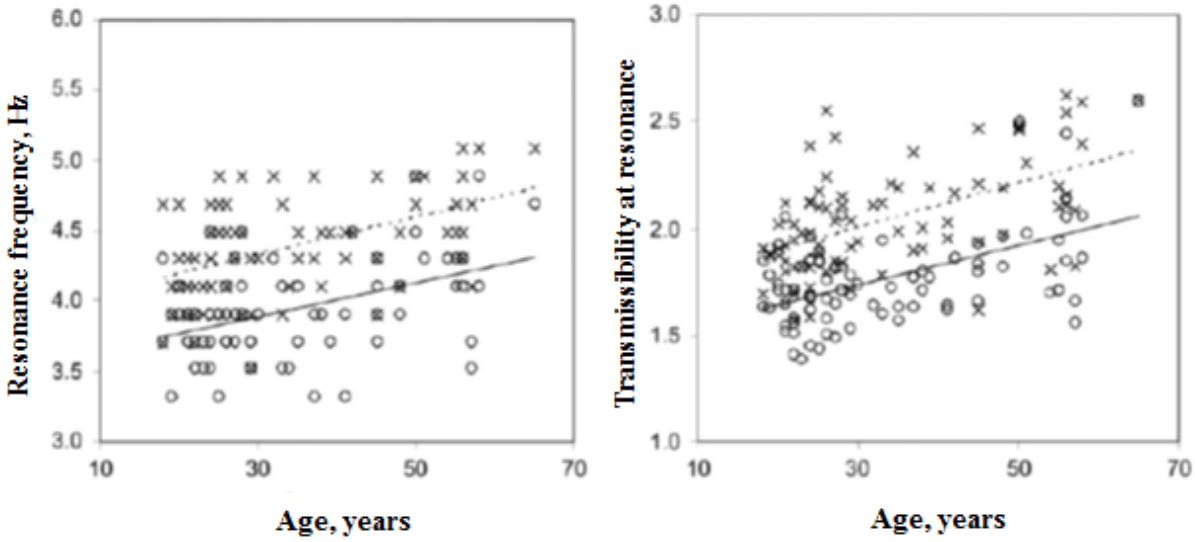

Figure 2.18: Effect of age on resonance frequency and seat transmissibility (Toward and Griffin, 2011).

2.3 Seat Comfort Measurement Methods

In the literature, it is concluded that under vibration exposure the most significant vibration which causes largest discomfort is in the vertical direction (Griffin, 1990). Therefore, the

following part of this literature review focuses on measurement methods of vertical vibration exposure.

The most common way to measure seat transmissibility is using accelerometers placed at the surface of seat and at the base of seat to compare results (Griffin, 1990). On the other hand, some studies discussed that transmissibility can also be measured using mechanical impedance of seat (e.g. Wei and Griffin, 1998).

Miwa and Yonekawa have published series of studies regarding the whole–body exposure in various conditions. In one of their studies, Miwa and Yonekawa (1971) compared three different methods of seat transmissibility measurements (threshold shift, mechanical impedance and acceleration ratio). Methods were subjected to vertical and horizontal vibrations at frequencies between 2 and 100 Hz. They found that the results of three methods are similar to each other and can be used individually for transmissibility measurements. It is also remarked that acceleration ratio method is most useful because it can be used for both transmissibility and vibration spectrum measurements.

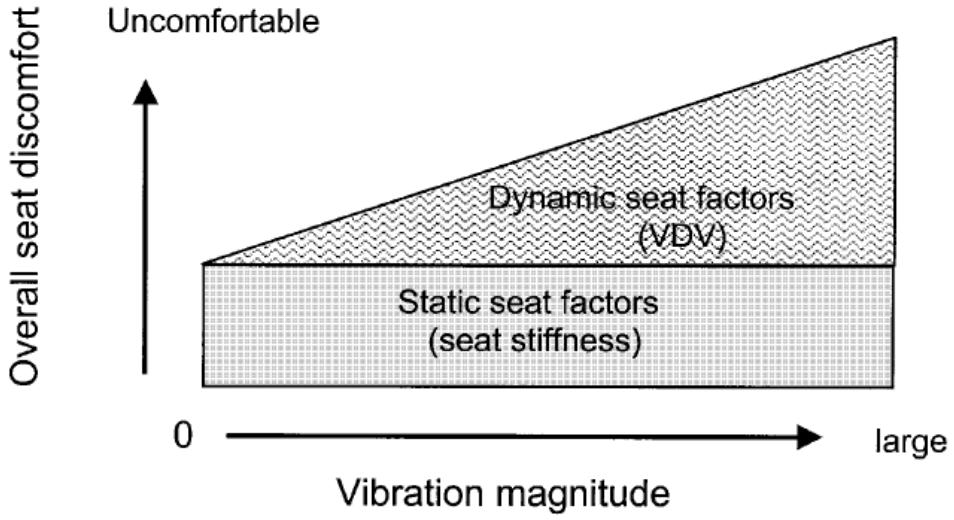

Figure 2.19: A model of overall seat discomfort on linear scales (Ebe and Griffin, 2000).

Ebe and Griffin (2000) developed qualitative model to measure overall discomfort including static and dynamic factors. Figure 2.19 describes the general trend of the proposed model. The model was tested with 12 subjects with four different cushions to provide different static and dynamic conditions under one-third octave band random vertical vibration with frequencies between 2.5 and 5.5 Hz at magnitudes of 0.25 and 2 r.m.s.

A model to describe sensation magnitude is developed according to Steven's psychophysical power law (1975):

$$\psi = k\varphi^{\beta} \tag{2.1}$$

where k is constant that depends on the units of measurement, φ is stimulus magnitude and β is the exponent that varies according to stimulus which was obtained from previous studies and it was reported to be approximately 1.10 in Fothergill and Griffin (1977). Hence, as shown in Figure 2.20, as the vibration magnitude increases, discomfort due to dynamic properties increases linearly.

To provide full linearity, the equation which gives the relationship between sensation magnitude and stimulus magnitude is written in log–log scales because, in log–log scale differences in the exponents results with differences in the slopes as shown in Figure 2.20 (Ebe and Griffin, 2000).

$$\log \psi = \beta \log \varphi + \log k \tag{2.2}$$

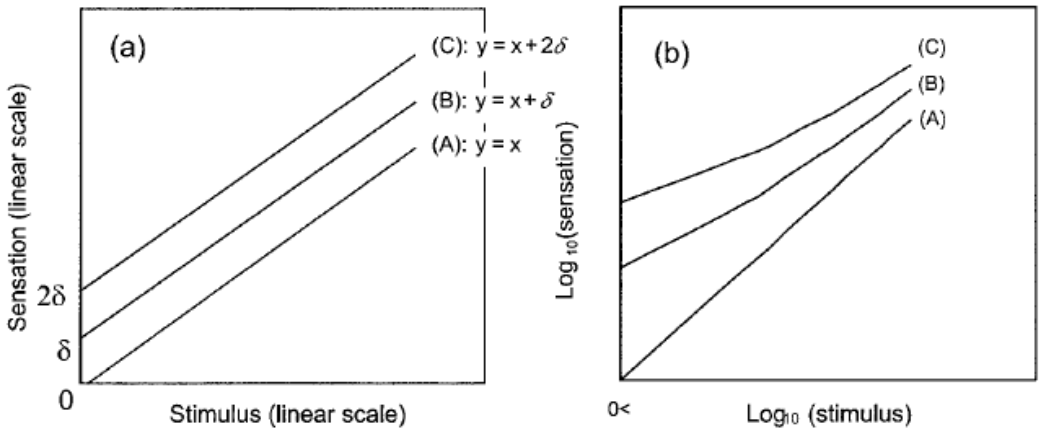

Figure 2.20: Effect of initial values on features of graphs: (a) linear scales, (b) log-log scale (from Ebe and Griffin, 2000).

In their study, Fothergill and Griffin (1977) strongly recommended that when measuring overall seat comfort, both static and dynamic factors should be considered and influence of static discomfort depends on the magnitude of vibration.

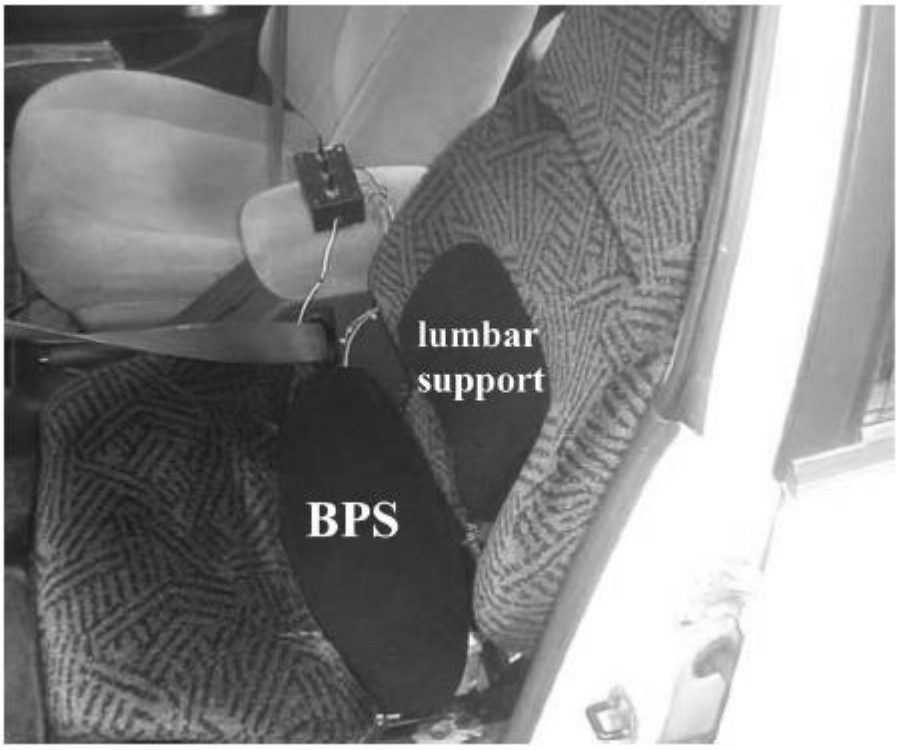

Figure 2.21: The new proposed design as implemented in testing vehicle (Makhsous et al., 2005).

Makhsous et al. (2005) have proposed a new seat design to reduce the whole-body vibration. The main idea of the proposed design is having an adjustable back part of seat and a lumbar cushion to support the spine and compared it to the traditional seat as shown in Figure 2.21. As the adjustable back part of the seat goes down to reduce contact surface area, lumbar cushion supports the back of the occupant to prevent discomfort. By reducing the contact area between seat and occupant, the new seating design provides lower contact pressure and amplitude of vibration transmitted through the body. Seat effective amplitude transmissibility (S.E.A.T.)

values presented for both situations (with lowered back part and without lowered back part) with subjects sitting in normal posture. Measurements were done for six body locations IT (ischial tuberosities), lumbar spine, shoulder, elbow, ankle and knee. Among these locations four of them showed significant reduction in terms of root mean square vibration values, especially in the lumbar spine 36% when the new design used. RMS vibration values did not show significant change at shoulder and knee.

Considering these benefits of the new seat design, 2.5h daily longer travelling is stated until reaching to critical zone and having health issues in the lumbar spine. The studies mentioned above are focusing on the reduction of vibration transmissibility and consequently to increase seat comfort. However, all of them had investigated, evaluated and developed a system that can reduce whole-body vibration for vehicles but not for aircrafts. The developments presented above towards the reduction of the input vibration either from road to vehicle or vehicle to seat for vehicles can also be implemented for the aircrafts for the given flight conditions.

Since this thesis focuses on the vibration transmissibility through seat to occupant in aircrafts for take–off, landing and cruise flight conditions, the positive results from the above mentioned studies can be partially implemented for the aircraft. Among these three flight conditions, take–off and landing cases might be affected by the tire characteristics consequently can change the seat comfort. Moreover, the studies mentioned above covering the tire inflation to increase seat comfort provides good handling characteristics as well considering catastrophic accidents due to mishandling of the airplanes.

Based on the literature review, it is observed that there is a lack of comprehensive analysis and documentation that consists of complete methodology for assessment of dynamic aircraft seat suspension characteristics as well as understanding the aircraft interior constraints.

Chapter 3

Experimental Setup and Procedure

In this chapter, a background for signal processing, a detailed explanation of experimental operations, and a step–by–step description of simulation development process are explained. A simple procedure of the conducted work is given in Figure 3.1.

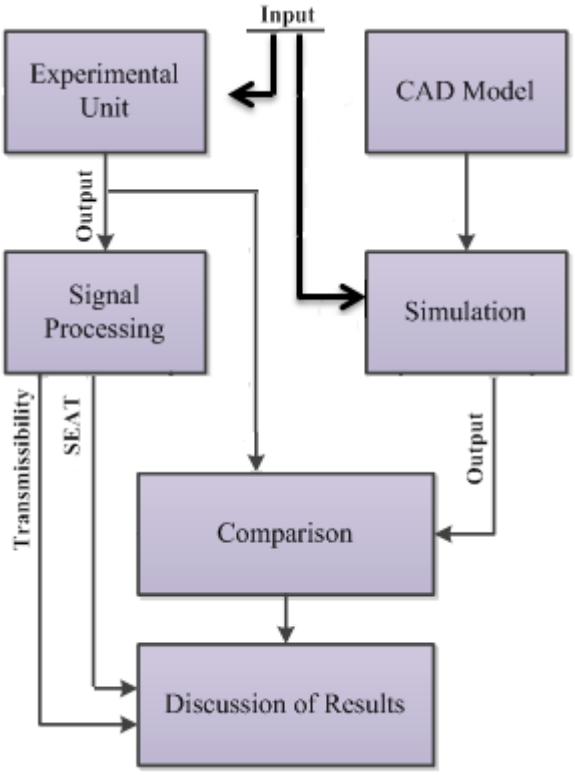

Figure 3.1: Schematic description of the conducted work.

Figure 3.1 indicates a typical experimental vibration simulation and signal processing procedure highlighting the essential steps. Vibrations are generated in response to some excitation. In some experimental procedures, mostly in vibration testing, a signal generator is used to meet the requirements, such as amplification or conditioning the signal.

3.1 Experimental Setup

3.1.1 Vibration Exciters

In controlled experiments where the level of vibration is applied to the test object and the resulting response is monitored, an external exciter is needed to generate the necessary vibration. A variety of vibration exciters are available, with different capabilities and principles of operation.

There are three types of vibration exciters that are commonly used in the industry which are: hydraulic shakers, inertial shakers, and electromagnetic shakers. Table 3.1 summarizes the capabilities of the categorized exciters.

Table 3.1: Typical operation – capability ranges for various shaker types.

Shaker Type	**Typical Operational Capabilities**					
	Frequency (Hz)	**Maximum Displacement (Stroke)**	**Maximum Velocity**	**Maximum Acceleration**	**Maximum Force**	**Excitation Waveform**
Hydraulic (electrohydraulic)	Low (0.1–500 Hz)	High (50 cm)	Int. (125 cm/sec)	Int. (20 g)	High (450,000 N)	Average flexibility
Inertial (counter-rotating mass)	Int. (2–50 Hz)	Low (2.5 cm)	Int. (125 cm/sec)	Int. (20 g)	Int. (4,500 N)	Sinusoidal only
Electromagnetic (electrodynamic)	High (2– 10,000 Hz)	Low (2.5 cm)	Int. (125 cm/sec)	High (100 g)	Low (2,000 N)	High flexibility and accuracy

In this study, hydraulic shakers are used to replicate the actual flight conditions due to their advantage of providing high flexibility of operation during the test. Hydraulic shakers also have the capability of variable and constant–force and wide–band random–input testing. The velocity

and acceleration capabilities of hydraulic shakers are moderate. Moreover, any general excitation input motion can be used in hydraulic shakers. In order to replicate the actual flight conditions required to perform the experiments, a large multi-axis-shaker-table (MAST) in hemi-anechoic chamber provided by the Automotive Centre of Excellence (ACE) at the University of Ontario Institute of Technology (UOIT) is used. The MAST is originally designed to test the durability of large automotive parts and it meets the requirements of the experimental requirements of this study. Despite its advantages, the MAST does not produce vibration exceeding 150 Hz and has a maximum displacement range of ±150mm. Attaching aircraft seats to the MAST requires additional parts. The design of the aircraft seats are such that only one side of the seats have a leg attached to the floor and the other sides are designed to be attached to the fuselage. In order to attach the aircraft seats to the MAST, steel plates are used (Figure 3.2) to have the seats leveled and rigidly fixed to the shaker table.

Figure 3.2: Designed fixations to the MAST using steel plates.

3.1.2 Performance Specification and Measurement

Proper selection and integration of sensors and transducers are crucial in a vibrating system. The tri-axial accelerometer pad used to measure vibration in this study is shown in Figure 3.3. The

measurement device is an ENDEVCO model 2560 with excitation of 10 V (dc) and with sensitivities of 1.83 mV/g, 2.05 mV/g and 1.76 mV/g on -x, -y and -z directions, respectively.

Figure 3.3: Seat pad accelerometer.

3.1.3 Data Acquisition and Processing

Commercial data–acquisition and processing systems with a wide range of properties to meet the required processing such as FFT analysis, frequency–response function, and transmissibility, and mechanical-impedance analysis, natural–frequency and modal analysis, and system-parameter identification (e.g. damping parameters) are available.

Generally most processing is done in real time which providing the advantage of noticing any changes in the signal since the input and output signals can be monitored as they are being measured.

In this study, NI PCI- 6221 data acquisition board, as shown in Figure 3.4, together with LabView software by National Instruments is used to receive and process the signals from the accelerometers.

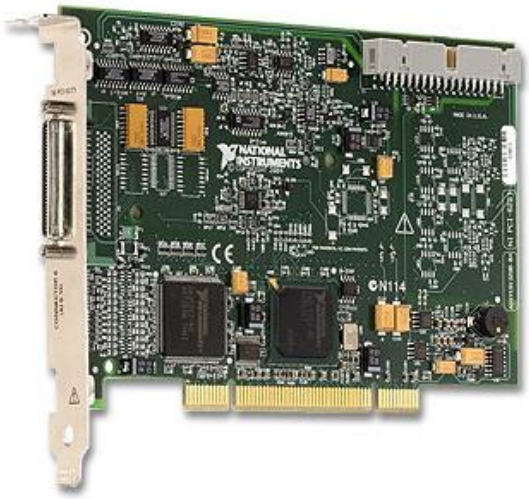

Figure 3.4: National Instruments DAQ card.

3.1.4. Complete Experimental Setup

The complete aircraft seat and the MAST instrumentation setup is shown in Figure 3.5. Since the ACE safety policies prohibit any person to be seated on the seat replica connected to MAST setup during operations, 150 lb weights are used on the seats to replicate human subjects.

Figure 3.**5**: Complete attachments of aircraft seat with the accelerometer under the dummy.

In addition to economy class and business class seats, different cushion materials are also examined replacing the original cushions with laboratory made cushions shown in Figure 3.6. These additional cushions were cut in same shape of original cushions from two different sound isolation materials. Cushion A and B are from same material but different thicknesses, 2 and 4 inches respectively. Cushion C is made of a second material with 3 inch thickness.

For these cushions shown in Figure 3.6, a stiffness test conducted. Using TA instruments model DMA Q 800 dynamic mechanical analyzer, as shown in Figure 3.7, 3 point bending tests are performed. For each cushion stress vs. strain curves are produced. Figures 3.8 and 3.9 show the stress–strain curves for cushion A and C, respectively. From these curves, the slope of the linear part yields the Young's modulus of elasticity. For cushion A, the linear part in the curve is very clear but for cushion C, it is not possible to obtain a curve with a clear linear part. The Young's modulus of cushion A and C is calculated to be 1.45 MPa and 30.3 kPa, respectively.

Figure 3.6: Laboratory–made cushions used in the experiments.

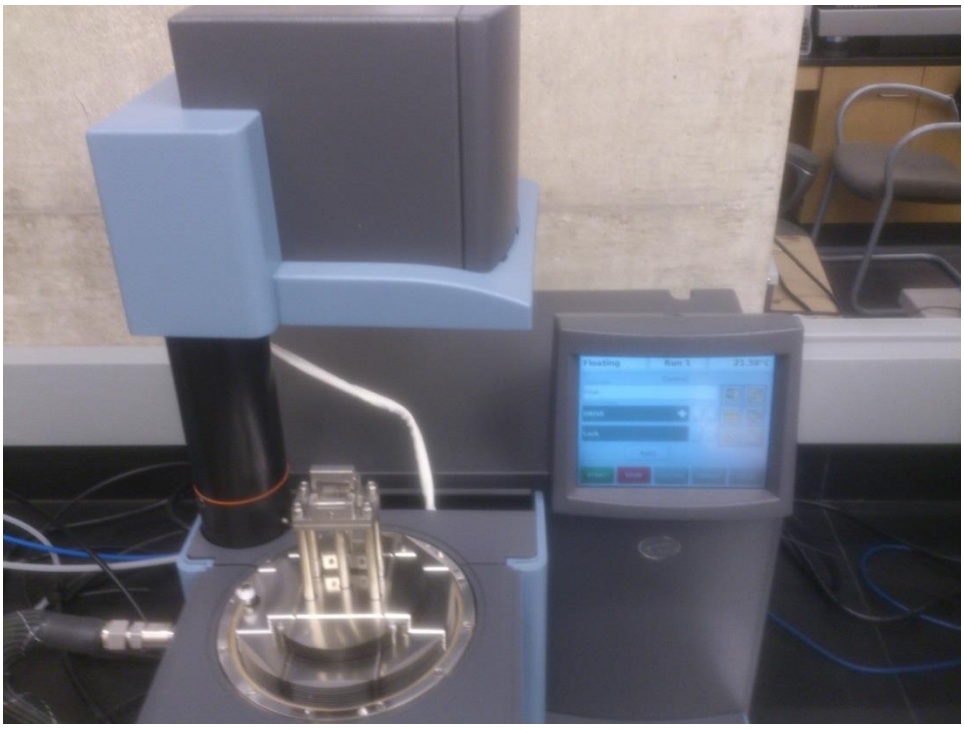

Figure 3.7: DMA Q 800 dynamic mechanical analyzer.

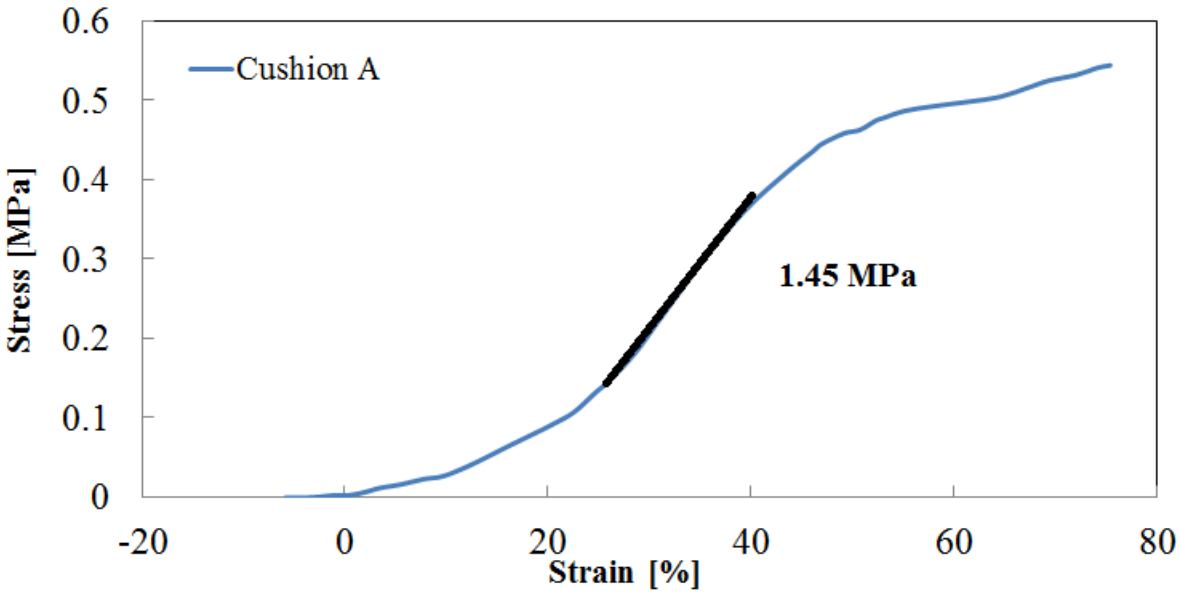

Figure 3.8: Stress–strain curve for cushion A.

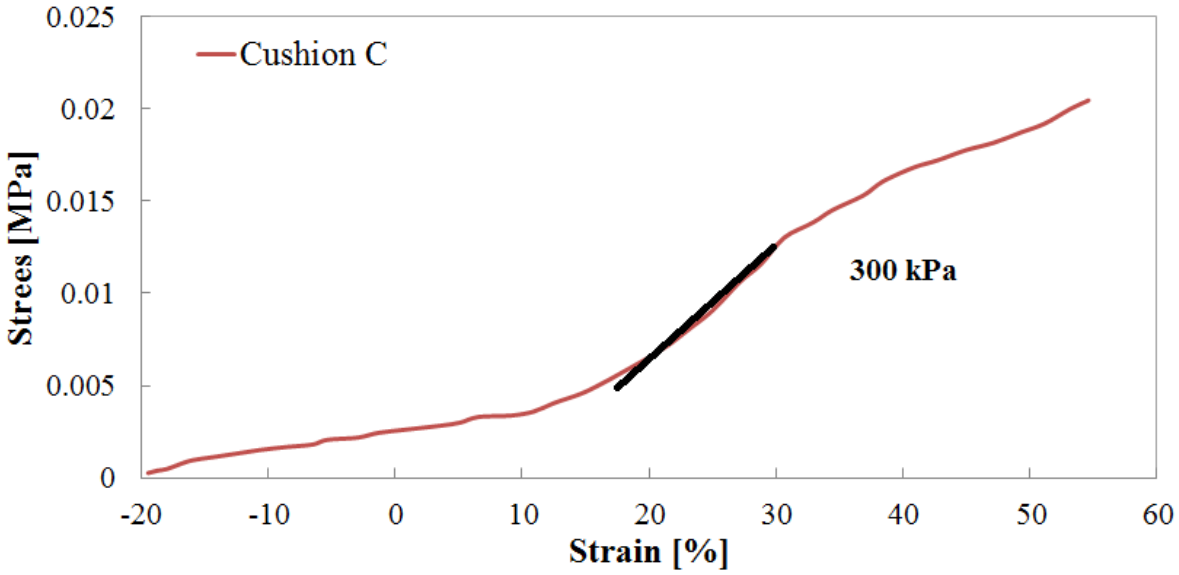

Figure 3.9: Stress–strain curve for cushion C

3.2 Experimental Procedure

To replicate the given flight conditions, the initial step was to recreate the given data because they were recorded during actual flight with 4096 Hz sampling rate. The MAST, on the other hand, has a sampling frequency of 1024Hz. This process was done through the control algorithm of the MAST. Once each flight condition was recreated for the MAST the seats were attached with the instruments on. Starting with economy class, each flight condition was replicated and obtained data from the accelerometers under the dummy on the seat surface and behind the dummy on the seat back. This process was repeated for business class seat as well as economy class seat base with laboratory made cushions.

3.2.1 Signal Processing

Once data obtained from the experiments, it is then processed to plot the transmissibility curves and to calculate the S.E.A.T. values using MATLAB via Fast Fourier Transform. The Fast Fourier transform (FFT) is a faster way to perform the Discrete Fourier Transform (DFT) by efficiently using the powers of two (2^n). There are many different FFT algorithms including wide range of mathematics.

The problem with DFT is that to compute the sequence $\{X(k)\}$ of N complex-valued numbers representing another sequence of data $\{x(n)\}$ of length N, according to the below formula as:

$$X(k) = \sum_{n=0}^{N-1} x(n) {W_N}^{kn}, \qquad 0 \leq \text{k} \leq \text{N-1} \tag{3.1}$$

where;

$$W_N = e^{-j2\pi/N} \tag{3.2}$$

and;

$$x(n) = \frac{1}{N} \sum_{n=0}^{N-1} X(k) {W_N}^{-nk}, \; 0 \leq \text{n} \leq \text{N-1} \tag{3.3}$$

Thus computation of the DFT becomes inefficient mainly due to lack of symmetry as well as the properties that define the periodicity of the phase factor $W_{N.}$ Considering the computation of $N=2^n$ point DFT by the divide-and-conquer approach, splitting data sequence consisting of N points in to two N/2 point data sequences as f_1 (n) and f_2 (n) providing a representation for the odd and even numbered samples of the data sequence x (n) , that is;

$$f_1(n) = x(2n) \tag{3.4}$$

$$f_2(n) = x(2n+1), n = 0,1, \ldots., {}^{N}/_{2} - \tag{3.5}$$

therefore, f_1 (n) and $f_{2\,(}$n) are found by reducing the data sequence x (n) by a factor of 2 resulting an efficient FFT is called a decimation-in-time algorithm. However substituting $W_N{}^2$ with $W_{N/2}$ equation can be expressed as;

$$X(k) = \sum_{n=0}^{\left(\frac{N}{2}\right)-1} f_1(m) {W_{\frac{N}{2}}}^{km} + {W_N}^{k} \sum_{n=0}^{N-1} f_2(m) {W_{\frac{N}{2}}}^{km} \tag{3.6}$$

$$= F_1(k) + {W_N}^{k} F_2(k), \; k = 0, 1 \ldots \text{N-1} \tag{3.7}$$

where $F_1(k)$ *and* $F_2(k)$ are the N/2 point DFT's of the sequences $f_1(m)$ and $f_2(m)$, respectively.

However, converting the data obtained in time domain to frequency domain is not sufficient to generate transmissibility curves and to calculate the S.E.A.T. value. In order to generate

transmissibility curves and calculate S.E.A.T. one should observe the data regarding its power spectrum density. The power spectrum density (PSD) for a signal is a measure of its power distribution as a function of frequency. Consequently, power spectrum density is obtained through FFT, therefore first the signal in the time domain obtained from experiments should be converted to frequency domain, which is FFT, then should be extracted to its power spectrum.

Using FFT, one can estimate power spectral densities using a function called periodogram. The periodogram of an N point sequence *y*(n) can be defined as follows:

$$I_N(W) = \frac{1}{N} |Y(W)|^2 \tag{3.8}$$

where,

$$Y(W) = \sum_{n=0}^{N-1} y[n] e^{-jWnT} \tag{3.9}$$

is the Fourier transform of *y*(n) and the inverse transform of the periodogram is sample autocorrelation function as,

$$R(n) = \begin{cases} \frac{1}{N} \sum_{k=0}^{N-1} y[n+k]\bar{y}[k] & for\ |n| \leq N-1 \\ 0 & elsewhere \end{cases} \tag{3.10}$$

The variable, *n*, in the autocorrelation function is called *lag.* Assuming 0 lag above equation yields;

$$R(0) = \frac{1}{N} \sum_{k=0}^{N-1} |y[k]|^2 = \frac{1}{W_s} \int_{-W_s/2}^{W_s/2} I_N(W) dW \tag{3.11}$$

is the average power in the sequence. This equation provides a representation for the periodogram that shows the power distribution depending on the frequency.

Chapter 4

Evaluation of Input Acceleration

As mentioned in the previous chapter, the objective of this study is to evaluate the seat comfort of an aircraft passenger during takeoff, landing and cruise through turbulence flight conditions. To perform this evaluation on the multi-axis-shaker-table, introduced vibrations to the aircraft seats through MAST must be the same as in the aircraft. Figure 4.1 shows the setup employed to record data during actual flight conditions.

Figure 4.1: Experimental setup during actual flight conditions.

Two single axis accelerometers attached perpendicularly to each other are used to record the vibration coming from the airplane floor as shown in figure 4.1. The recorded vibrations are then replicated by the MAST and a comparison for each flight condition is described below.

4.1 Input Comparison for Takeoff

Figure 4.2 and 4.3 show the comparison between the replicated vibrations by the MAST and recorded data during actual flight in –z and –y directions, respectively. Since comparing two signals in time domain can be deceiving, comparison of two signals in frequency domain is also provided.

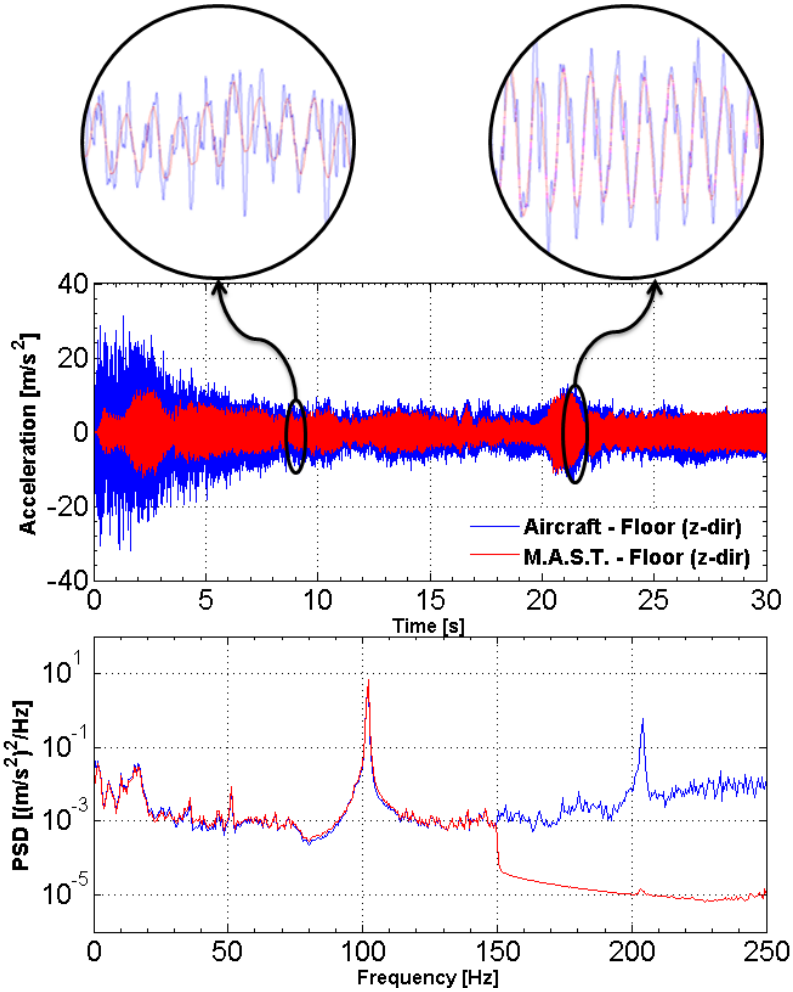

Figure 4.2: Input comparison for take–off in z–direction.

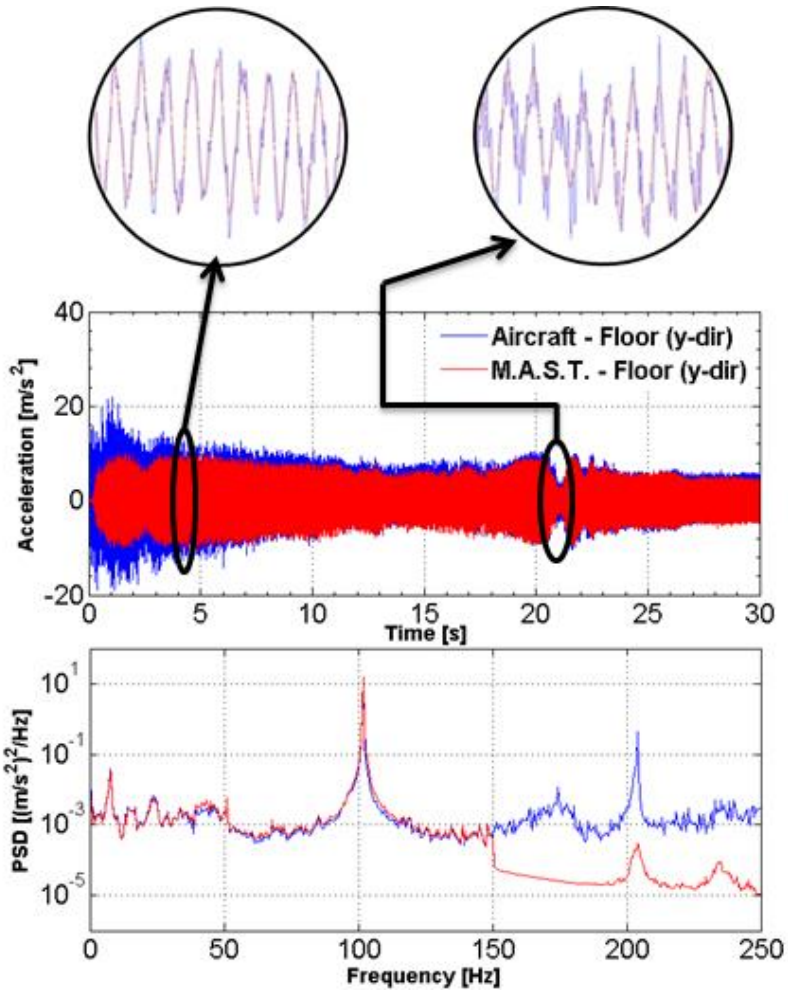

Figure 4.3: Input comparison for take–off in y–direction.

It is clear from figures 4.2 and 4.3 that the MAST replicates the takeoff flight condition perfectly until its cut-off frequency of 150Hz. It is therefore, the high frequency components in the original signal that cannot be simulated on the MAST causes the difference in amplitude in time domain.

4.2 Input Comparison for Landing

For landing flight condition, comparison between the vibrations recorded during actual flight and that replicated by the MAST show some differences in the time domain as shown in Figure 4.4 and 4.5 in –z and –y direction, respectively. However, power spectral density comparison of two

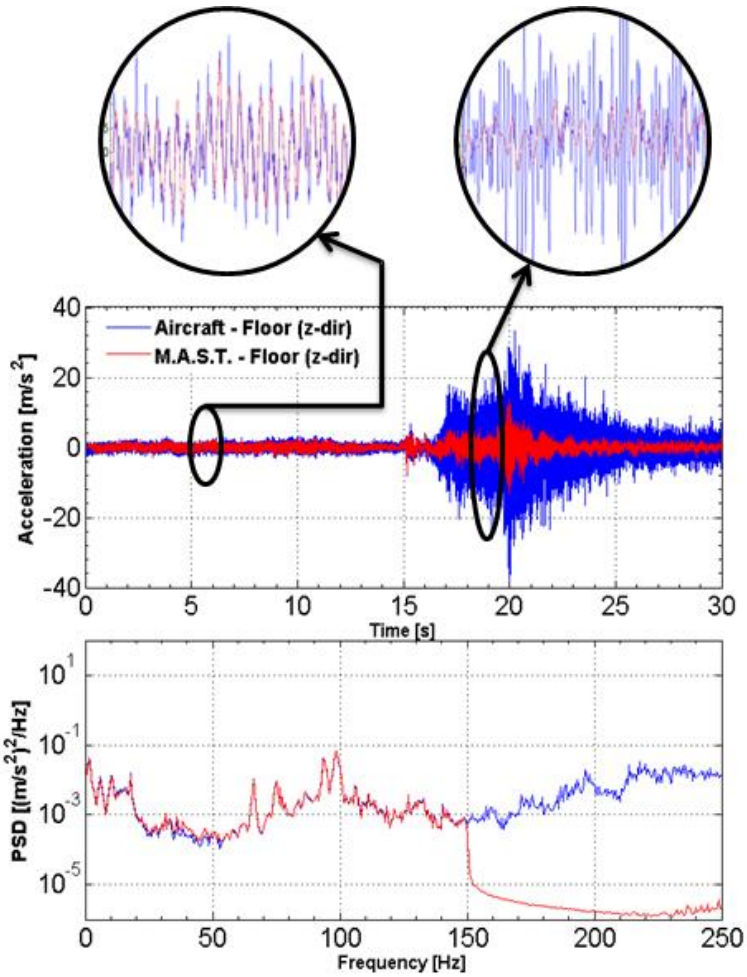

Figure 4.4: Input comparison for landing in z–direction.

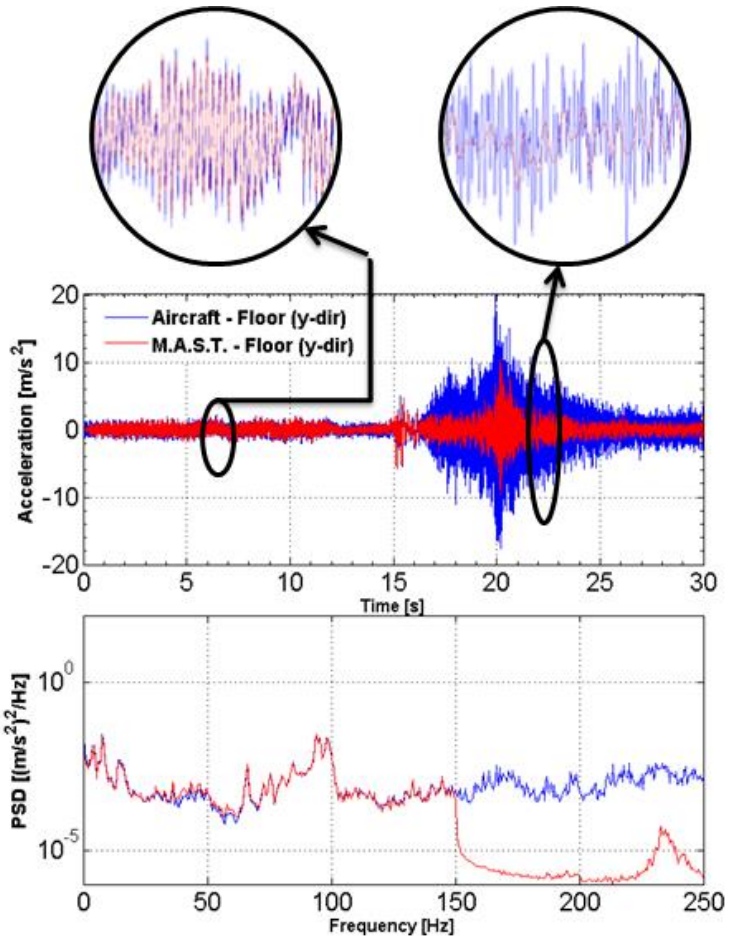

Figure 4.5: Input comparison for landing in y–direction.

signals show that they are almost identical until 150Hz. As seen from the acceleration values in the time domain, landing flight condition resulted with higher values compared to takeoff flight condition. It is therefore, resulted with greater discrepancy in time domain compared to takeoff flight condition.

4.3 Input Comparison for Cruise

The comparison method employed for takeoff and landing flight conditions also employed for cruise flight condition. Results showed that cruise through turbulence seem to be least matching flight condition among the three. In the 150Hz frequency range, the simulated input signal which was introduced to the MAST differs from the original recordings of actual flight. This difference

is attributed to the large displacements during the flight through a turbulence which the MAST cannot produce a displacement more than 150mm, hence, resulting with discrepancy between the two signals. Figures 4.6 and 4.7 show the comparison of the original signal and the signal replicated by the MAST for the given flight condition in –z and –y directions, respectively.

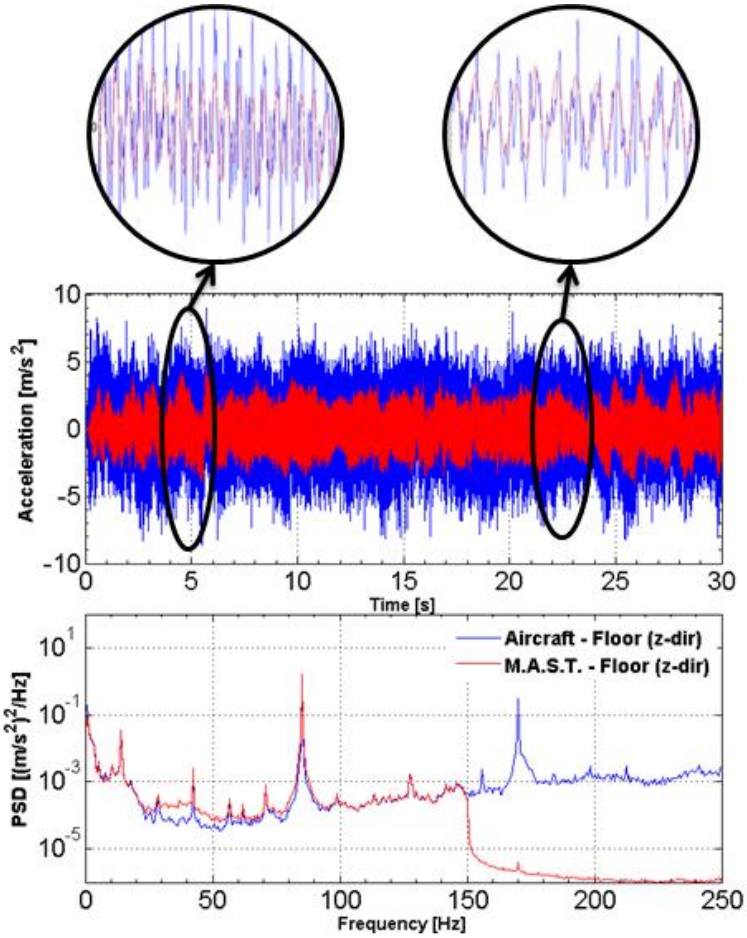

Figure 4.6: Input comparison for cruise in z–direction.

Comparison between the two signals that are introduced to the MAST and the original recordings from flight for takeoff and landing flight conditions seem perfectly match within the 150Hz frequency range. The slight difference between the two signals for cruise flight condition is tolerable since the difference occurs at very small magnitudes.

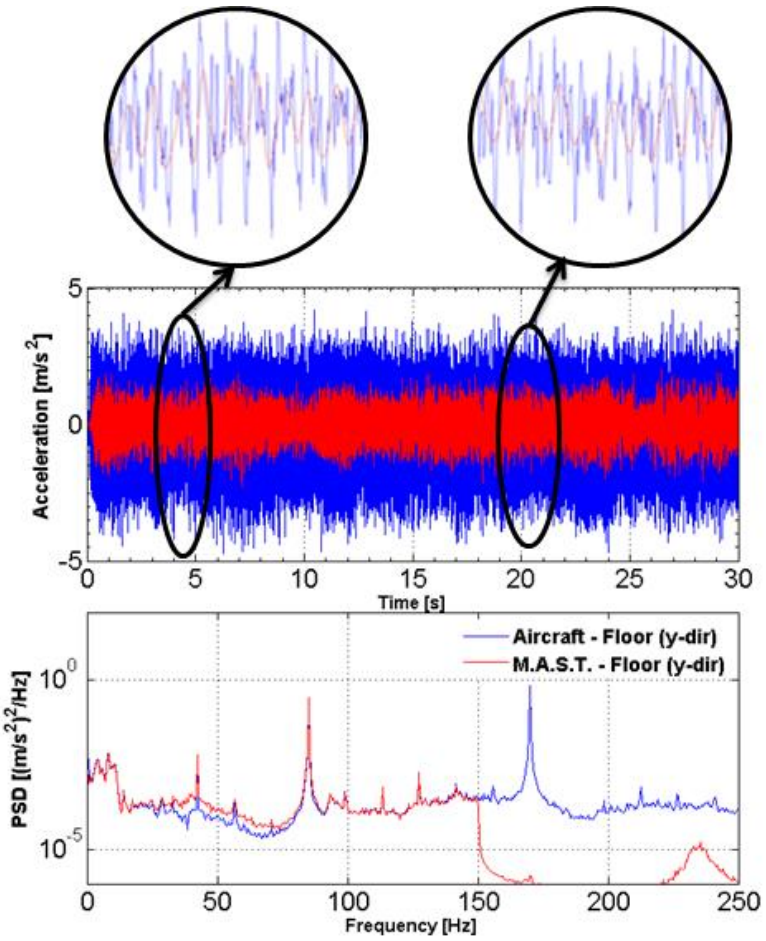

Figure 4.7: Input comparison for cruise in y–direction.

Any vibration in the –y direction is not the interest of this study. However, they are shown in order to validate that a given flight condition can be fully replicated on the MAST. Moreover, the MAST not being able to operate beyond 150Hz is not a concern since the seat comfort is evaluated in much lower frequency range which will be shown in the following sections.

Chapter 5

Evaluation of Vibration Transmissibility and S.E.A.T.

5.1 Transmissibility

Transmissibility is assumed to be the initial step for comfort evaluations. It is calculated through the ratio of output power spectral density (on seat surface or seat back) and input power spectral density of acceleration measurements (Griffin, 1978).

$$Transmissibility = \frac{G_s}{G_f} \tag{5.1}$$

where G_f is the power spectral density of the input acceleration on the floor and G_s is the power spectral density of output acceleration. The transmissibility points out the frequency range which primarily should be dealt with depending on the discomfort produced by input vibration. Since transmissibility curves are plotted by taking ration of output and input power spectral densities of vibrations Figures 5.1, 5.2 and 5.3 show the input and output vibrations in PSD domain for economy and business class seats for takeoff, landing and cruise flight conditions respectively. Closer inspections revealed that around 10 Hz measured vibrations on top of the seat cushion for both economy and business class seat resulted with higher magnitude comparing to input vibration magnitude. This is due to the resonance of the seat including the effect of dummy weigh. However, this resonance frequency can be changed depending on the applied force by the dummy. However relying only on the vibration transmissibility for overall comfort evaluations may be inaccurate.

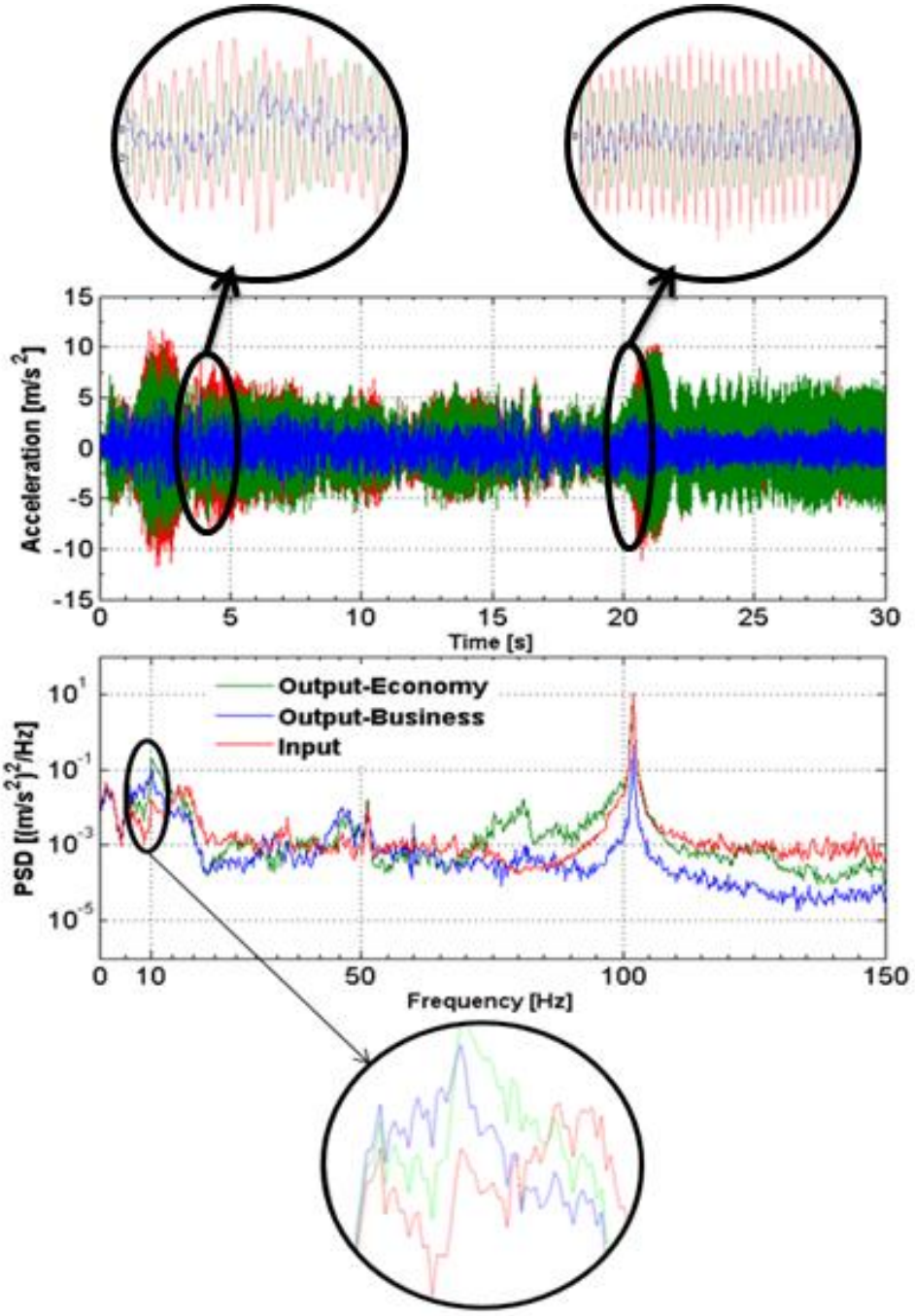

Figure 5.1: Comparison of input and output vibration on the seat surface (z-direction) for takeoff.

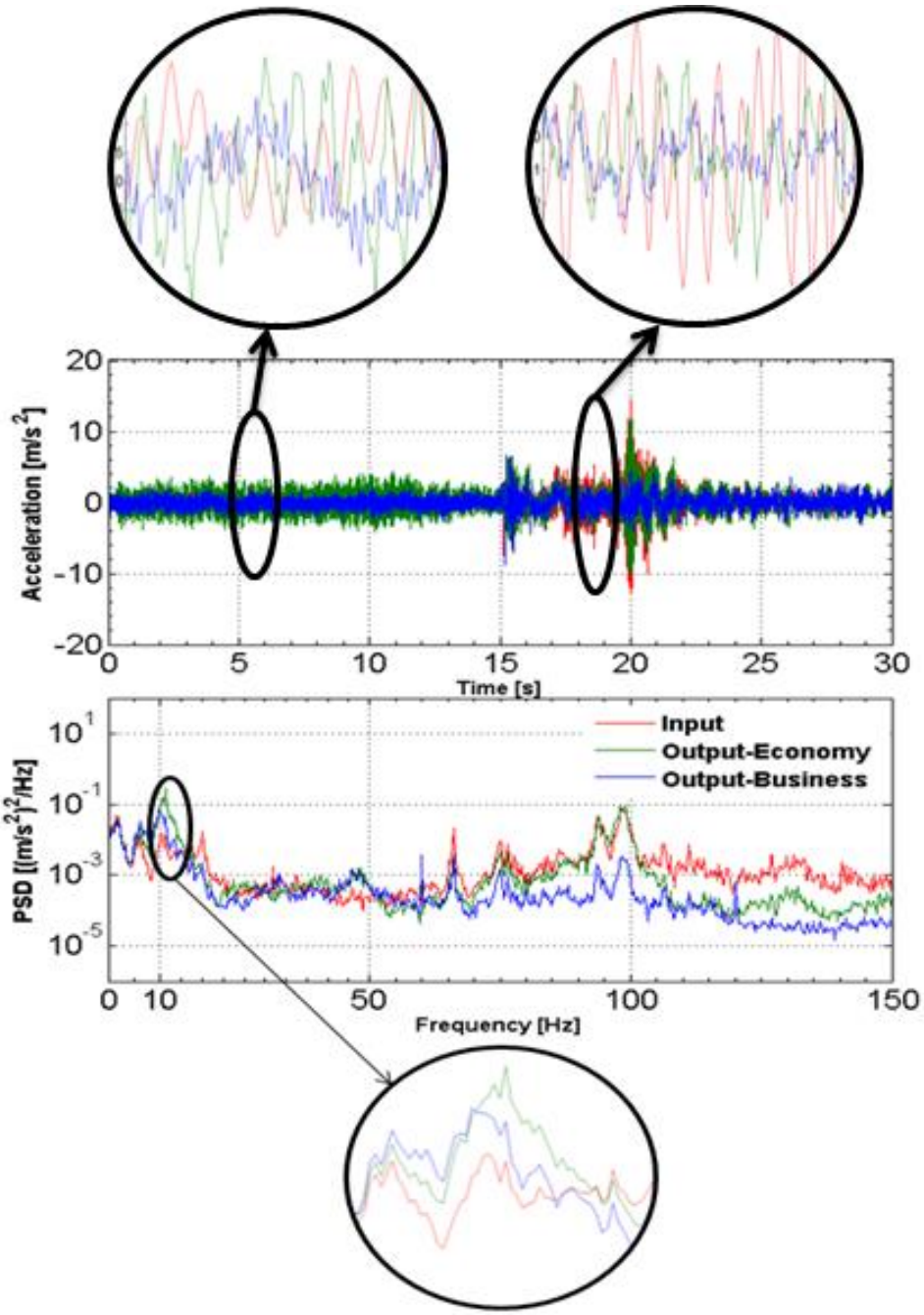

Figure 5.2: Comparison of input and output vibration on the seat surface (z-direction) for landing.

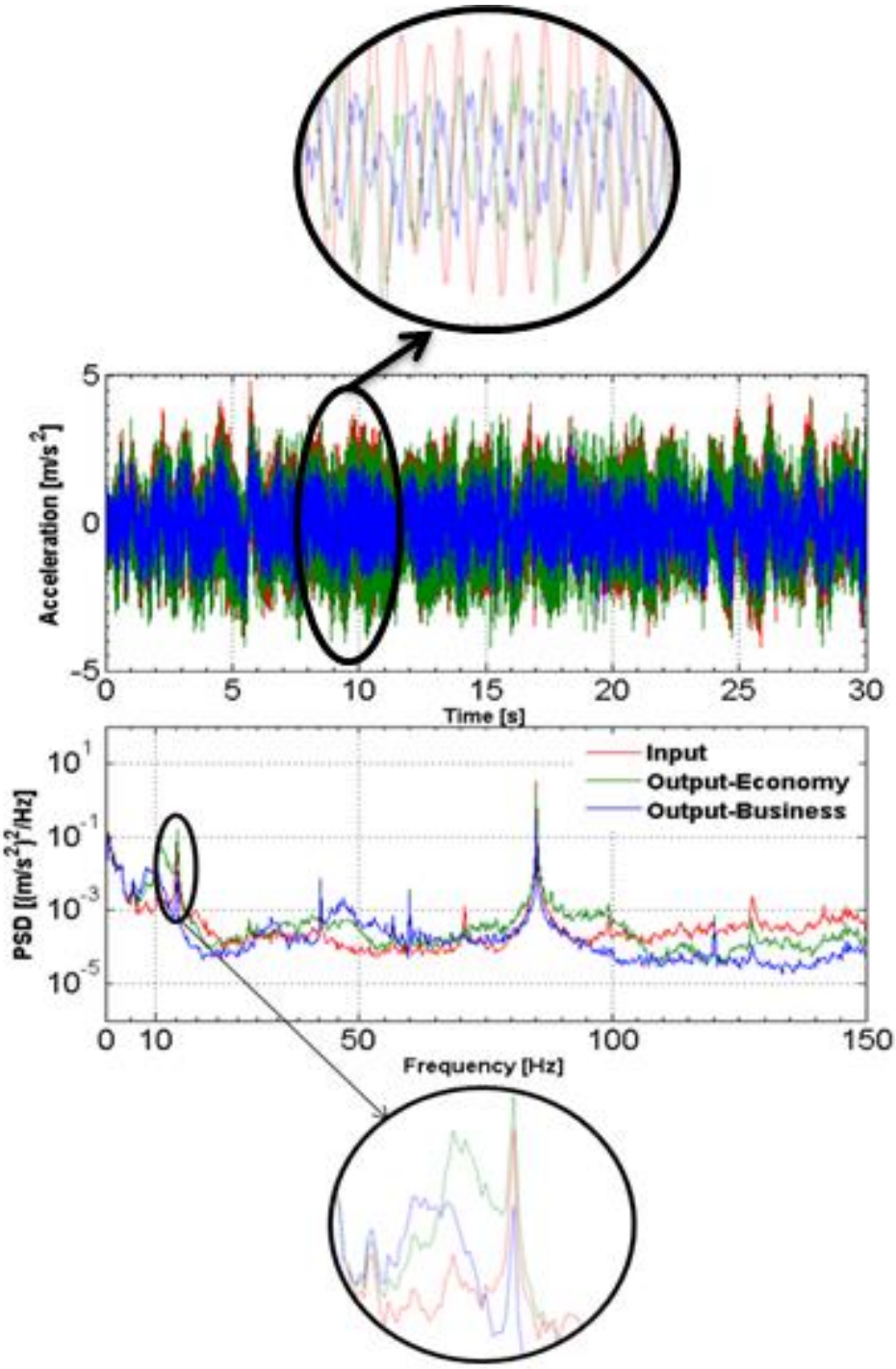

Figure 5.3: Comparison of input and output vibration on the seat surface (z-direction) for cruise.

Nevertheless, generating transmissibility curves is a very common technique to evaluate the dynamic comfort and has been used in many investigations for evaluation of seat comfort in vehicles. Most of these investigations considered only the vertical component of input vibrations,

because it is more severe compared to the other components. However, since the focus of this thesis is the comfort evaluation in aircraft seats, it is assumed that the discomfort produced on the seat back in the fore-aft direction is as crucial as the vertical component on the seat surface. Therefore, the transmissibility curves for both the seat back (*x*–direction) and the seat surface (*z*–direction) are generated. Each transmissibility curve is based on the vertical component of the input vibration to the seat. Figures 5.4 and 5.5 show the transmissibility calculated on the seat surface (*z*-direction) for both economy and business class seats and their variation during the three different flight conditions.

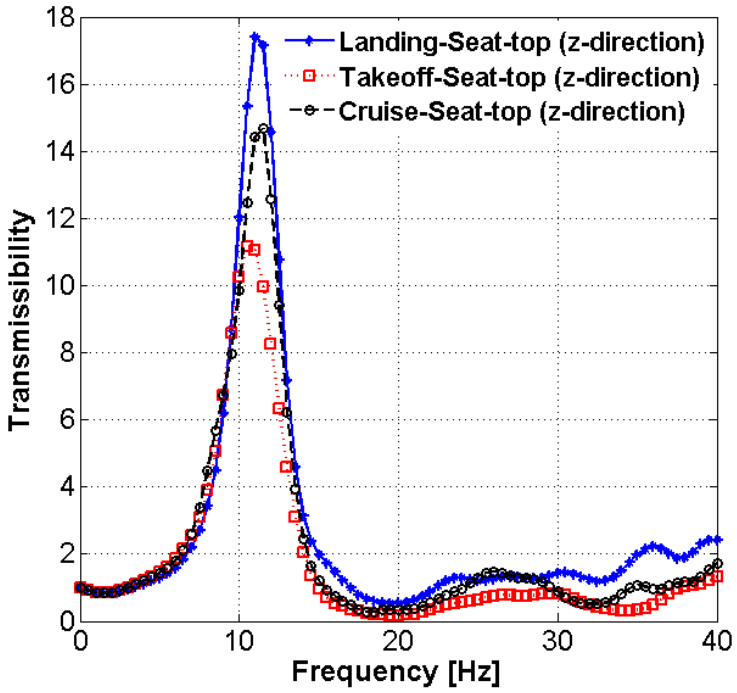

Figure 5.4: Transmissibility in z–direction for economy class seats.

The results show that among the three different flight conditions, landing seems to be the most severe one. Moreover, as expected the transmissibility values for economy class seat are higher than those for the business class seat for the same flight conditions. It is interesting to note that all transmissiblity curves have a well defined peak around 10 Hz for the economy class seat and about 8 Hz for the business class seat.

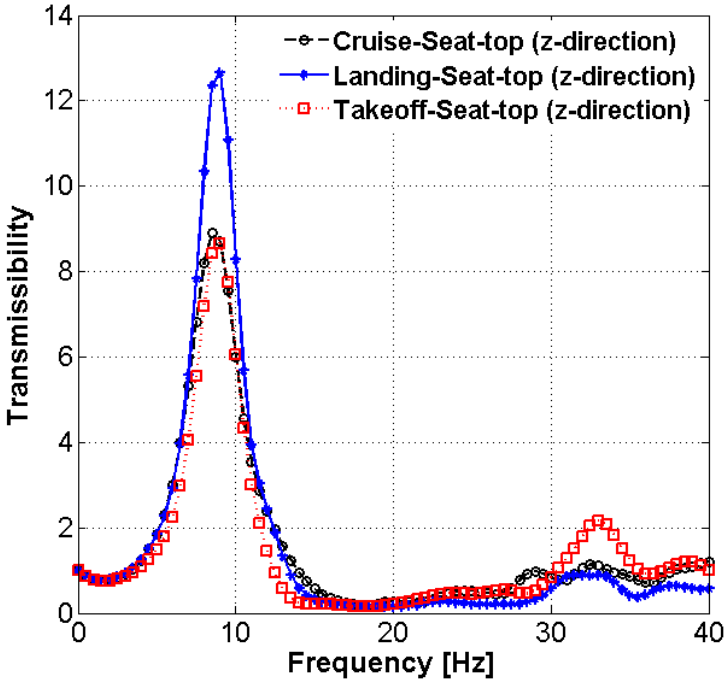

Figure 5.5: Transmissibility in z–direction for business class seats.

As it can be seen from Figures 5.4 and 5.5, there is a difference in the transmissibility values between economy class and business class seats. Business class seats seem to absorb more vibration compared to economy class seats. Moreover, it is also clear that the peak transmissibility curves occur at slightly different frequencies between economy and business class seats. As discussed by Corbridge et al. (1989), stiffness of the cushion plays a role at the resonance frequency thus; business class seats with better cushions tend to reach its maximums at slightly lower frequencies compared to economy class. Furthermore, conducted experiments on economy class seat with half-full dummy and without dummy are presented in Figures 5.8, 5.9 and 5.10 in terms of transmissibility. It is clear from figures that there is a shift in the frequency of peak transmissibility towards higher frequencies when the dummy weight is reduced. This agrees with what has been presented in the literature as the change in the stiffness of the cushion due the applied force, the resonance occurs at different frequencies. Figures 5.6 and 5.7 show the transmissibility curves of seat backrest (x–direction) for both economy class seat and business class seat; respectively, and their comparison for different flight conditions. Transmissibility values for seat backrest (x–direction) for both economy and business class seats seem to reach their maximum at different frequency range comparing to z–direction. Moreover,

economy class seat produced maximum transmissibility around 22 Hz for all flight conditions whereas business class seat produced around 33 Hz.

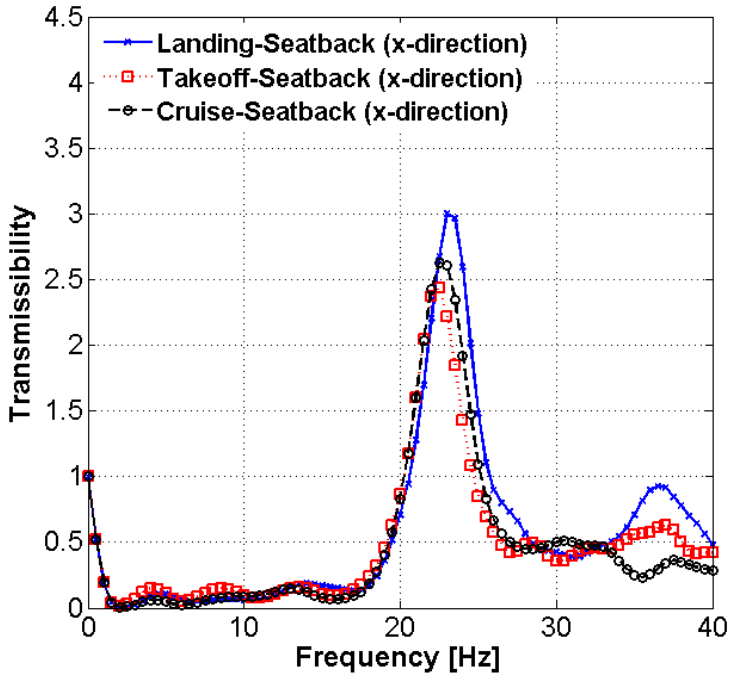

Figure 5.6: Transmissibility in x–direction for economy class seats.

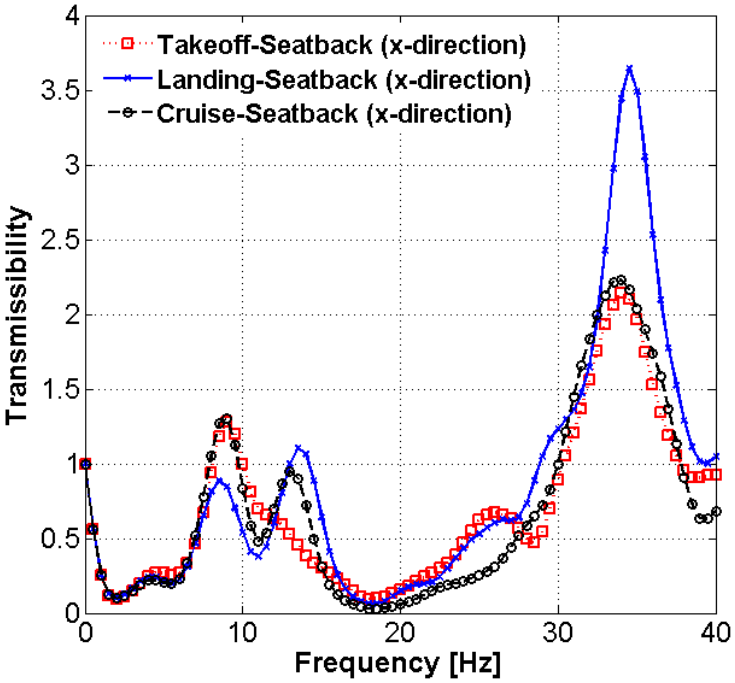

Figure 5.7: Transmissibility in the x–direction for business class seats.

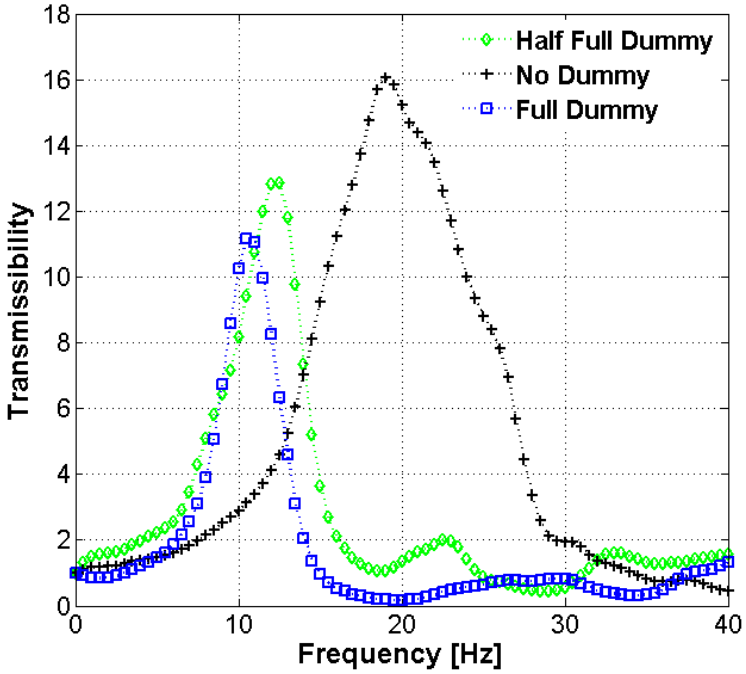

Figure 5.8 Change in the peak transmissibility depending on the weight for takeoff.

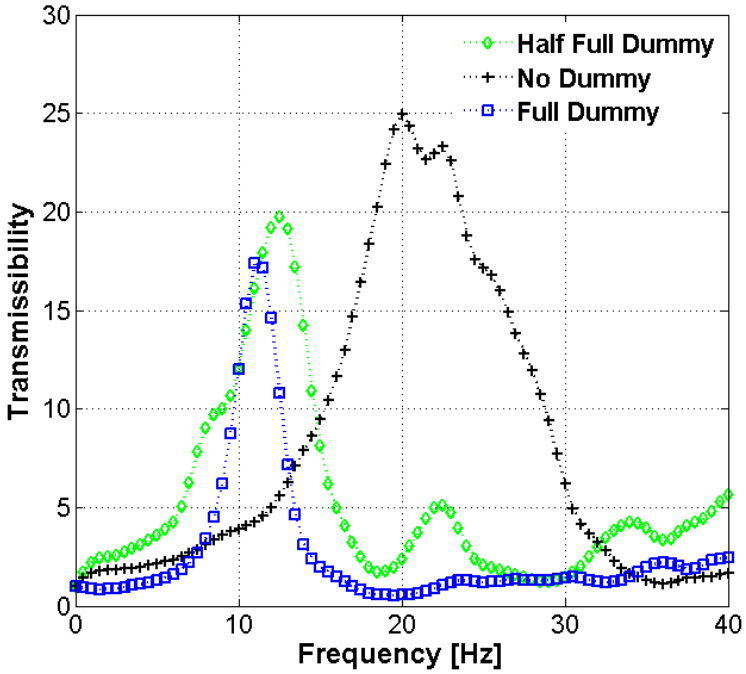

Figure 5.9 Change in the peak transmissibility depending on the weight for landing

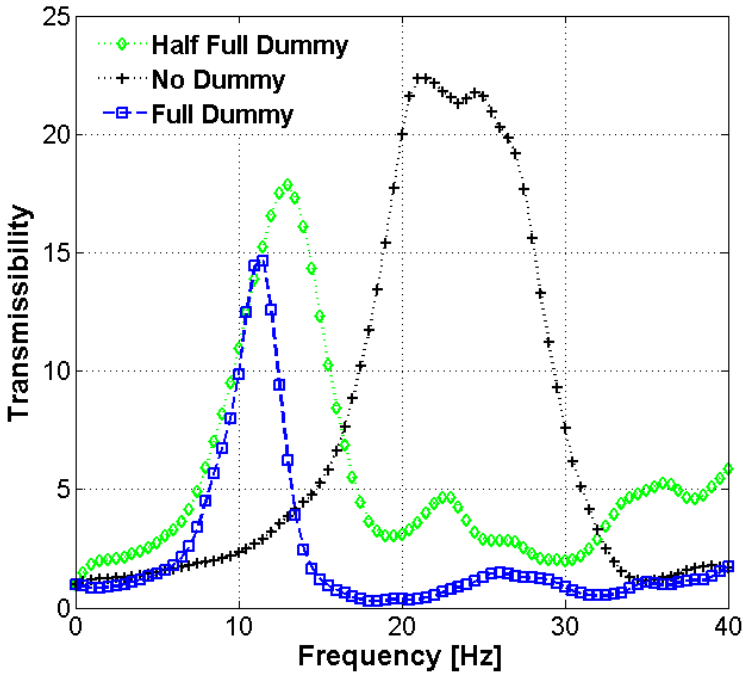

Figure 5.10 Change in the peak transmissibility depending on the weight for cruise

From the Figures 5.8, 5.9 and 5.10 it can be concluded that the response of the peak transmissibility changes depending on the applied force. As the force increases, the cushion compresses and the reduced thickness changes the stiffness thus changing the natural frequency of the seat. Moreover, it is very hard to determine the resonance frequency depending on the compression since the material of the cushion is highly nonlinear.

These transmissibility curves provide a general idea of the severity of vibration depending on its frequency. However, they are not sufficient for overall comfort evaluation.

5.2 Seat Effective Amplitude Transmissibility

Griffin (1978), has developed a new model for measuring transmissibility (S.E.A.T) after his observations on the existence transmissibility functions were not sufficient (Transmissibility = (cross spectrum of floor and seat vibration) / (power spectrum of floor vibration).

The existing transmissibility model was not sufficient to determine whether the vibration characteristics of a seat are good or bad because, isolation efficiency of a seat is determined not by the amplification at resonance but by the extent to which it amplifies or attenuates the motion producing discomfort over the complete spectrum of frequencies (Griffin, 1978).

First a mathematical expression of frequency weighting method is developed to compare vibration spectra with ISO standards:

$$a_n = \left(\int_{f=1}^{f=80} G_s\,(f)\, S^2(f)\, df \right)^{1/2} \tag{5.2}$$

where *S(f)* is the frequency function of human response to vibration given by ISO 2631, a_n is weighted vibration level and $G_s(f)$ is the power spectrum of seat. In addition to these, vibration power spectrum in the same axis on the floor beneath the seat is described as $G_f(f)$, therefore the useful attenuation provided by the seat is given by S.E.A.T. (Seat Effective Amplitude Transmissibility).

In the literature, seat comfort has been evaluated (e.g. Niekerk et al. 2003) by using Seat Effective Amplitude Transmissibility formula which was introduced in 1978 by M.J. Griffin. It gives an objective evaluation using the transmissibility curve and the human weighting functions (normalized perception functions) standardized by ISO and BS, as shown in equation below:

$$\boldsymbol{SEAT}\ \% = \left[\frac{\int \boldsymbol{G_s(f)\, W_i^2(f) df}}{\int \boldsymbol{G_f(f)\, W_i^2(f) df}} \right]^{\boldsymbol{1/2}} * \boldsymbol{100} \tag{5.3}$$

If the weighted vibration levels give a good indication of the effects of the motion, when the value of S.E.A.T is equal to 100%, the motion of the floor and seat produce same discomfort. However, if S.E.A.T is greater than 100%, this indicates that motion of the seat is greater than that on the floor and if the S.E.A.T. values are less than 100% indicates the amount of useful isolation provided by the seat. Values above 100% indicate the perception of the transmitted vibration is amplified.

Seat Effective Amplitude Transmissibility (S.E.A.T) is the second step of transmissibility evaluation which represents the overall seat comfort and has been widely used by many researchers [e.g. Hostens et al. 2004; Niekerk et al. 2003; Griffin 1978]. Transmissibility curves are not sufficient for overall seat comfort because they do not consider the human response to vibration hence, the vibration weighting for overall comfort. There are two sets of human weighting functions, one is based on the ISO-2631 standard and is shown in Figure 5.11, where the other one is based on BS-6841 standard and is shown in Figure 5.12.

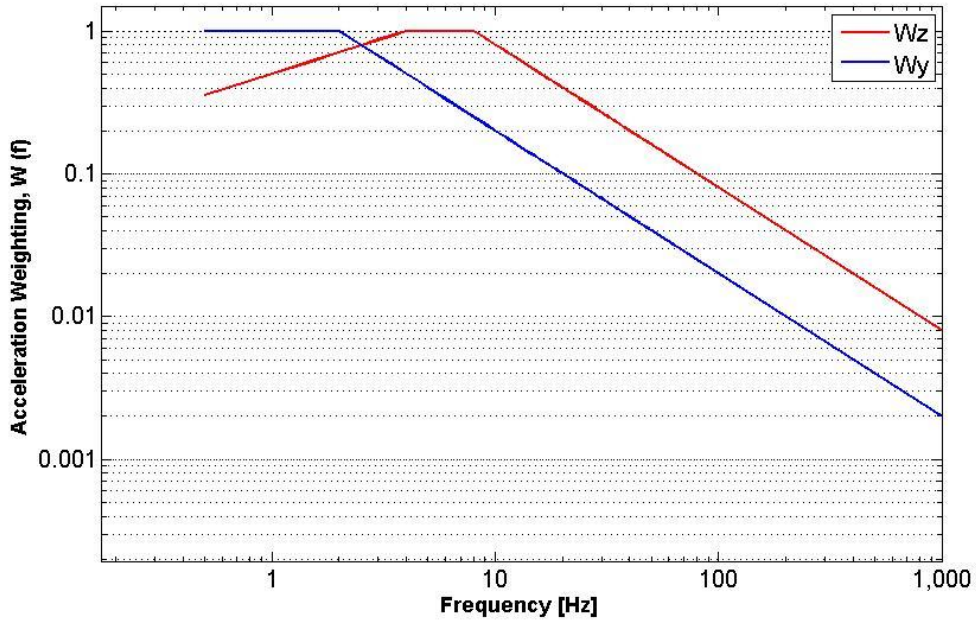

Figure 5.11: ISO–2631 human response functions W_z =z–direction, W_y = x–direction.

In ISO–2631, shown in Figure 5.11, W_z is used for seat-top surface acceleration (*z*–direction) and W_y is used for seat back acceleration (*x* and *y*–directions). In BS–6841, shown in Figure 5.12, W_d is used for seat-top surface acceleration (*z*–direction) and W_c is used for seat back acceleration(*x* and *y*–directions). Tables 5.1 and 5.2 show a summary of the S.E.A.T. values in the frequency range between 1 Hz to 40 Hz using ISO–2631 and BS–6841 weighting functions; respectively, for both the economy class and business class seats during the three different flight conditions.

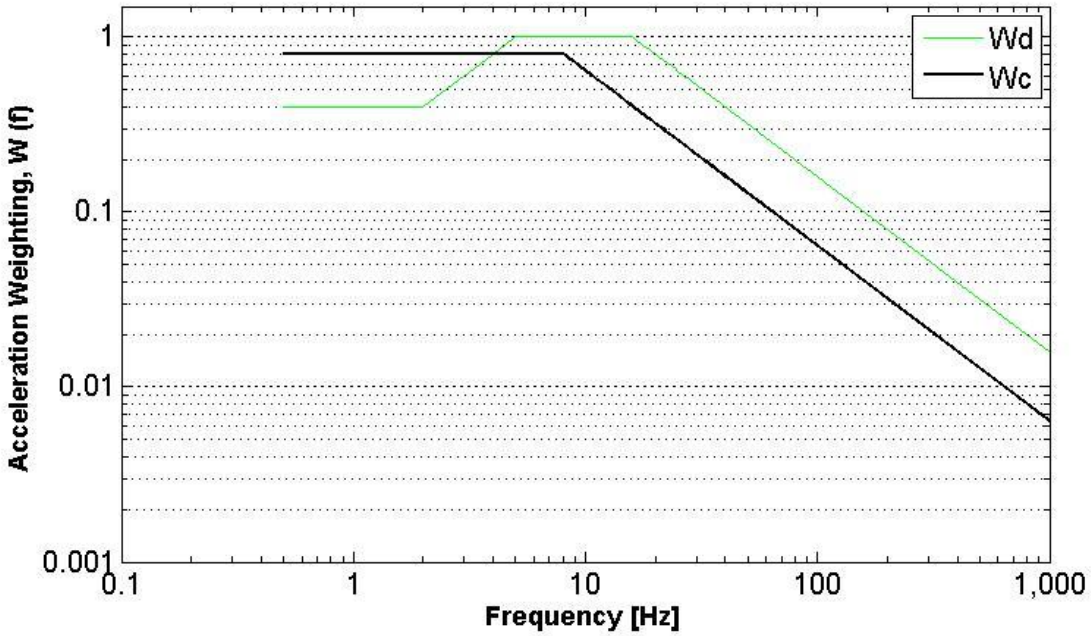

Figure 5.12: BS–6841 human weighting functions W_d = z–direction, W_c = x–direction.

Table 5.1: Calculated S.E.A.T. values using ISO–2631.

	Flight Condition					
	Takeoff		**Landing**		**Cruise**	
	***z*-dir.**	***x*-dir.**	***z*-dir.**	***x*-dir.**	***z*-dir.**	***x*-dir.**
Economy Class	169.2	8.84	186.4	10.3	146.7	8.9
Business Class	151.9	25.8	162.1	24.6	112.6	35.3

Table 5.2: Calculated S.E.A.T. values using BS–6841.

	Flight Condition					
	Takeoff		**Landing**		**Cruise**	
	***z*-dir.**	***x*-dir.**	***z*-dir.**	***x*-dir.**	***z*-dir.**	***x*-dir.**
Economy Class	162.5	17.1	210.2	20.42	180.4	18.3
Business Class	129.9	36.2	153.1	41.1	109.2	43.1

Calculated S.E.A.T. values using both ISO–2631 and BS–6841 weighting functions agree in the sequence of the given flight conditions in terms of overall comfort. However, there is no ratio between two weighting functions due to the nonlinearity of the input and output power spectral densities.

Chapter 6

Factors Affecting Dynamic Seat Comfort

6.1 Effect of Weight on the Transmissibility and S.E.A.T

To investigate the effect of the passenger weight on the vibration transmissibility, an identical second dummy was used. The two dummies were placed on economy class seat base but using the business class seat cushion. This way, placing the business class seat cushion on top of the economy class seat base provided data to compare cushions on the same seat base as shown in the following section. This experiment is performed for the three different flight conditions. Figures 6.1, 6.2, and 6.3 show a comparison of the transmissibility curves for 1 and 2 identical dummies placed on the seat during takeoff, landing and cruise flight conditions.

Table 6.1 shows a summary of the calculated S.E.A.T. values using the BS-6841 standards. As the passenger weight increases the S.E.A.T. value decreases, which means an increase in the dynamic comfort level. The calculated S.E.A.T. values for economy and business class seat cushions on economy class seat base using the BS–6841 weighting functions are summarized in table 6.1. Moreover, it is also observed that additional dummy caused a slight shift in the peak transmissibility towards higher frequencies.

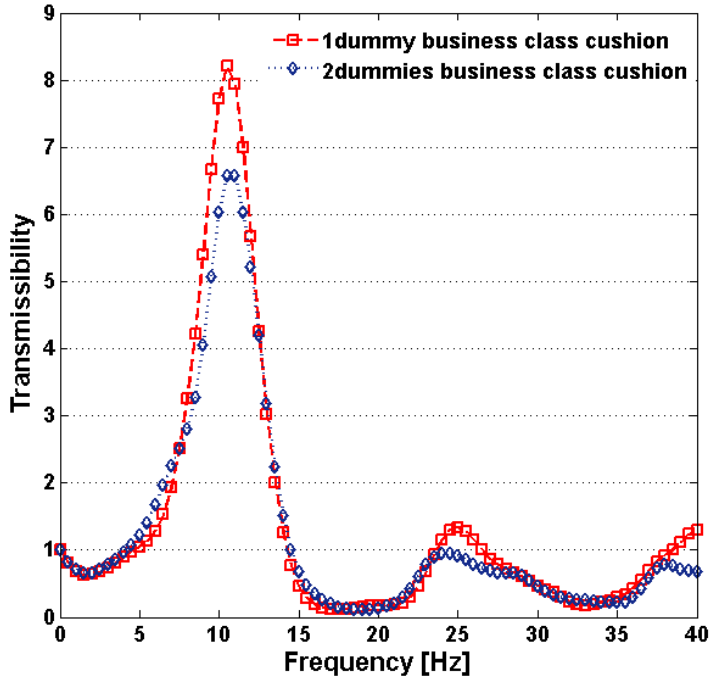

Figure 6.1: Effect of number of passengers in transmissibility during take–off.

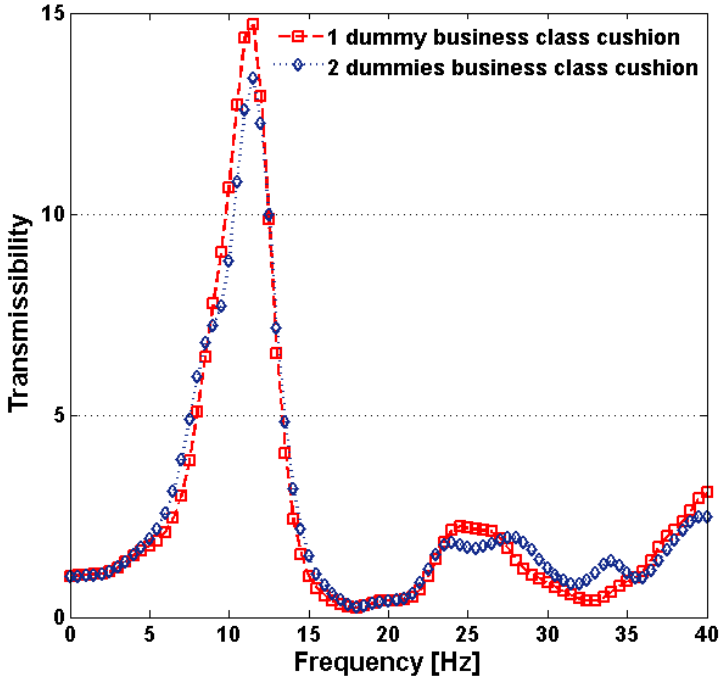

Figure 6.2 Effect of number of passengers in transmissibility during landing.

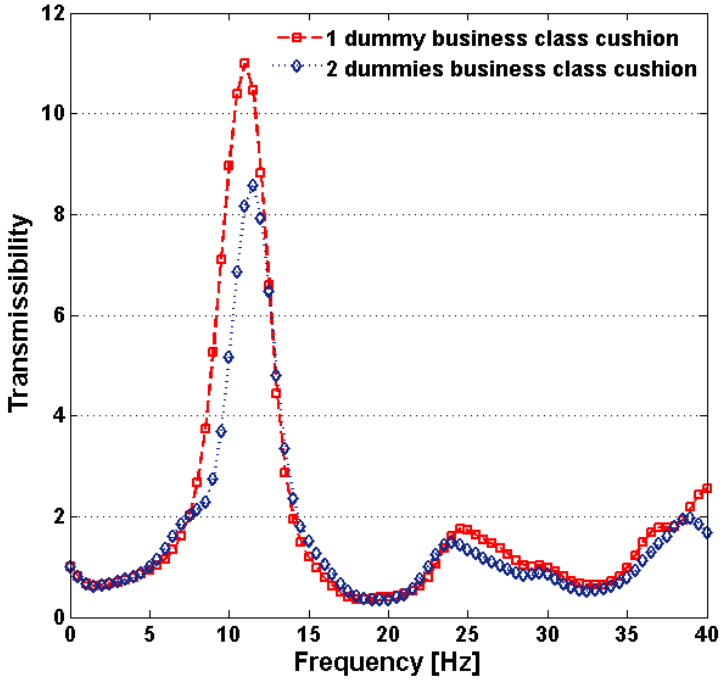

Figure 6.3: Effect of number of passengers in transmissibility during cruise.

Table 6.1: Calculated S.E.A.T. values using BS–6841 human weighting functions.

	Takeoff	**Landing**	**Cruise**
1 dummy business cushion	148.1	159.4	143.5
2 dummies business cushion	142.3	155.7	126.8

6.2 Effect of Cushion on the Transmissibility and S.E.A.T.

Previous sections showed that there is significant difference between economy and business class seats. It is however, may be due to the cushion or the difference in the structures of the two seats base. To understand this, economy and business class seat cushions were placed on top of the economy class base along with the laboratory made cushions. Figures 6.4, 6.5, and 6.6 show the comparison of five cushions during takeoff, landing, and cruise, respectively.

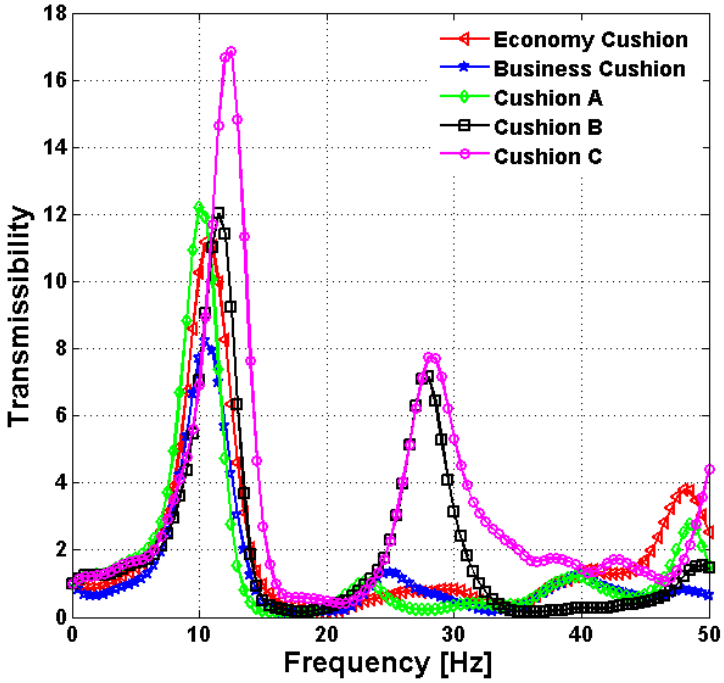

Figure 6.4: Transmissibility comparison of different cushions during take–off.

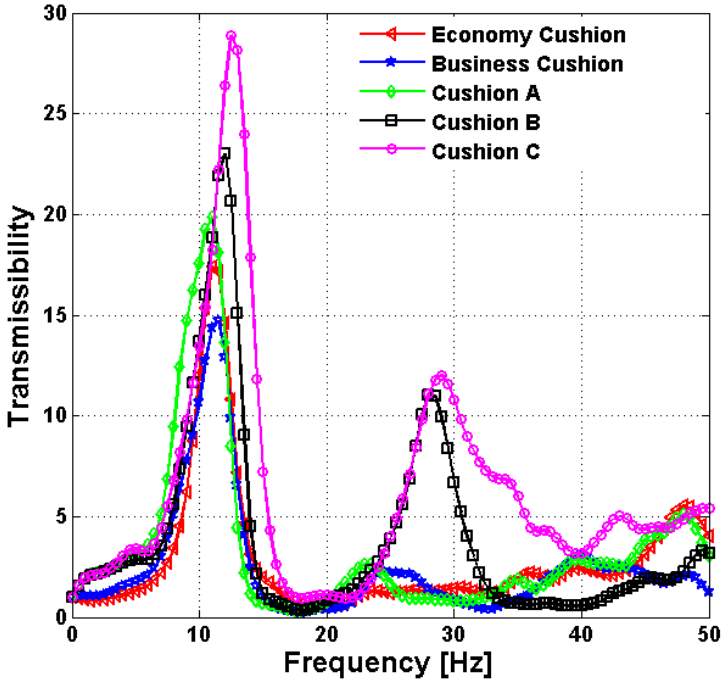

Figure 6.5: Transmissibility comparison of different cushions during landing.

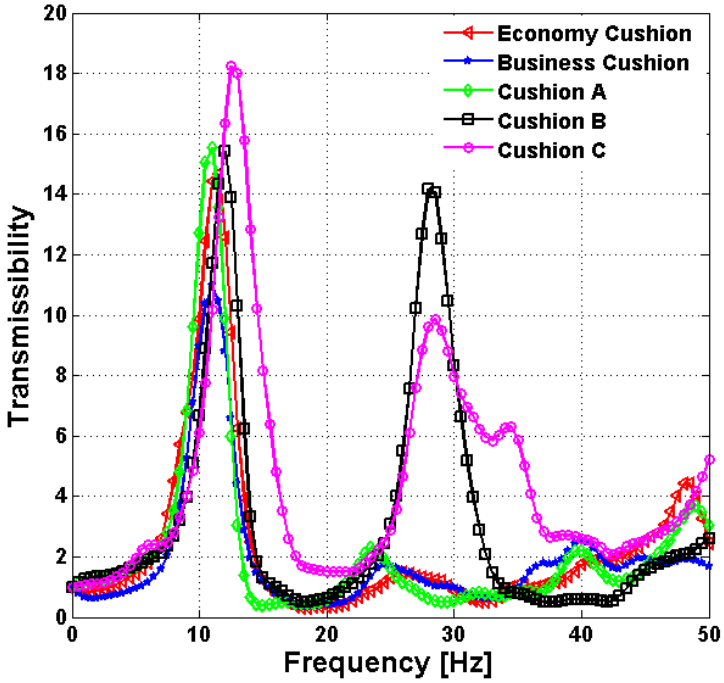

Figure 6.6: Transmissibility comparison of different cushions during cruise.

Figures 6.4 – 6.6 provide a good comparison between all five cushions and as expected all the transmissibility values for landing are much higher than takeoff and cruise. Cushion B and C produced a second peak around 27 Hz for each flight condition which can be assumed as second mode frequency for those cushions. The cushion with large thickness but low stiffness resulted with highest transmissibility. Calculated S.E.A.T. values with ISO–2631 human functions for 5 different cushions on top of economy class base are presented in Table 6.2. Moreover, transmissibility values for business class cushion shown in the figures are slightly larger when compared to the results when it was on business class seat base which, indicates that the large difference in the transmissibility between business and economy class is mainly due to the cushion difference but also slightly related to the base structure.

Table 6.2: Calculated S.E.A.T. values for different cushions.

	Takeoff	**Landing**	**Cruise**
Economy cushion	169.2	186.4	146.7
Business cushion	159.3	176.6	127.8
Cushion A	184.2	201.4	169.3
Cushion B	180.6	197.8	162.6
Cushion C	198.1	221.2	178.7

Chapter 7

Finite–Element Simulation

As mentioned in the previous chapters one of the main objectives of this study is to provide a theoretical model that can predict the dynamic seat comfort as close as possible to experimental results. For this purpose, a CAD model is developed as shown in Figure 7.1. However, since it was not practical to disassemble the seats into components considering the welding process employed for the production, some parts of the seats, such as joints and connections were considered as one body with the main parts of the seat.

Figure 7.1: CAD model of economy class seats.

Finite-element analysis is very common technique in the industry. It provides variety of solutions such as; stress–strain, modal, random vibration, and transient analysis for different structures. It does not only reduce the expenses but also any development and changes in the structure can be done easily.

7.1 Mesh Development and Mesh Sensitivity

The quality of the mesh plays a significant role in the accuracy of the simulation. On the other hand, increased mesh element number significantly increases the solving time. Therefore, an optimum number of elements should be selected in order to the present a fine mesh and keeping the solving time as low as possible.

To find the optimum number of elements, one should first perform either modal analysis or stress & strain analysis with the given mesh element number initially by ANSYS. The reason behind that is modal analysis and stress & strain analysis are solved very fast. Then, same analysis should be performed with an increased number of elements. This process should be repeated until there is no significant change in the solutions.

For this study, modal analysis is performed first with initial number of elements given by the program which is approximately 70000, and then the number of elements is reduced while monitoring the results of modal analysis.

7.1.1 Modal Analysis

The results of modal analysis for the first four modes with different element numbers are presented in Figure 7.2. It is clear from the figure that resulted frequencies for each mode did not change when the number of mesh elements is reduced from 70000 to 40000. Therefore, for the rest of FE analysis, the number elements of the mesh is set to be 40000 so the results will be as

accurate as it would be with 70000 elements and time for the solving process would be much less.

The results of the model analysis are presented in Table 7.1 for the first nine modes as the model analysis was limited to 600 Hz and the affected areas on the structure for the first two modes are presented in Figure 7.3 and third and fourth modes are presented in Figure 7.4 respectively.

Table 7.1: Identified model frequencies by using FE.

Mode	**Frequency [Hz]**
1	61
2	90
3	129
4	145
5	187
6	344
7	452
8	494
9	590

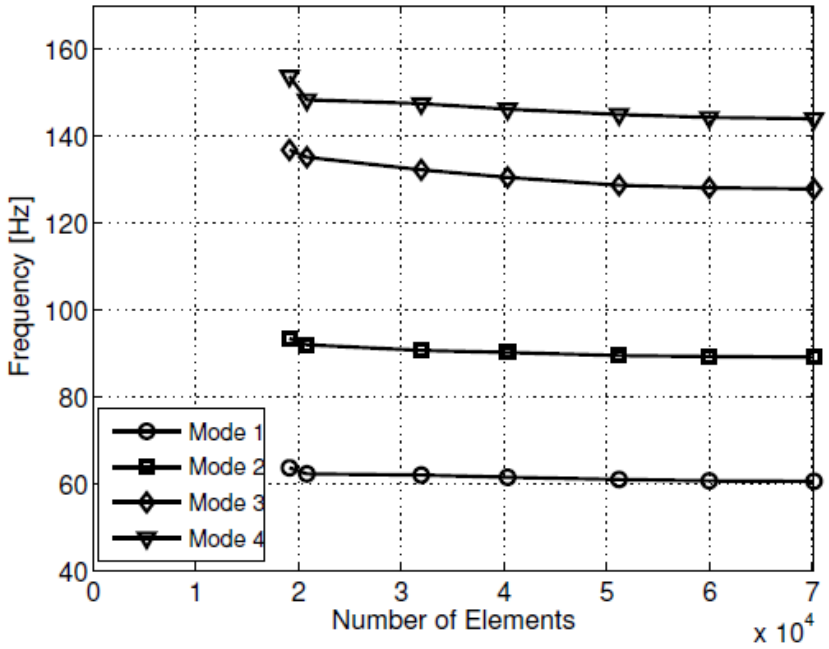

Figure 7.2: Change in the model frequencies with the increase of tetrahedral element number.

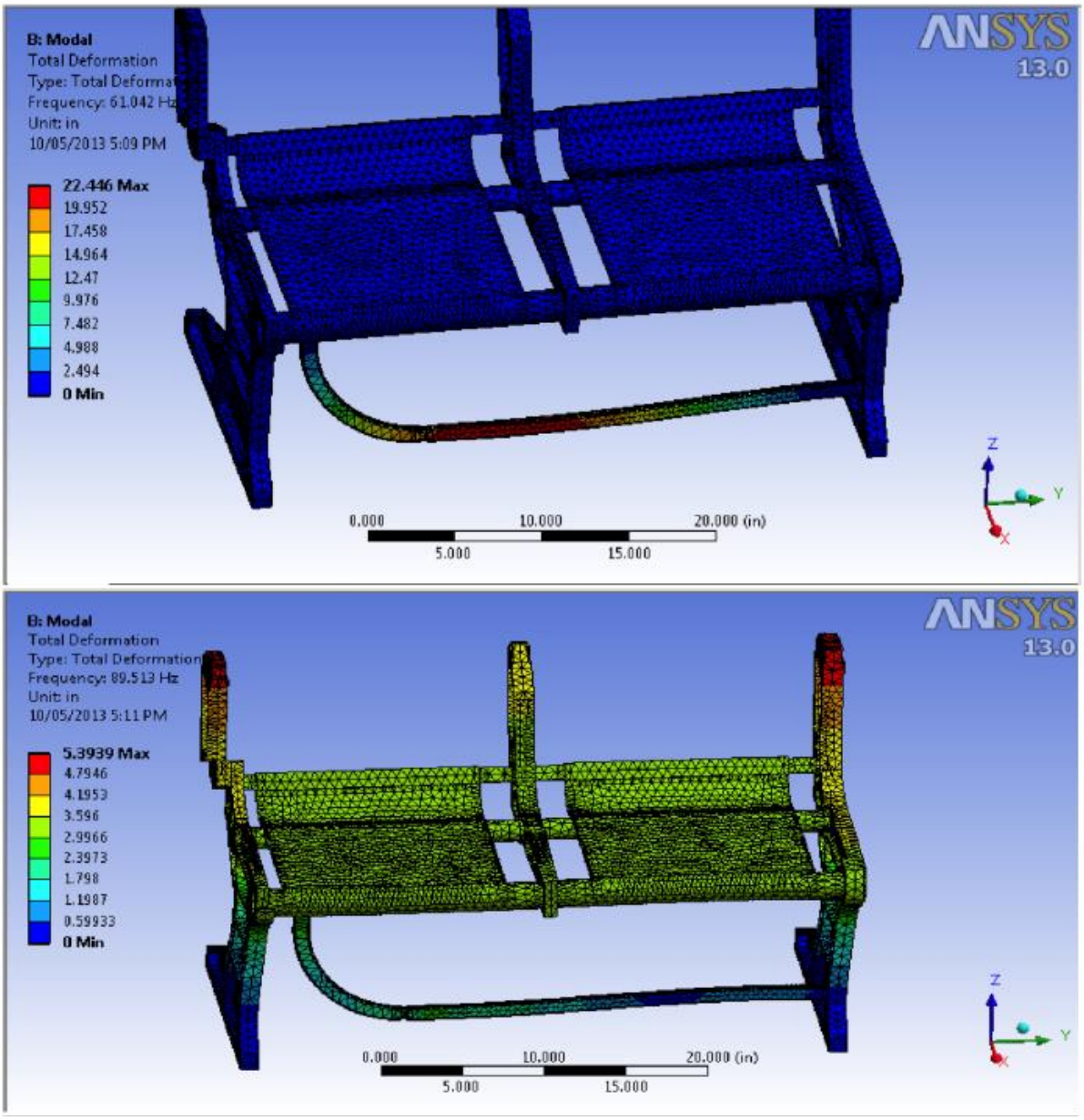

Figure 7.3: First and second mode shapes.

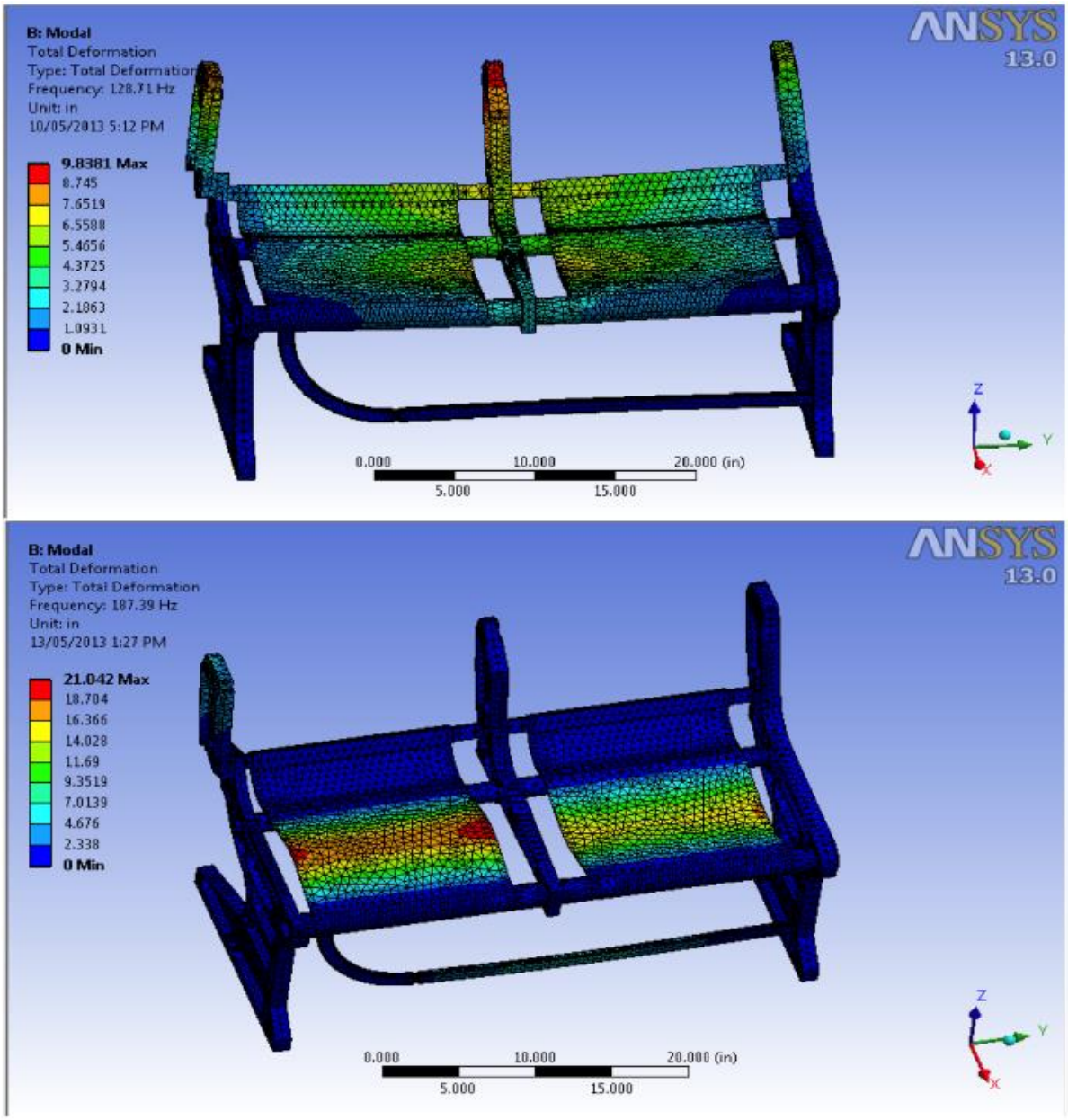

Figure 7.4: Third and fourth mode shapes.

7.2 FEA Response for the Given Flight Conditions

Using the optimized mesh parameters, the model is used to predict the dynamic seat comfort and the output acceleration measurements of FE are compared to experimental results. In the first step however, the model is tested without any cushions. Figure 7.5, 7.6, and 7.7 show the

comparison between FEA and experimental results for a total of two second data points during takeoff, landing, and cruise, respectively.

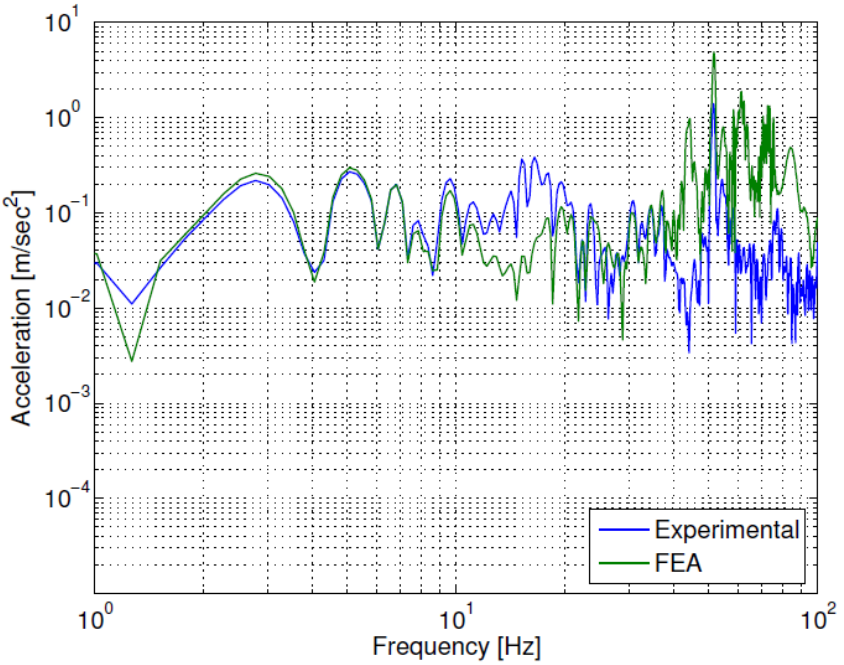

Figure 7.5: Output acceleration comparison for takeoff without cushion.

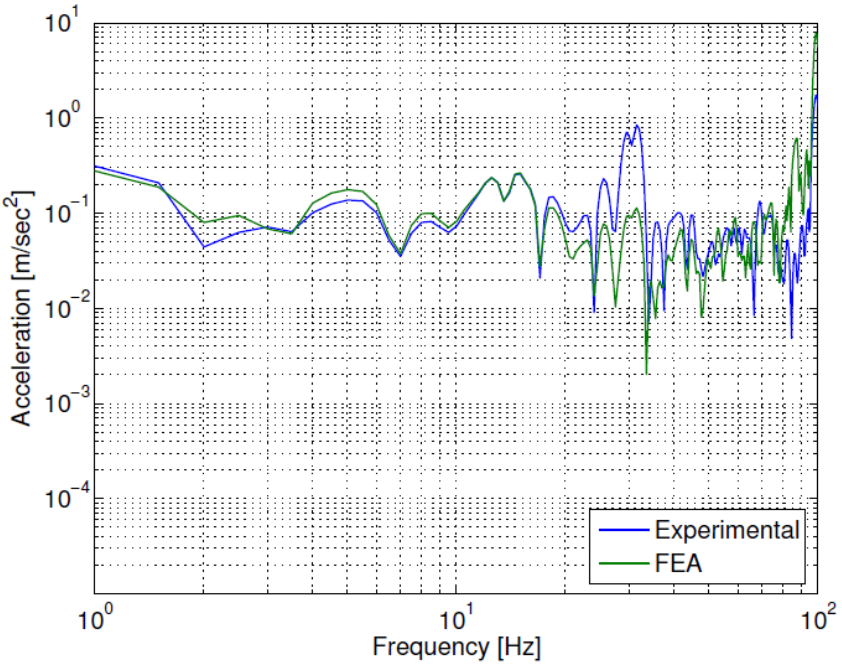

Figure 7.6: Output acceleration comparison for landing without cushion.

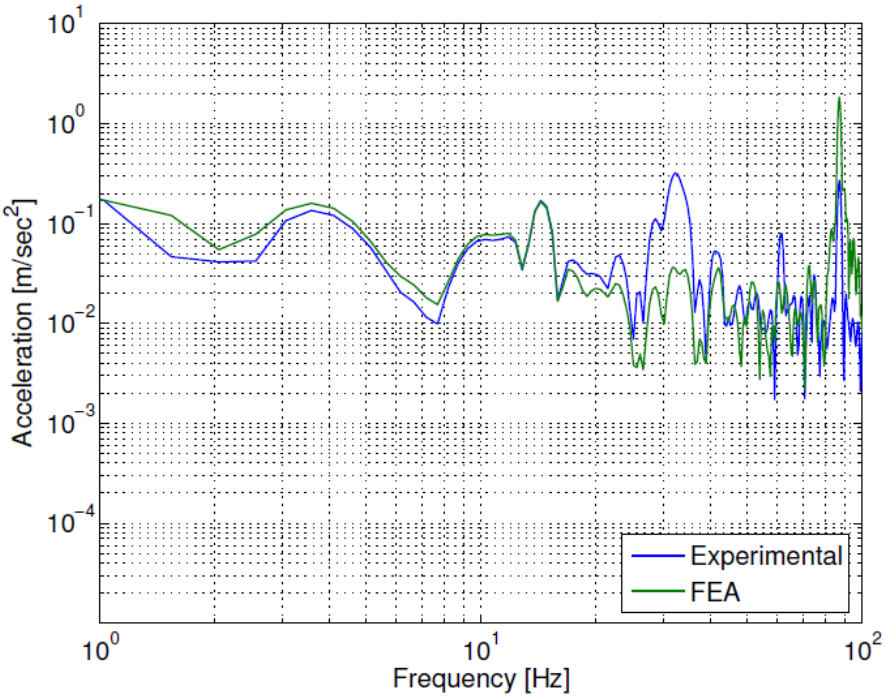

Figure 7.7: Output acceleration comparison for cruise without cushion.

The input acceleration values only contain first two seconds of the original acceleration values taken from experiments since it was not practical to input the whole data series for 30 second due to time, equipment and hard drive memory limitations.

Figures 7.5, 7.6, and 7.7 indicate that there is good correlation between FEA and experimental results until 20 Hz. At higher frequencies however, discrepancy observed. This can be due to joints and connections that were not included in the CAD model. Moreover, some of the materials used in the structure of the seat are unknown. However in the FEA, the seat base is assumed to be purely aluminium.

Figures 7.8, 7.9, and 7.10 show the comparison between FEA and experimental results for the economy class seat including the cushion during takeoff, landing and cruise respectively. When FEA expected to run with cushion, the solving process took significantly more time than without

cushion. This was expected since the cushion is made of hyper elastic material and behaves nonlinearly.

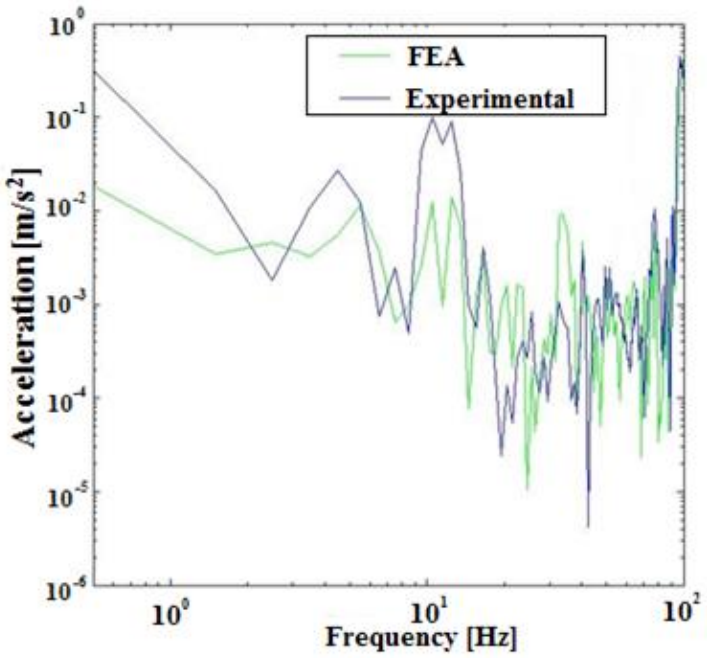

Figure 7.8: Output acceleration comparison for takeoff including cushion.

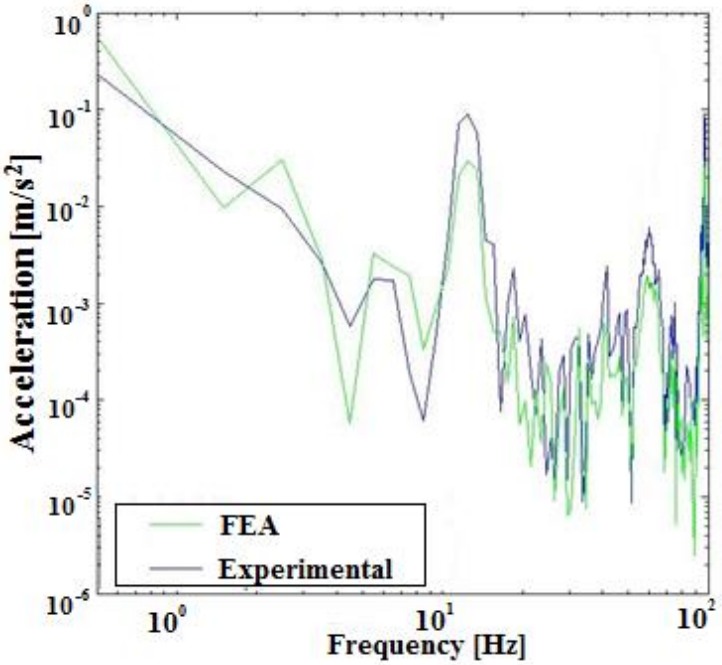

Figure 7.9: Output acceleration comparison for landing including cushion.

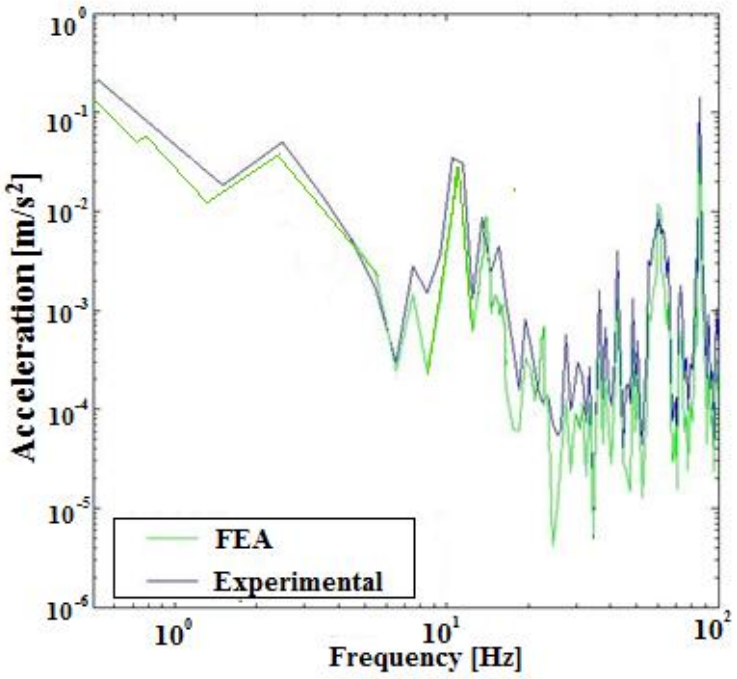

Figure 7.10: Output acceleration comparison for cruise including cushion.

It should be noted that the undertaken FEA with cushion had a one second of data points input acceleration. Therefore, the generated curves for FE analysis with cushion as not smooth as the ones without cushion and since the cushion increases the solving time dramatically, it also requires a larger hard drive memory.

Moreover, the difference between FEA and experimental output accelerations are more significant when the cushion is included. This is mainly due to the unknown properties of the cushion in addition to unknown properties of the seat base. It was also not practical to perform any property test on the original cushions since the tests require cutting samples from the cushions. Nevertheless, the FEA results show similar behaviour to the experimental results.

Chapter 8

Conclusions and Recommendations

8.1 Conclusions

In this study experimental and theoretical analysis are performed to evaluate dynamic seat comfort in the aircraft for given flight conditions; takeoff, landing and cruise through turbulence. Moreover, some of the effecting factors are also investigated.

To perform the experiments, input acceleration values that are obtained from actual flight conditions are introduced to multi-axis-shaker-table (MAST) to replicate the given flight conditions. It is proved that the original flight conditions were perfectly created on the MAST until which, reaches the cut-off frequency of 150 Hz. However, in this study as well as in the literature it is shown that the comfort evaluations are performed within a range much less than 150 Hz since, the peak transmissibility occurs at low frequencies.

Performed experiments clearly show that among the three flight conditions, landing appears to produce the most discomfort by having high vibration transmissibility. However, for overall dynamic seat comfort calculated S.E.A.T. values do not present valuable information since all the results are more than 100%. The S.E.A.T. equation was initially created for automotive industry and since the vibration levels that are introduced to the passenger seats in aircrafts and

automotive are very different, this equation appears to be not valid for aircraft industry. The results provide good comparison between different seats however they are not sufficient to measure any improvement since there is not an absolute value.

To investigate the effect of weight a second identical dummy is added and comfort evaluations are performed. The results agree what with has been published in the literature, saying that an increase in the passenger weight dynamic comfort results in an increase.

The other comfort affecting factor investigated in this study, which concluded to be the most effective one, is the characteristics of seat cushion. To express the importance of cushion, in addition to comparison between economy and business class cushions three additional cushions from two different materials are investigated as well. Among the three additional cushions, two of them are from same material but having different thicknesses. This way the change of dynamic comfort due to different thickness of same cushions is also observed. Performing a three-point bending test, the Young's modulus of two cushions is obtained. As a result, Cushion C with the smallest Young's modulus resulted with the highest vibration transmissibility for each flight condition. Moreover, experiments with different cushions are performed only on economy class seat base showed that using business class cushion on economy class seat base resulted with a small decrease in the comfort score comparing to original business class results, indicating that the base structure of the aircraft seats also play a role in vibration transmission.

In addition to experimental investigations, a CAD model is developed to be used for Finite Element Analysis using ANSYS software. Due to time constraints, only a small portion of the original input vibration signals could be applied for the FE analysis. Although there are some differences in the measured vibrations on the seat surface especially at low frequencies, FE model presented similar results as in experiments.

8.2 Recommendations

The method to predict the dynamic seat comfort used in automotive industry seems to be not a valid approach for the comfort evaluations in aircrafts because all the results that are presented in this study are more than 100%. Therefore, it is recommended that a new set of weighting functions could be introduced to be used in S.E.A.T. equation that can provide an absolute value to observe any improvement in dynamic seat comfort.

The proposed FE model still can be improved since the results of FE analysis show some differences compared to the experimental results mainly due to unknown parameters, such as cushion properties. Therefore, the model can be enhanced by improving the CAD model, setting the correct properties for seat cushion as well as seat structure including the dynamic connections. Also, this kind of analysis requires high speed CPU and very large hard drive memory to fully simulate the given flight conditions.

References

[1]Air Transport Action Group, ATAG (2008) "The Economic and Social Benefits of Air Transport, 2008, website: www.iata.org [accessed: 06/10/2013].

[2]Air Transport Association of America, ATAA (2008) "Economic Report 2008" website: www.airlines.org [accessed: 06/10/2013].

[3]American Conference of Governmental Industrial Hygienists (ACGIH) "2002 TLVs and BEIs Based on the Documentation of the Threshold Limit Values for Chemical Substances and Physical Agents and Biological Exposure Indices".

[4]American National Standards Institute, Inc. (ANSI) "Mechanical Vibration and Shock– Evaluation of Human Exposure to Whole-body Vibration – Part 1: General requirements" ANSI S3.18-2002.

[5]Basri, B., Griffin, M. J. (2012). Equivalent comfort contours for vertical seat vibration: effect of vibration magnitude and backrest inclination. Ergonomics,55(8), 909-922.

[6]Blood, R. P., Rynell, P. W., Johnson, P. W. (2012). Whole-body vibration in heavy equipment operators of a front-end loader: Role of task exposure and tire configuration with and without traction chains. Journal of safety research.

[7]Boileau, P.E., Rakheja, S., (1990). Vibration attenuation performance of suspension seats for off-road forestry vehicles. International Journal of Industrial Ergonomics 5, 275–291.

[8]Corbridge, C., Griffin, M. J., Harborough, P. R. (1989). Seat dynamics and passenger comfort. Proceedings of the Institution of Mechanical Engineers, Part F: Journal of Rail and Rapid Transit, 203(1), 57-64.

[9]Ebe, K., Griffin, M. J. (2001). Factors affecting static seat cushion comfort.Ergonomics, 44(10), 901-921.

[10]Ebe, K., Griffin, M. J. (2000). Qualitative models of seat discomfort including static and dynamic factors. Ergonomics, 43(6), 771-790.

[11]Eberle, W. R., Steele, M. M. (1975). Investigations of fluidically controlled suspension systems for tracked vehicles. NASA STI/Recon Technical Report N, 76, 31484.

[12]Elmadany, M.M., Abduljabbar, Z., (1990). Design evaluation of advanced suspension systems for truck ride comfort. Computers and Structures 36(2), 321–331.

[13]Els, P.S., Theron, N.J., Uys, P.E., Thoresson, M.J., (2007). The ride comfort vs. handling compromise for off-road vehicles. Journal of Terramechanics 44, 303–317.

[14]Fairley, T. E., Griffin, M. J. (1989). The apparent mass of the seated human body: vertical vibration. Journal of Biomechanics, 22(2), 81-94.

[15]Fothergill, L. C., Griffin, M. J. (1977). The evaluation of discomfort produced by multiple frequency whole-body vibration. Ergonomics, 20(3), 263-276.

[16]Furness, T. A., Lewis, C. H. (1978) "Helmet-mounted Display Reading Performance under Whole-body vibration" Proceedings of the United Kingdom Informal Group on Human Response to Vibration, National Institute of Agricultural Engineering, Silsoe, Bedfordshire.

[17]Griffin, M. J. (1978). The evaluation of vehicle vibration and seats. Applied Ergonomics, 9(1), 15-21.

[18]Griffin, M. J. (1990). Handbook of human vibration. Academic press.

[19]Gouw, G. J., Rakheja, S., SANKAR, S., Afework, Y. (1990). Increased comfort and safety of drivers of off-highway vehicles using optimal seat suspension. SAE transactions, 99(2), 541-548.

[21]Guignard, J. C., King, P. F. (1972) "Aeromedical Aspects of Vibration and Noise" AGARD-AG-151, 1972.

[20]Gunston, T. P. (2003, September). The apparent mass of the seated human body in response to lateral and roll vibration. In 38th United Kingdom Conference on Human Response to Vibration, Institute of Naval Medicine, Alverstoke, Gosport, PO12 2DL, England (pp. 17-19).

[23]Hostens, I., Ramon, H. (2003). Descriptive analysis of combine cabin vibrations and their effect on the human body. Journal of sound and vibration,*266*(3), 453-464.

[24]Hostens, I., Deprez, K., Ramon, H., (2004). An improved design of air suspension for seats of mobile agricultural machines. Journal of Sound and Vibration 276, 141–156.

[25]Ieluzzi, M., Turco, P., Montiglio, M. (2006). Development of a heavy truck semi-active suspension control. Control Engineering Practice, 14(3), 305-312.

[26]International Air Transport Association, IATA (2007) "Fact Sheet: World Industry Statistics" website: www.iata.org [accessed: 06/10/2013].

[27]International Air Transport Association, IATA (2008) "Airlines to Lose $5.2 billion in 2008 – Slowing Demand and High Oil to Blame," Press Release, September 3.

[28]International Civil Aviation Organization, ICAO (1971–2005) "Statistical Yearbook and Annual Reviews of Civil Aviation"

[29]International Standards Organization (ISO) "Mechanical Vibration and Shock – Evaluation of Human Exposure to Whole-body Vibration – Part 1: General Requirements" ISO 2631-1:1997(E).

[30]Ishutkina, M. A., Hansman, R. J. (2008) "Analysis of Interactions between Transportation and Economic Activity" International Center for Air Transportation, Massachusetts Institute of Technology, Cambridge, MA.

[31]Japan Aircraft Development Corporation, JADC (2002) "Worldwide Market Forecast for Commercial Air Transport between 2002 and 2021".

[32]Malchaire, J., Piette, A., Mullier, I. (1996). Vibration exposure on fork-lift trucks. The Annals of Occupational Hygiene, 40(1), 79-91.

[33]Mandapuram, S., Rakheja, S., Boileau, P. É., Maeda, S. (2012). Apparent mass and head vibration transmission responses of seated body to three translational axis vibration. International Journal of Industrial Ergonomics, 42(3), 268-277.

[34]Magid, E. B., Coermann. R. R., Ziegenruecker, G. H. (1960) "Human Tolerance to Whole Body Sinusoidal Vibration" Aerospace Medicine, 31: 915–924.

[35]Makhsous, M., Hendrix, R., Crowther, Z., Nam, E., Lin, F. (2005). Reducing whole-body vibration and musculoskeletal injury with a new car seat design.Ergonomics, 48(9), 1183-1199.

[36]Miwa, T., Yonekawa, Y. (1971). Evaluation methods for vibration effect. Part 10. Measurement of Vibration Attenuation; Effect of Cushions. Industrial Health,9, 81.

[37]Moseley, M. J., Griffin, M. J. (1986) "Effects of Display Vibration and Whole-body Vibration on Visual Performance" Ergonomics, 29.8: 977–983.

[38]Nell, S., Steyn, J. L. (2003). Development and experimental evaluation of translational semi-active dampers on a high mobility off-road vehicle. Journal of terramechanics, 40(1), 25-32.

[39]Patil, M.K., Palanichamy, M.S., (1988). A mathematical model of tractor-occupant system with a new seat suspension for minimization of vibration response, Applied Mathematical Modelling 12, 63–71.

[40]Paddan, G. S., Mansfield, N. J., Arrowsmith, C. I., Rimell, A. N., King, S. K., Holmes, S. R. (2012). The influence of seat backrest angle on perceived discomfort during exposure to vertical whole-body vibration. Ergonomics, 55(8), 923-936.

[41]Pope, M. H., Donnermeyer, D., Wilder, D. G., Hundal, M. (1983) "The Effects of Helicopter Vibration on the Spinal System" University of Vermont, Annual Progress Report, Contract No. DAMD 17-82-C-2153, U.S. Army Medical Research and Development Command, Fort Detrick, MD.

[42]Smith, S. D. (2002) "Characterizing the Effects of Airborne Vibration on Human Body Vibration Response" Aviation, Space, and Environmental Medicine, 73.2: 36–45.

[43]Smith, S. D. (2006) "Seat Vibration in Military Propeller Aircraft: Characterization, Exposure Assessment, and Mitigation" Aviation, Space, and Environmental Medicine, 77.1: 32–40.

[44]Smith, S. D., Smith, J. A. (2006) "Head and Helmet Biodynamics and Tracking Performance in Vibration Environments" Aviation, Space, and Environmental Medicine, 77.4: 388–397.

[45]Shen, W., Vertiz, A. M. (1997). Redefining seat comfort. Technical Paper No. 970597. Society of Automotive Engineers. Inc., Warrendale, PA, USA.

[46]Sherwin, L. M., Owende, P. M. O., Kanali, C. L., Lyons, J., Ward, S. M. (2004). Influence of tyre inflation pressure on whole-body vibrations transmitted to the operator in a cut-to-length timber harvester. Applied Ergonomics, 35(3), 253-261.

[47]Tewari, V.K., Prasad, N., (1999). Three-DOF modelling of tractor seat-operator system. Journal of Terramechanics 36, 207–219.

[48]Toward, M. G., Griffin, M. J. (2011). Apparent mass of the human body in the vertical direction: Inter-subject variability. Journal of Sound and vibration,330(4), 827-841.

[49]Yusof, M.B. (2005). Development of an automotive seat for ride comfort. Universiti Teknologi Malaysia, Research Vote No.: 74113

[50]Uys, P. E., Els, P. S., Thoresson, M. (2007). Suspension settings for optimal ride comfort of off-road vehicles travelling on roads with different roughness and speeds. Journal of Terramechanics, 44(2), 163-175.

[51]Verma, M.R. (1970). Tractor seat design, fabrication and testing. Unpublished M.Tech. thesis. Agricultural Engineering Department, I.I.T., Kharagpur, India.

[52]Von Gierke, H. E. (1975). The ISO Standard Guide for the Evaluation of Human Exposure to Whole-Body Vibration.

[53]Wei, L., Griffin, M. J. (1998). Mathematical models for the apparent mass of the seated human body exposed to vertical vibration. Journal of Sound and Vibration, 212(5), 855-874.

[54]Wilder, D., Magnusson, M.L., Fenwiek, J., Pope, M., (1994). The effect of posture and seat suspension design on discomfort and back muscle fatigue during simulated truck driving. Applied Ergonomics 25(2), 66–76.

[55]White, S. W., Kim, S. K., Bajaj, A. K., Davies, P., Showers, D. K., & Liedtke, P. E. (2000). Experimental techniques and identification of nonlinear and viscoelastic properties of flexible polyurethane foam. Nonlinear Dynamics, 22(3), 281-313.

[56]Wells, M. J., Griffin, M. J. (1984) "Benefits of Helmet-mounted Display Image Stabilisation Under Whole-body Vibration" Aviation, Space, and Environmental Medicine, 55.1: 13–18.

[57]Zehsaz, M., Sadeghi, M. H., Ettefagh, M. M., Shams, F. (2011). Tractor cabin's passive suspension parameters optimization via experimental and numerical methods. Journal of Terramechanics, 48(6), 439-450.